Theses and Dissertations

2014

Investigating Detergent and Lipid Systems for the Study of Membrane Protein Interactions: Characterizing Caveolin Oligomerization

Monica D. Rieth
Lehigh University

Follow this and additional works at: http://preserve.lehigh.edu/etd

Part of the Chemistry Commons

Recommended Citation

Investigating Detergent and Lipid Systems for the Study of Membrane Protein
Interactions: Characterizing Caveolin Oligomerization

by

Monica D. Rieth

A Dissertation

Presented to the Graduate and Research Committee

of Lehigh University

in Candidacy for the Degree of

Doctor of Philosophy

in

Chemistry

Lehigh University

January 12, 2014

Approved and recommended for acceptance as a dissertation in partial fulfillment of the requirements for the degree of Doctor of Philosophy

Monica D. Rieth
Investigating Detergent and Lipid Systems for the Study of Membrane Protein Interactions: Characterizing caveolin oligomerization

_____

Defense Date

_____
Dissertation Director
Kerney Jebrell Glover

_____

Approved Date

Committee Members:

_____
Robert Flowers, II

_____
Dmitri Vezenov

_____
Julia Koeppe

ACKNOWLEDGMENTS

TABLE OF CONTENTS

Chapter 2. Analysis of Caveolin-1 Oligomerization in DPC Micelles

Chaper 3. Evaluating Caveolin-1 Oligomerization in a Bilayer

LIST OF FIGURES

Chapter 1

Chapter 2

Chapter 3

xii

LIST OF APPENDICES

xv

LIST OF TABLES

LIST OF ABBREVIATIONS

DPC: Dodecylphosphocholine

LMPG: *lyso*-Myristoylphosphatidylglycerol

LMPC: *lyso*-Myristoylphosphatidylcholine

PFOA: Pentafluorooctanoic acid

HFIP: Hexafluoroisopropanol

AUC: Analytical Ultracentrifugation

SE: Sedimentation Equilibrium

HPLC: High Performance Liquid Chromatography

MALDI-TOF: Matrix-Assisted Laser Desorption/Ionization time-of-flight

DHPC: Dihexanoyl-glycero-phosphatidylcholine

DMPC: Dimyristoyl-glycero-phosphatidylcholine

Cav1: Caveolin-1

WT: wild type

IPA: Isopropanol

PCR: Polymerase Chain Reaction

LB: Luria-Bertani media

MDAG: minimal media supplemented with amino acids

KAN: Kanamycin

IPTG: Isopropyl β-D-1-thiogalactopyranoside

EDTA: Ethylenediaminetetraacetic acid

TAE: Tris-acetate EDTA buffer

DPH: 1,6-diphenyl-1,3,5-hexatriene

C8E5: pentaethylene glycol monooctyl ether (n-octylpentaoxyethylene)

NMR: Nuclear Magnetic Resonance Spectrometry

HSQC: Heteronuclear Single Quantum Coherence Spectroscopy

TROSY: Transverse Relaxation-Optimized Spectroscopy

ABSTRACT

Membrane proteins represent an important class of proteins that closely associate or reside within the plasma membrane of the cell. They play a multitude of roles in cell function such as signaling, trafficking, and recently discovered, scaffolding and shaping of the plasma membrane itself. For example, caveolin is a membrane protein that is believed to have the ability to curve the plasma membrane forming invaginations that serve as signaling platforms called caveolae. The curvature of the plasma membrane is believed to be a result of caveolin oligomerization. Caveolin oligomerization was characterized using sedimentation equilibrium analytical ultracentrifugation. Due to the extremely hydrophobic nature of caveolin it was necessary to explore different detergents and lipid systems that support membrane protein structure and function. Not all detergents are conducive to studies of membrane proteins and it is often necessary to determine empirically the best detergent / lipid mimic best suited for biophysical studies. One membrane mimic that has been well-characterized and used successfully to study membrane proteins are bicelles. Bicelles are discoidal phospholipid structures comprised of a long-chain and short-chain phospholipid, typically 1,2-dimyristoyl-*sn*-glycero-3-phosphocholine (DMPC) and 1,2-dihexanoyl-*sn*-glycero-3-phosphocholine (DHPC), respectively. Bicelles provide a true bilayer environment in which to study membrane protein structure and function. These lipid structures were successfully density matched using the method of sedimentation equilibrium in the analytical ultracentrifuge by adding 71.7% D_2O as a density modifier. We explored the utility of bicelles as a medium for studying membrane protein interactions in the analytical ultracentrifuge (AUC) by investigating the interactions of caveolin-1. The results of this work show that caveolin-1 does not have the capacity to

1

oligomerize in detergent micelles or in a bilayer environment (bicelles). On the other hand, a naturally-occuring breast cancer mutant, P132L, forms a strong dimer in detergent micelles. A close investigation of the mutant reveals that an extension of helix 2 in the intramembrane region of the protein where dimerization was shown to occur may play a key role in the dimerization of the mutant.

An alternative bicelle system was also investigated using pentaethylene glycol monooctyl ether (C_8E_5) instead of DHPC to form the rim of the bicelle. The C_8E_5 / DMPC lipid aggregates were density matched and their properties were characterized using ^{31}P-phosphorus NMR to assess the heterogeneity of the lipid / detergent arrangement, which confirms a bicellar-like arrangement. C_8E_5 has a density similar to water (1.007 g / mL) and was shown to form lipid aggregate structures with DMPC that are less dense and require significantly lower quantity of D_2O to density match in the AUC making them better suited to the study of membrane protein interactions of small peptides.

Chapter 1. Membrane Protein Biochemistry

INTRODUCTION

Membrane Proteins

Proteins are the foundation for all living organisms. These soluble macromolecules are very diverse in both structure and function. One special class of proteins called membrane proteins are encoded for in approximately one-third of most mammalian genomes. Though they are fewer in number compared to their soluble counterparts, their importance is not to be underestimated. Membrane proteins describe proteins that interact with the plasma membrane of cells; although, not all membrane proteins interact with the lipid bilayer of the plasma membrane in the same way. Membrane proteins can be divided into three broad classes: peripheral, integral, and lipid-anchored (Figure 1-1). Peripheral membrane proteins interact with the plasma membrane of cells superficially where only a small portion of the protein is in contact with the lipids of the bilayer. These proteins can typically be extracted using traditional biochemical techniques and are often soluble in aqueous buffers. Lipid-anchored proteins are soluble in aqueous buffers as well, and are only anchored to the plasma membrane through the covalent attachment of a lipid (i.e. palmitoylation) or a glycolipid (i.e. glycophosphatidylinositol (GPI-anchored)) (Figure 1-1). Integral membrane proteins are embedded in the lipid bilayer of the plasma membrane (Figure 1-1). The extent to which integral membrane proteins associate with the lipids varies. Integral membrane proteins are a particularly challenging group of proteins to study due to their extreme hydrophobicity. Their extreme hydrophobicity is due to the need to situate the majority of their polypeptide backbone in the hydrophobic side of the lipid bilayer. Examples of some of the most highly studied integral membrane proteins include bacteriorhodopsin

3

and G-protein coupled receptors. Because integral membrane proteins are so closely associated with the plasma membrane, their chemical properties highly differ from those of soluble proteins. The most distinguishing feature of membrane proteins is that they have a high fraction of non-polar amino acid residues. These non-polar residues impart a high degree of hydrophobicity to membrane proteins making them very challenging to study using traditional biochemical techniques. Biochemical and biophysical techniques such as analytical ultracentrifugation, solution NMR, and chromatography have been adapted to the study of these proteins, but it is often necessary to modify these techniques empirically to make them suitable to the study of new membrane proteins.

Membrane Associated / Peripheral

Integral Polytopic

Lipid Anchored
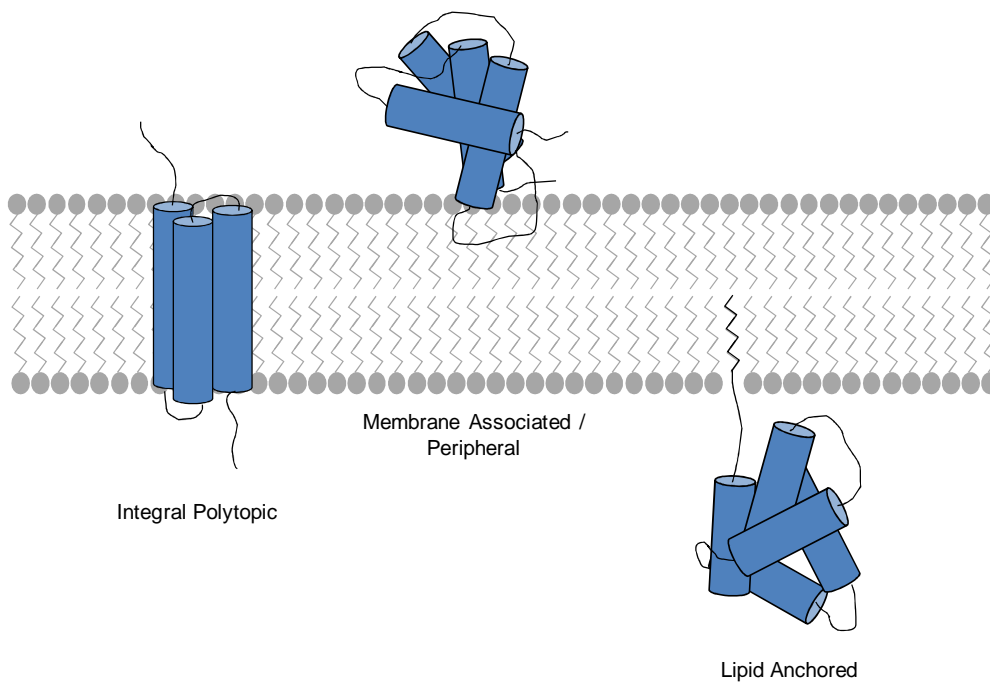
Figure 1-1. Schematic representation of three different classes of membrane proteins.

Detergents and Lipids are Used in Studies of Membrane Proteins

Membrane proteins reside in a lipid bilayer inside the plasma membrane. This lipid bilayer is crucial to the stability and integrity of membrane protein structure. In order to study membrane proteins, it is necessary to carry out these studies using a lipid-like environment so that the structure and behavior of the membrane protein under scrutiny is preserved. Detergents provide a powerful medium in which to study membrane proteins. These amphipathic molecules typically consist of a long hydrophobic carbon chain and highly hydrophilic headgroup (Figure 1-2a). When these molecules are exposed to water they spontaneously assemble into aggregates called micelles (Figure 1-2a). Micelles facilitate the dissolution of membrane proteins in aqueous buffers by enshrouding the hydrophobic portion of the membrane protein with the hydrophobic lipid tails thereby protecting it from the surrounding aqueous environment. Micelles are a powerful medium in which to study membrane protein structure and function; however, they can project undesirable properties onto proteins.

Detergents can either be non-ionic, cationic, anionic, or zwitterionic. Non-ionic detergents such as Triton X-100 are more mild and tend to be less denaturing than ionic detergents, although they are not always powerful enough to solubilize highly hydrophobic membrane proteins. Ionic detergents such as sodium dodecylsulfate (SDS), a powerful anionic detergent, can be used to solubilize membrane proteins, however, it is also highly denaturing (1). Zwitterionic detergents such as dodecylphosphocholine (DPC) and lyso-myristoylphosphatidylglycerol (LMPG) are powerful enough to solublize hydrophobic proteins, and they have been used with success in partial protein structure determination (2, 3). Other micellar systems employ the use of short-chain phospholipids such as dihexanoylphosphatidylcholine (DHPC), which have been successfully used in determination of membrane protein structure (4,

5). Clearly, micellar systems have been used successfully in the study of membrane protein structure and function. However, micellar systems must be used with caution when studying membrane proteins. They are highly curved structures which have the potential to influence elements of protein structure due to the high curvature. In some cases, protein structure can be altered enough that it can affect the activity of proteins, in particular, enzymes. The enzymatic activity of proteins can be affected by the nature of the detergent in which it resides (6). Lastly, although micelles have become an invaluable tool in which to study membrane proteins, they do not provide a true bilayer environment, which can complicate data interpretation under certain circumstances. Nonetheless, micellar systems have been used to obtain valuable information about membrane proteins (5).

In addition to micelles, two other systems that have been explored for the study of membrane proteins are vesicles and bicelles. Vesicles are often comprised of phospholipid molecules such as dimyristoylphosphatidylcholine (DMPC) which differ from detergent molecules in that they contain two fatty acid tails rather than one (Figure 1-2b). Phospholipid molecules are amphipathic and spontaneously form bilayers in an aqueous environment. When compared to micelles, vesicles are larger lipid aggregates that have a distinct cavity inside that is similar to a real cell. The inside cavity of vesicles is aqueous and membrane proteins can be incorporated into the bilayer region of vesicles (7). Vesicles are not equilibrium structures meaning that lipid molecules are not in flux with their vesicle counterpart. This can be undesirable when studying membrane protein interactions because the protein is not free to interact with other proteins.

To capture the bilayer feature of cells and maintain a dynamic system that supports protein interactions, bicelles have emerged as a powerful tool. Bicelles are discoidal lipid aggregates that are comprised of a long chain phospholipid like DMPC,

6

and short-chain phospholipid such as DHPC (Figure 1-2b). The size of bicelles can be tailored to different applications simply by adjusting the mole ratio, *q*, of the long chain lipid, DMPC, to that of the short chain lipid, DHPC. This ratio is also affected by the overall lipid concentration (c_L). In most applications, a *q* of 0.5 to 3.0 is used. The bilayer thickness can also be adjusted by changing the length of the long chain lipid that is used.

q = moles of DMPC / moles of DHPC
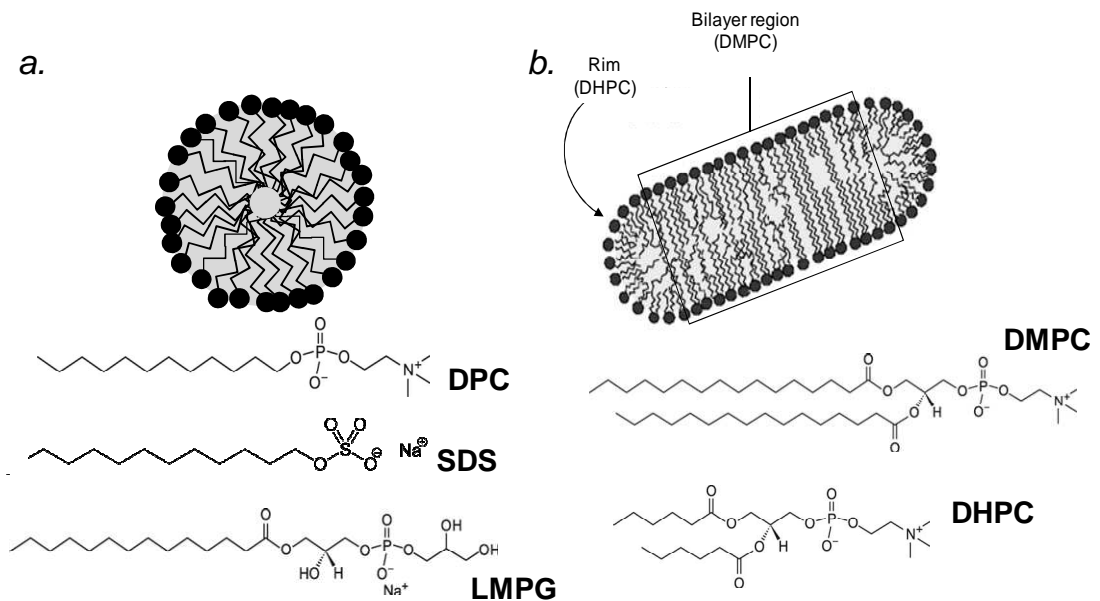
Figure 1-2. a) Schematic diagram of a micelle and common detergents that form them. DPC = dodecylphosphocholine, SDS = sodium dodecyl sulfate, LMPG = *lyso*-myristoylphosphatidylglycerol b) Schematic diagram of a bicelle and two common phospholipids that comprise bicelles.

Of the three different systems, bicelles share the advantages of micelles in that they are dynamic and allow proteins to freely associate thereby supporting any inherent protein interactions, yet they also provide a bilayer environment for the study membrane proteins, which is a more accurate reflection of the natural membrane environment of membrane proteins. Bicelles have been successfully used as a tool in which to study membrane protein structure (8). Their utility as a medium in which to study membrane protein interactions is only beginning to emerge. Traditionally, membrane protein interactions have been evaluated in micellar systems (9, 10, 11). While the information gleaned from these studies has been insightful, the uncertainty or inaccuracies inherently presented by a micelle system cannot be avoided. The use of bicelles as a means of studying membrane protein interactions in a true bilayer, this would eliminate the uncertainty or bias present in the use of micelles. The goal of the work presented in the following dissertation is to explore the utility of bicelles in the study of membrane protein interactions. Bicelles will be used to characterize the oligomeric behavior of the integral membrane protein, caveolin.

Caveolae and Caveolin

Caveolae (plural, caveola singular) are a feature of mammalian cells which have gained much attention over the last two decades. They are non-clathrin coated indentations of the plasma membrane that are approximately 50-100 nm in diameter and are found in many different cell types but are particularly abundant in smooth muscle cells, skeletal muscle cells, endothelial cells, fibroblasts and adipocytes (12). These flask-like structures consist of a myriad of proteins that work together to mediate the dynamic signaling and trafficking platforms that are the hallmark of caveolae (13, 14, 15, 16, 17, 18, 19, 20). Caveolin is a 21-24 kDa integral membrane protein that is central to caveolae formation. It is the single most abundant protein found in caveolae and when this protein is not present, caveolae are unable to form (13). Not only are caveolae unable to form when caveolin is not present, caveolae can also be introduced to lymphocytes, which normally do not express caveolin, by transforming these cells with the caveolin gene (21).

Three isoforms of caveolin have been identified; 1, 2, and 3, yet caveolin-1 is by far the most ubiquitous. Caveolin-2 is not as abundant as caveolin-1 and its role in caveolae formation is less understood; however, it does appear to associated very closely with caveolin-1. Caveolin-3 is most commonly found in smooth and skeletal muscle cells and it is not as ubiquitous as caveolin-1. Caveolin-3 is specific to skeletal muscle cells, cardiac myocytes, and smooth muscle cells (22, 23, 24, 25). Like caveolin-1, caveolin-3 is sufficient to support caveolae formation; when caveolin-3 is over-expressed in transgenic mice an increase in muscle cell caveolae is observed (26). All three caveolin isoforms show a high degree of sequence homology; however, caveolin-1 and -3 have the highest degree of homology (Figure 1-3). One distinguishing feature

9

between the three caveolin isoforms is that the soluble N-terminal region of each protein varies in length. The membrane interacting region of all three proteins, the portion of the protein that is predicted to be buried within the lipid bilayer of the plasma membrane, is highly conserved (Figure 1-3). This suggests that the intramembrane region is critical to the function of the protein and without it, caveolin does not function properly.

```
Caveolin-1 1    MSGGKYVDSE GHLYTVPIRE QGNIYKPNNK AMADELSEKQ 40
Caveolin-2 1               MGLETE KADVQLFMDD DSYSHHSGLE 26
Caveolin-3 1                  MMA EEHTDLEAQI 13

Caveolin-1 41   VYDAHTKEID LVNRDPKHLN DDVVKIDFED VIAEPEGTHS 80
Caveolin-2 27   YADPEKFADS DQDRDP-HRL NSHLKLGFED VIAEPVTTHS 66
Caveolin-3 14   VKDIHCKEID LVNRDPKNIN EDIVKVDFED VIAEPVGTYS 53

Caveolin-1 81   FDGIWKASFT TFTVTKYWFY RLLSALFGIP MALIWGIYFA 120
Caveolin-2 67   FDKVWICSHA LFEISKYVMY KFLTVFLAIP LAFIAGILFA 105
Caveolin-3 54   FDGVWKVSYT TFTVSKYWCY RLLSTLLGVP LALLWGFLFA 93

Caveolin-1 121  ILSFLHIWAV VPCIKSFLIE IQCISRVYSI YVHTVCDPLF 160
Caveolin-2 106  TLSCLHIWIL MPFVKTCLMV LPSVQTIWKS VTDVIIAPLC 145
Caveolin-3 94   CISFCHIWAV VPCIKSYLIE IQCISHIYSL CIRTFCNPLF 133

Caveolin-1 161  EAVGKIFSNV RINLQKEI 178
Caveolin-2 146  TSVGRCFSSV SLQLSQD  162
Caveolin-3 134  AALGQVCSSI KVVLRKEV 151
```

Figure 1-3. Sequence alignment of three caveolin isoforms 1, 2, 3. Dark gray highlights conserved amino acid residues. Light gray highlights similar amino acid residues.

Caveolin and Disease

Cancer

Many biological studies aimed at investigating changes in protein expression levels in abnormal cells have uncovered a link between changes in normal caveolin expression and the development and progression of different diseases. Caveolin expression levels are altered and mutations are found in diseases such as heart disease, Alzheimer's disease, muscular dystrophy, diabetes, and cancer (27, 28, 29, 30, 31). The exact role caveolin plays in the development of these diseases remains ambiguous, which further emphasizes the need for more studies to understand how caveolin is linked to these diseases.

Caveolae are intimately connected to cell signaling processes and it is possible that mutations to the caveolin protein or changes in the expression levels result in the disruption of key signaling events in the cell which can lead to various disease states. For example, mutations to caveolin and changes in expression levels have been linked to breast cancer recurrence and metastasis. One particular mutation that has been heavily investigated due to its strong association to breast cancer development is caveolin-1 P132L. This mutant is found in approximately 16% of breast cancers (32). In vivo the P132L mutant localizes to the Golgi apparatus, and it also acts as a dominant negative mutation whereby it leads to the retention of wild-type caveolin-1 when both are mutually expressed (27, 33). The retention of caveolin-1 P132L in the Golgi apparatus results in a loss of caveolae from the plasma membrane. The P132L mutant upregulates ERα receptor and this mutant is present in approximately 19% of ERα-positive breast cancers which is linked to aggressive breast carcinomas (27, 34). In addition to the P132L mutation, six other point mutations in caveolin were isolated from

11

breast cancer tissue, but P132L is by far the most commonly occurring mutant and the most studied due to its strong presence and association with breast cancer (34).

Alzheimer's Disease

Alterations in caveolin expression and function have been linked to other diseases as well including Alzhemier's disease. In senile plaques of Alzheimer's patients an upregulation of caveolin-3 was observed in the cells surrounding these plaques. Immunoprecipitation experiments reveal that caveolin-3 co-localizes with amyloid pre-cursor protein (APP) both in vivo and in vitro, and the over-expression of caveolin-3 in cultured cells stimulates β-secretase-mediated cleavage of APP. The product of β-secretase cleavage has direct implications for the development of Alzheimer's disease (35, 36).

Heart Disease

The tight regulation of caveolin-1 and -3 is also crucial to proper physiological heart function and deviations from controlled caveolin expression levels leads to cardiac myopathies. For example, when caveolin-3 levels were quantified from the cardiac myocytes of canines with heart disease, caveolin-3 levels were elevated (37). Caveolin-3 over-expression in transgenic mice show severe cardiac tissue degeneration, fibrosis, and impaired cardiac function and also leads to the down-regulation of nitric oxide synthase (29). Interestingly, a P104L mutant of caveolin-3 leads to impaired calcium channel function in skeletal muscle cells (38). This P104L mutant is arguably synonymous to the P132L mutant that was identified in caveolin-1.

Diabetes

Caveolin-1 expression has been linked to insulin signaling in diabetes. Insulin co-localizes within caveolae and has been shown to recruit caveolin-1 to plasma membrane (39, 40). In hyperglycemic rats, alveolar epithelial cells were found to contain a 1.3-fold

12

higher level of caveolae, which is accompanied by higher caveolin-1 expression levels, and when caveolin-null mice were evaluated significant increases in insulin resistance were observed along with impairment of glucose uptake by skeletal muscle cells in mice (41, 42). When the expression of this protein was restored in diabetic obese mice improvements to glucose metabolism followed (42, 43). Caveolin is an integral player in the maintenance of normal cell function and it is clear that mutations and alterations in expression levels can lead to the development and progression of disease.

Caveolin Structure

Caveolin has been described as possessing regions or domains based on its primary sequence analysis: An N-terminal domain, a scaffolding domain, a highly insoluble intramembrane domain, and a C-terminal domain. The N-terminal domain consists of mostly polar amino acid residues making this region extremely soluble (Figure 1-4). Following the N-terminal domain is a small region comprised of both polar and non-polar amino acids called the scaffolding domain (Figure 1-4). This region of the protein is very small compared to the other regions described in the caveolin protein.
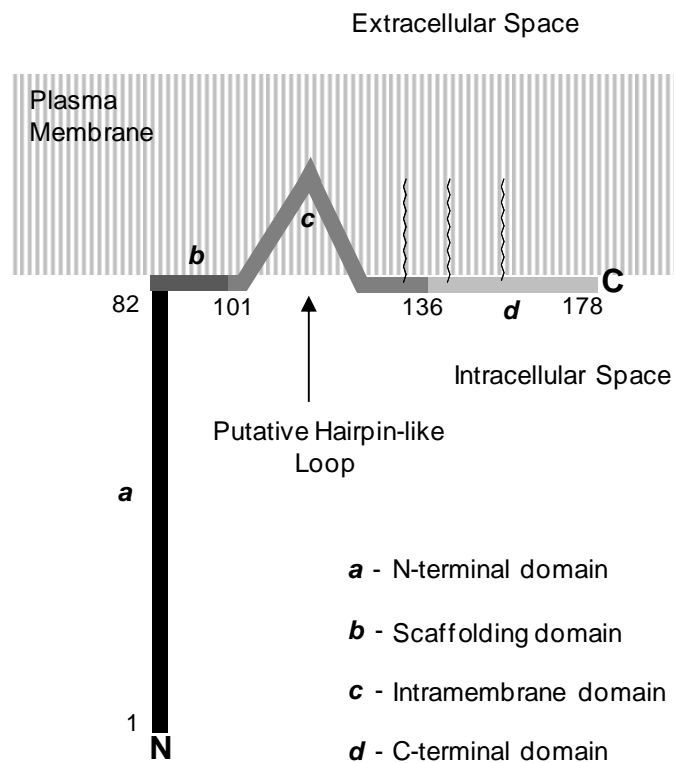
Figure 1-4. Schematic diagram of the proposed regions of the caveolin-1 protein.

Though it has been well-studied, its role remains ambiguous. It has been charged with binding caveolin to the plasma membrane, and it has been described as an oligomerization platform where many caveolin proteins come together to form a caveola (44, 45, 46, 47). Succeeding the scaffolding domain is a sequence of hydrophobic amino acids called the intramembrane domain which is proposed to be entirely situated in the plasma membrane (Figure 1-4). A careful analysis of the primary sequence of all three caveolin isoforms reveals that this region is comprised entirely of hydrophobic amino acid residues, which suggests that it is embedded almost entirely in the lipid bilayer of the plasma membrane. The C-terminal domain of caveolin is also comprised of polar and non-polar amino acids which are predicted to form an amphipathic helix that, like the scaffolding domain, also rests on the surface of the plasma membrane (Figure 1-4). This region has also been described as an attachment site for caveolin to the plasma membrane (45).

The intramembrane domain is a particularly intriguing region of the caveolin protein. Preliminary studies probing the location of the caveolin protein in cells revealed that the N- and C- termini lie on the same side of the plasma membrane (48, 49, 50). From these studies it can be inferred that caveolin forms a turn in the lipid bilayer of the plasma membrane. Also, a mechanism of caveolae curvature can be hypothesized: If caveolin only inserts partially into the plasma membrane, this creates an asymmetric displacement of the lipids on the inner leaflet of the membrane while pushing the lipids of the outer membrane leaflet closer together causing the membrane to curve (Figure 1-5). When multiple caveolin proteins come together, self-associate, or oligomerize, this event leads to the creation of the observed caveolar invaginations. It is not clear how many caveolin proteins associate to form a single caveola.

Extracellular Space

50-100 nm

Intracellular space
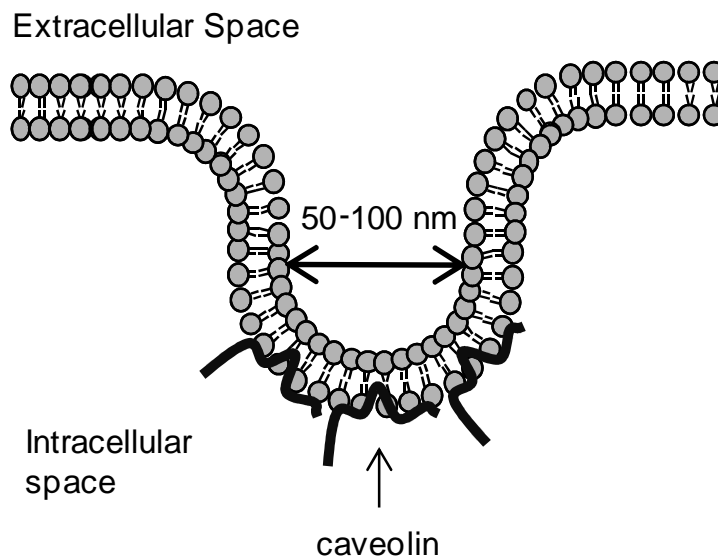
caveolin

Figure 1-5. Proposed mechanism of caveolin induced membrane curvature.

Caveolin Oligomerization

Studies of the caveolin protein are heavily aimed at investigating the effects of caveolin in cell signaling and its effect on organism pathology in animal models. Expression and knockout studies of the protein were employed to determine the effects of caveolin on caveolae formation, signaling, and animal physiology (51, 52, 53, 54, 55). The results of these studies demonstrate a clear causal relationship between impaired caveolin function and aberrant organism physiology. However, they are unable to address the exact role that caveolin plays in normal cellular function. Studies aimed at looking closely at the precise role of caveolin focused on isolating and characterizing the protein. Caveolin was first isolated from cells using a sucrose density gradient containing a mild detergent such as Triton X-100. Caveolin migrates with the Triton X-100 insoluble fraction. By isolating the Triton X-100 insoluble fractions from whole cell lysates, and using a combination of SDS-PAGE and western blot analysis to probe for the presence of caveolin, it was found that caveolin could be isolated in 200, 400, and 600 kD molecular weight complexes which were characterized by SDS-PAGE (47, 48, 56). Based on these findings it was concluded that caveolin self-assembles into high-order oligomers, which may drive the formation of caveolae. Although insightful, these studies do not account for the presence of other biomolecules in the large complexes because only the caveolin protein was probed for, and the role of other molecules cannot be accounted for. With this limitation in mind definitive conclusions about the oligomeric state of caveolin cannot be drawn.

In biology studies, caveolin has been isolated in large insoluble complexes from cells. Based on these studies, it was believed that caveolin oligomerizes to form the observed high molecular weight complexes leading to the creation of caveolae in cells. The full characterization of all molecules present in these complexes had not been

accomplished and isolating caveolin from these complexes was likely difficult due to the highly insoluble nature of the complexes. Further attempts to characterize the oligomeric state using biochemical methods have been limited to soluble pieces of the protein. For example, residues 1-62 do not have any oligomeric properties, yet residues 1-82 oligomerize into a heptameric complex (46). This data led to the conclusion that the scaffolding domain was responsible for the oligomerization of caveolin-1. However, in this study there were no detergents or lipid mimics present in this study the lack of which can lead to aggregation. Other studies suggest that the C-terminal domain may be responsible for the oligomerization (57). Definitely conclusions from this study are difficult to formulate because the C-terminal region of does not necessarily capture the true nature of caveolin.

The main objective of this work is to characterize the precise oligomeric state of caveolin using biophysical techniques. If caveolin forms high-order oligomers, then it is reasonable to believe that the intramembrane region plays a critical role. To explore this hypothesis current biophysical techniques were adapted to the study of membrane proteins. These studies are outlined in Chapters 2 through 5. Chapter 6 describes the expression and purification of membrane proteins from *E. coli* and the subsequent methods used to reconstitute these highly hydrophobic proteins into lipid bilayers.

Introduction to Analytical Ultracentrifugation

Analytical ultracentrifugation is a powerful tool that is used to study the hydrodynamic and thermodynamic properties of proteins. Two types of experiments can be executed to measure these parameters: sedimentation velocity and sedimentation equilibrium. The former can be used to determine the size and shape of proteins that are traveling down a solution column. The latter is used to measure protein interactions and determine stoichiometric ratios of hetero-interactions as well as oligomeric states. In the membrane protein field, sedimentation velocity experiments incur challenges when detergents are present. Protein size and shape can be heavily influenced when it is enshrouded in detergent and lipid molecules. The presence of lipid and detergent molecules can inflate the protein size and distort information about protein shape. Because of the bias introduced when working in a detergent or lipid system, sedimentation equilibrium experiments are much more useful in membrane protein studies because typically the oligomeric state of the protein is of interest. Sedimentation equilibrium experiments differ from velocity experiments, because instead of measuring the time it takes for a protein to travel down a solution column it measures the concentration profile created by a protein at equilibrium. In other words, the forces acting on the sedimenting protein, diffusion and gravity, are balanced by one another and the protein no longer moves down the solution column. The mathematical expression that has been derived to describe the equilibrium concentration profile of a protein is called the Lamm equation:

$$\frac{\ln(c_r)}{r^2} = \frac{M(1 - \bar{v}\rho)\omega^2}{2RT}$$

19

From the Lamm equation, the molecular weight of a protein, M, can be calculated by measuring its absorbance at 280 nm, which is directly related to the concentration of the protein, c, at a given radius from the center axis of rotation, r. The density of the solution, ρ, is known as well as the angular velocity, ω, which can be determined from the centrifugal force measured in revolutions per minute (rpm). The ideal gas constant, R, and the temperature, T, in Kelvin are also used to describe an ideally sedimenting species. Lastly, the partial specific volume of the protein, v, is determined from the method of Cohn and Edsall where the average of the sum of the partial specific volumes of each amino acid in the protein sequence is used to determine the overall partial specific volume of the protein (58). Sedimentation equilibrium is advantageous to other methods used to evaluate protein interactions, because it allows interactions to be observed in solution without modifications to the protein. With the advent of computers which can facilitate the processing of large quantities of data, analytical ultracentrifugation is becoming a powerful tool to characterize protein interactions. In particular, sedimentation equilibrium presents significant advantageous to study membrane protein interactions, because the bias introduced by the presence of detergents can be circumvented.

Membrane proteins are highly insoluble and spend their time interacting closely with the plasma membrane of cells. In order to study these types of proteins it is crucial to use a suitable membrane mimic that will both facilitate the solubility of these highly hydrophobic proteins in aqueous buffers and that will provide the same stability and support of the native plasma membrane. Detergents are employed because of their amphipathic properties, which is similar to the plasma membrane of cells. Detergents contain a hydrophilic carboxylate headgroup that is attached to a hydrocarbon tail resembling the phospholipids found in the native plasma membrane. They

spontaneously aggregate to form micelles, which are dynamic systems meaning that the lipid aggregate is in constant equilibrium with monomeric detergent molecules. This is ideal when studying membrane proteins because it supports native protein interactions. Sedimentation equilibrium is ideal for studying membrane proteins in detergent systems because the method of density matching can be employed to subtract away the molecular weight contribution of the lipid or detergent aggregate to the protein.

Most density matching studies that have been carried out employ the use of a detergent to analyze protein interactions. For example, studies of the anti-apoptotic membrane protein Bcl-xL were carried out dodecylphosphocholine (DPC) micelles. In this study, sedimentation equilibrium density matching experiments were carried out according to the method of Tanford and Reynolds (59). In this method it was determined that approximately 52.5% D_2O is necessary to successfully subtract out the molecular weight contribution of DPC to the Bcl-xL protein (60). Other studies have utilized detergents such as C_8E_5 and $C_{12}E_8$ as well to determine the oligomeric state of the protein, glycophorin A. In this study, no density modifier was required since the density of the detergents are approximately equal to the density of the buffer (61).

Not all detergents are suited to analytical ultracentrifugation studies. The most commonly used detergents like C_8E_5, $C_{12}E_8$, and DPC are unique in that the densities of these detergents is very close to that of water, approximately 1.0 cm^3 / g. As detergents deviate further from the density of water, it is necessary to use larger quanitites of density modifiers such as D_2O, glycerol, and sucrose. It is possible for the density of the detergent to exceed the density of 100% D_2O (greater than 1.10 g / cm^3) in which case it may be necessary to use heavier isotopes of water such as D_2O^{18}. DPC micelles are often used in analytical ultracentrifugation for two reasons: DPC is powerful enough to reconstitute highly hydrophobic proteins, and DPC is often used in NMR studies where

21

protein structures have been accurately solved (62, 63). Because DPC is often used in

structural studies of proteins it has the ability to preserve important structural features of

proteins.

REFERENCES

1. Otzen, D. E. (2002) Protein Unfolding in Detergents: Effect of Micelle Structure, Ionic Strength, pH, and Temperature. *Biophys. J. 83*, 2219-2230.

2. Lee, J., and Glover, K. J. (2012) The Transmembrane Domain of Caveolin-1 Exibits a Helix-Break-Helix Structure. *Biochim Biophys Acta. 1818*, 1158-1164.

3. Neumoin, A., Arshava, B., Becker, J., Zerbe, O., and Naider, F. (2007) NMR Studies in Dodecylphosphocholine of a Fragment Containing the Seventh Transmembrane Helix of a G-Protein-Coupled Receptor from Saccharomyces Cerevisiae. *Biophys. J. 93*, 467-482.

4. Fernandez, C., Hilty, C., Wider, G., Guntert, P., and Wuthrich, K. (2004) NMR Structure of the Integral Membrane Protein OmpX. *J. Mol. Biol. 336*, 1211-1221.

5. Fernandez, C., and Wuthrich, K. (2003) NMR Solution Structure Determination of Membrane Proteins Reconstituted in Detergent Micelles. *FEBS Lett. 555*, 144-150.

6. Kronenburga, N. A., and de Bont, J. A. (2001) Effects of Detergents on Specific Activity and Enantioselectivity of the Epoxide Hydrolase from Rhodotorula Glutinis. *Enzyme Microb. Technol. 28*, 210-217.

7. Dewald, A. H., Hodges, J. C., and Columbus, L. (2011) Physical Determinants of Beta-Barrel Membrane Protein Folding in Lipid Vesicles. *Biophys. J. 100*, 2131-2140.

8. Mahalakshmi, R., Franzin, C. M., Choi, J., and Marassi, F. M. (2007) NMR Structural Studies of the Bacterial Outer Membrane Protein OmpX in Oriented Lipid Bilayer Membranes. *Biochim. Biophys. Acta. 1768*, 3216-3224.

9. Fleming, K. G., Ren, C. C., Doura, A. K., Eisley, M. E., Kobus, F. J., and Stanley, A. M. (2004) Thermodynamics of Glycophorin A Transmembrane Helix Dimerization in C14 Betaine Micelles. *Biophys. Chem. 108*, 43-49.

10. Noy, D., Calhoun, J. R., and Lear, J. D. (2003) Direct Analysis of Protein Sedimentation Equilibrium in Detergent Solutions without Density Matching. *Anal. Biochem. 320*, 185-192.

11. Losonczi, J. A., Olejniczak, E. T., Betz, S. F., Harlan, J. E., Mack, J., and Fesik, S. W. (2000) NMR Studies of the Anti-Apoptotic Protein Bcl-xL in Micelles. *Biochemistry. 39*, 11024-11033.

12. Razani, B., Woodman, S. E., and Lisanti, M. P. (2002) Caveolae: From Cell Biology to Animal Physiology. *Pharmacol. Rev. 54*, 431-467.

13. Lisanti, M. P., and Williams, T. M. (2004) The Caveolin Genes: From Biology to Medicine. *Ann Med. 36*, 584-595.

14. Thorn, H., Stenkula, K. G., Karlsson, M., Ortegren, U., Nystrom, F. H., Gustavsson, J., and Stralfors, P. (2003) Cell Surface Orifices of Caveolae and Localization of Caveolin to the Necks of Caveolae in Adipocytes. *Mol. Biol. Cell. 14*, 3967-3976.

15. Spisni, E., Tomasi, V., Cestaro, A., and Tosatto, S. C. (2005) Structural Insights into the Function of Human Caveolin 1. *Biochem. Biophys. Res. Commun. 338*, 1383-1390.

16. Luoma, J. I., Boulware, M. I., and Mermelstein, P. G. (2008) Caveolin Proteins and Estrogen Signaling in the Brain. *Mol. Cell. Endocrinol. 290*, 8-13.

17. Awasthi, V., Mandal, S. K., Papanna, V., Rao, L. V. M., and Pendurthi, U. R. (2007) Modulation of Tissue Factor-Factor VIIa Signaling by Lipid Rafts and Caveolae. *Arterioscler Thromb Vasc Biol. 27*, 1447-1455.

18. Balijepalli, R. C., Foell, J. D., Hall, D. D., Hell, J. W., and Kamp, T. J. (2006) Localization of Cardiac L-Type Ca2+ Channels to a Caveolar Macromolecular Signaling Complex is Required for Beta(2)-Adrenergic Regulation. *Proc Natl Acad Sci U S A. 103*, 7500-7505.

19. Bauer, P. M., Wertz, J. W., and Billiar, T. R. (2006) Reciprocal Regulation of Caveolin-1 Expression and Bone Morphogenetic Protein Signaling in Mouse Aortic Smooth Muscle Cells. *Circulation. 114*, 179-179.

20. Weerth, S. H., Holtzclaw, L. A., and Russell, J. T. (2007) Signaling Proteins in Raft-Like Microdomains are Essential for Ca2+ Wave Propagation in Glial Cells. *Cell Calcium. 41*, 155-167.

21. Fra, A. M., Williamson, E., Simons, K., and Parton, R. G. (1995) De Novo Formation of Caveolae in Lymphocytes by Expression of VIP21-Caveolin. *Proc. Natl. Acad. Sci. U. S. A. 92*, 8655-8659.

22. Kaakinen, M., Kaisto, T., Rahkila, P., and Metsikko, K. (2012) Caveolin 3, Flotillin 1 and Influenza Virus Hemagglutinin Reside in Distinct Domains on the Sarcolemma of Skeletal Myofibers. *Biochem. Res. Int. 2012*, 497572.

23. Parton, R. G., Hanzal-Bayer, M., and Hancock, J. F. (2006) Biogenesis of Caveolae: A Structural Model for Caveolin-Induced Domain Formation. *J. Cell. Sci. 119*, 787-796.

24. Song, K. S., Scherer, P. E., Tang, Z. L., Okamoto, T., Li, S. W., Chafel, M., Chu, C., Kohtz, D. S., and Lisanti, M. P. (1996) Expression of Caveolin-3 in Skeletal, Cardiac, and Smooth Muscle Cells - Caveolin-3 is a Component of the Sarcolemma and Co-Fractionates with Dystrophin and Dystrophin-Associated Glycoproteins. *J. Biol. Chem. 271*, 15160-15165.

25. Tang, Z. L., Scherer, P. E., Okamoto, T., Song, K., Chu, C., Kohtz, D. S., Nishimoto, I., Lodish, H. F., and Lisanti, M. P. (1996) Molecular Cloning of Caveolin-3, a Novel Member of the Caveolin Gene Family Expressed Predominantly in Muscle. *J. Biol. Chem. 271*, 2255-2261.

26. Galbiati, F., Volonte, D., Chu, J. B., Li, M., Fine, S. W., Fu, M., Bermudez, J., Pedemonte, M., Weidenheim, K. M., Pestell, R. G., Minetti, C., and Lisanti, M. P. (2000) Transgenic Overexpression of Caveolin-3 in Skeletal Muscle Fibers Induces a Duchenne-Like Muscular Dystrophy Phenotype. *Proc Natl Acad Sci U S A. 97*, 9689-94.

27. Bonuccelli, G., Casimiro, M. C., Sotgia, F., Wang, C., Liu, M., Katiyar, S., Zhou, J., Dew, E., Capozza, F., Daumer, K. M., Minetti, C., Milliman, J. N., Alpy, F., Rio, M. C., Tomasetto, C., Mercier, I., Flomenberg, N., Frank, P. G., Pestell, R. G., and Lisanti, M. P. (2009) Caveolin-1 (P132L), a Common Breast Cancer Mutation, Confers Mammary Cell Invasiveness and Defines a Novel Stem cell/metastasis-Associated Gene Signature. *Am. J. Pathol. 174*, 1650-1662.

28. Gaudreault, S. B., Dea, D., and Poirier, J. (2004) Increased Caveolin-1 Expression in Alzheimer's Disease Brain. *Neurobiol. Aging. 25*, 753-759.

29. Aravamudan, B., Volonte, D., Ramani, R., Gursoy, E., Lisanti, M. P., London, B., and Galbiati, F. (2003) Transgenic Overexpression of Caveolin-3 in the Heart Induces a Cardiomyopathic Phenotype. *Hum. Mol. Genet. 12*, 2777-2788.

30. Karam, J. A., Lotan, Y., Roehrborn, C. G., Ashfaq, R., Karakiewicz, P. I., and Shariat, S. F. (2007) Caveolin-1 Overexpression is Associated with Aggressive Prostate Cancer Recurrence. *Prostate. 67*, 614-622.

31. McNally, E. M., Moreira, E. D., Duggan, D. J., Lisanti, M. P., Lidov, H. G. W., Vainzof, M., Bonnemann, C. G., Passos-Bueno, M. R., Hoffman, E. P., Zatz, M., and Kunkel, L. M. (1998) Caveolin-3 in Muscular Dystrophy. *Hum. Mol. Genet. 7*, 871-877.

32. Hayashi, K., Matsuda, S., Machida, K., Yamamoto, T., Fukuda, Y., Nimura, Y., Hayakawa, T., and Hamaguchi, M. (2001) Invasion Activating Caveolin-1 Mutation in Human Scirrhous Breast Cancers. *Cancer Res. 61*, 2361-2364.

33. Lee, H., Park, D. S., Razani, B., Russell, R. G., Pestell, R. G., and Lisanti, M. P. (2002) Caveolin-1 Mutations (P132L and Null) and the Pathogenesis of Breast Cancer - Caveolin-1 (P132L) Behaves in a Dominant-Negative Manner and Caveolin-1 (-/-) Null Mice show Mammary Epithelial Cell Hyperplasia. *Am. J. Pathol. 161*, 1357-1369.

34. Li, T., Sotgia, F., Vuolo, M. A., Li, M., Yang, W. C., Pestell, R. G., Sparano, J. A., and Lisanti, M. P. (2006) Caveolin-1 Mutations in Human Breast Cancer: Functional Association with Estrogen Receptor Alpha-Positive Status. *Am. J. Pathol. 168*, 1998-2013.

35. Nishiyama, K., Trapp, B. D., Ikezu, T., Ransohoff, R. M., Tomita, T., Iwatsubo, T., Kanazawa, I., Hsiao, K. K., Lisanti, M. P., and Okamoto, T. (1999) Caveolin-3 Upregulation Activates Beta-Secretase-Mediated Cleavage of the Amyloid Precursor Protein in Alzheimer's Disease. *J. Neurosci. 19*, 6538-6548.

36. Schenk, D., Barbour, R., Dunn, W., Gordon, G., Grajeda, H., Guido, T., Hu, K., Huang, J., Johnson-Wood, K., Khan, K., Kholodenko, D., Lee, M., Liao, Z., Lieberburg, I., Motter, R., Mutter, L., Soriano, F., Shopp, G., Vasquez, N., Vandevert, C., Walker, S., Wogulis, M., Yednock, T., Games, D., and Seubert, P. (1999) Immunization with

Amyloid-Beta Attenuates Alzheimer-Disease-Like Pathology in the PDAPP Mouse. *Nature. 400*, 173-177.

37. Hare, J. M., Lofthouse, R. A., Juang, G. J., Colman, L., Ricker, K. M., Kim, B., Senzaki, H., Cao, S., Tunin, R. S., and Kass, D. A. (2000) Contribution of Caveolin Protein Abundance to Augmented Nitric Oxide Signaling in Conscious Dogs with Pacing-Induced Heart Failure. *Circ. Res. 86*, 1085-1092.

38. Couchoux, H., Allard, B., Legrand, C., Jacquemond, V., and Berthier, C. (2007) Loss of Caveolin-3 Induced by the Dystrophy-Associated P104L Mutation Impairs L-Type Calcium Channel Function in Mouse Skeletal Muscle Cells. *J. Physiol. (London). 580*, 745-754.

39. Gustavsson, J., Parpal, S., Karlsson, M., Ramsing, C., Thorn, H., Borg, M., Lindroth, M., Peterson, K. H., Magnusson, K. E., and Stralfors, P. (1999) Localization of the Insulin Receptor in Caveolae of Adipocyte Plasma Membrane. *FASEB J. 13*, 1961-1971.

40. Wang, H., Wang, A. X., Liu, Z., Chai, W., and Barrett, E. J. (2009) The trafficking/interaction of eNOS and Caveolin-1 Induced by Insulin Modulates Endothelial Nitric Oxide Production. *Mol. Endocrinol. 23*, 1613-1623.

41. Pascariu, M., Bendayan, M., and Ghitescu, L. (2004) Correlated Endothelial Caveolin Overexpression and Increased Transcytosis in Experimental Diabetes. *J. Histochem. Cytochem. 52*, 65-76.

42. Oshikawa, J., Otsu, K., Toya, Y., Tsunematsu, T., Hankins, R., Kawabe, J., Minamisawa, S., Umemura, S., Hagiwara, Y., and Ishikawa, Y. (2004) Insulin Resistance in Skeletal Muscles of Caveolin-3-Null Mice. *Proc. Natl. Acad. Sci. U. S. A. 101*, 12670-12675.

43. Otsu, K., Toya, Y., Oshikawa, J., Sakata, M., Yazawa, T., Okumura, S., Sato, M., Umemura, S., Minamisawa, S., and Ishikawa, Y. (2007) Caveolin Improves Glucose Metabolism in Diabetic Mice. *Am J Physiol Cell Physiol. 21*, C450-C456.

44. Schlegel, A., Schwab, R. B., Scherer, P. E., and Lisanti, M. P. (1999) A Role for the Caveolin Scaffolding Domain in Mediating the Membrane Attachment of Caveolin-1 - the Caveolin Scaffolding Domain is both Necessary and Sufficient for Membrane Binding in Vitro. *J. Biol. Chem. 274*, 22660-22667.

45. Schlegel, A., and Lisanti, M. P. (2000) A Molecular Dissection of Caveolin-1 Membrane Attachment and Oligomerization - Two Separate Regions of the Caveolin-1 C-Terminal Domain Mediate Membrane Binding and oligomer/oligomer Interactions in Vivo. *J. Biol. Chem. 275*, 21605-21617.

46. Fernandez, I., Ying, Y., Albanesi, J., and Anderson, R. G. (2002) Mechanism of Caveolin Filament Assembly. *Proc. Natl. Acad. Sci. U. S. A. 99*, 11193-11198.

47. Sargiacomo, M., Scherer, P. E., Tang, Z., Kubler, E., Song, K. S., Sanders, M. C., and Lisanti, M. P. (1995) Oligomeric Structure of Caveolin: Implications for Caveolae Membrane Organization. *Proc. Natl. Acad. Sci. U. S. A. 92*, 9407-9411.

48. Monier, S., Parton, R. G., Vogel, F., Behlke, J., Henske, A., and Kurzchalia, T. V. (1995) VIP21-Caveolin, a Membrane Protein Constituent of the Caveolar Coat, Oligomerizes in Vivo and in Vitro. *Mol. Biol. Cell. 6*, 911-927.

49. Dupree, P., Parton, R. G., Raposo, G., Kurzchalia, T. V., and Simons, K. (1993) Caveolae and Sorting in the Trans-Golgi Network of Epithelial Cells. *EMBO J. 12*, 1597-1605.

50. Scherer, P. E., Tang, Z. L., Chun, M. Y., Sargiacomo, M., Lodish, H. F., and Lisanti, M. P. (1995) Caveolin Isoforms Differ in their N-Terminal Protein-Sequence and Subcellular-Distribution - Identification and Epitope Mapping of an Isoform-Specific Monoclonal-Antibody Probe. *J. Biol. Chem. 270*, 16395-16401.

51. Gaudreault, S. B., Dea, D., and Poirier, J. (2004) Increased Caveolin-1 Expression in Alzheimer's Disease Brain. *Neurobiol Aging. 25*, 753-9.

52. Zhao, Y. Y., Liu, Y., Stan, R. V., Fan, L., Gu, Y., Dalton, N., Chu, P. H., Peterson, K., Ross, J.,Jr, and Chien, K. R. (2002) Defects in Caveolin-1 Cause Dilated Cardiomyopathy and Pulmonary Hypertension in Knockout Mice. *Proc. Natl. Acad. Sci. U. S. A. 99*, 11375-11380.

53. Patel, H. H., Zhang, S., Murray, F., Suda, R. Y., Head, B. P., Yokoyama, U., Swaney, J. S., Niesman, I. R., Schermuly, R. T., Pullamsetti, S. S., Thistlethwaite, P. A., Miyanohara, A., Farquhar, M. G., Yuan, J. X., and Insel, P. A. (2007) Increased Smooth Muscle Cell Expression of Caveolin-1 and Caveolae Contribute to the Pathophysiology of Idiopathic Pulmonary Arterial Hypertension. *FASEB J. 21*, 2970-2979.

54. El-Yazbi, A. F., Cho, W. J., Schulz, R., and Daniel, E. E. (2006) Caveolin-1 Knockout Alters Beta-Adrenoceptors Function in Mouse Small Intestine. *Am J Physiol Gastrointest Liver Physiol. 291*, G1020-G1030.

55. Capozza, F., Combs, T. P., Cohen, A. W., Cho, Y. R., Park, S. Y., Schubert, W., Williams, T. M., Brasaemle, D. L., Jelicks, L. A., Scherer, P. E., Kim, J. K., and Lisanti, M. P. (2005) Caveolin-3 Knockout Mice show Increased Adiposity and Whole Body Insulin Resistance, with Ligand-Induced Insulin Receptor Instability in Skeletal Muscle. *American Journal of Physiology-Cell Physiology. 288*, C1317-C1331.

56. Kurzchalia, T. V., Dupree, P., Parton, R. G., Kellner, R., Virta, H., Lehnert, M., and Simons, K. (1992) VIP21, a 21-kD Membrane Protein is an Integral Component of Trans-Golgi-Network-Derived Transport Vesicles. *J. Cell Biol. 118*, 1003-1014.

57. Schlegel, A., and Lisanti, M. P. (2000) A Molecular Dissection of Caveolin-1 Membrane Attachment and Oligomerization. Two Separate Regions of the Caveolin-1 C-Terminal Domain Mediate Membrane Binding and oligomer/oligomer Interactions in Vivo. *J. Biol. Chem. 275*, 21605-21617.

58. Cohn E.J. & Edsall J.J. (1943) *Proteins, Amino Acids, and Peptides as Ions and Dipolar Ions.* , 375.

59. Tanford, C., and Reynolds, J. A. (1976) Characterization of Membrane Proteins in Detergent Solutions. *Biochim Biophys Acta. 457*, 133-70.

60. Losonczi, J. A., Olejniczak, E. T., Betz, S. F., Harlan, J. E., Mack, J., and Fesik, S. W. (2000) NMR Studies of the Anti-Apoptotic Protein Bcl-xL in Micelles. *Biochemistry. 39*, 11024-11033.

61. Fleming, K. G., Ackerman, A. L., and Engelman, D. M. (1997) The Effect of Point Mutations on the Free Energy of Transmembrane Alpha-Helix Dimerization. *J Mol Biol. 272*, 266-75.

62. Arora, A., Abildgaard, F., Bushweller, J. H., and Tamm, L. K. (2001) Structure of Outer Membrane Protein A Transmembrane Domain by NMR Spectroscopy. *Nat. Struct. Biol. 8*, 334-8.

63. Tamm, L. K., Abildgaard, F., Arora, A., Blad, H., and Bushweller, J. H. (2003) Structure, Dynamics and Function of the Outer Membrane Protein A (OmpA) and Influenza Hemagglutinin Fusion Domain in Detergent Micelles by Solution NMR. *FEBS Lett. 555*, 139-143.

Chapter 2. Analysis of Caveolin-1 Oligomerization in DPC Micelles

ABSTRACT

Caveolin-1 is the most important protein found in caveolae, which are cell surface invaginations of the plasma membrane that act as signaling platforms. A single point mutation in the transmembrane domain of caveolin-1 (proline 132 to leucine) has deleterious effects on caveolae formation in vivo, and has been implicated in various disease states, particularly aggressive breast cancers. Using a combination of gel filtration chromatography and analytical ultracentrifugation we found that a fully-functional construct of caveolin-1 (Cav1(62–178)) was a monomer in dodecylphosphocholine micelles. In contrast, the P132L mutant of Cav1(62–178) was dimeric. To explore the dimerization of the P132L mutant further, various truncated constructs (Cav1(82–178), Cav1(96–178), Cav1(62–136), Cav1(82–136), Cav1(96–136)) were prepared which revealed that oligomerization occurs in the transmembrane domain (residues 96–136) of caveolin-1. To characterize the mutant structurally, solution-state NMR experiments in *lyso*-myristoylphosphatidylglycerol were undertaken of the Cav1(96–136) P132L mutant. Chemical shift analysis revealed that compared to the wild type, helix 2 in the transmembrane domain was lengthened by four residues (wild type, residues 111 to 129; mutant, residues 111–133), which corresponds to an extra turn in helix 2 of the mutant. Lastly, point mutations at position 132 of Cav1(62–178) (P132A, P132I, P132V, P132G, P132W, P132F) revealed that no other hydrophobic amino acid can preserve the monomeric state of Cav1(62-178) which indicates that proline 132 is critical in supporting proper caveolin-1 behavior.

INTRODUCTION

Caveolae are a feature of mammalian cells which have been the subject of heavy investigation over the last two decades. They are non-clathrin coated indentations of the plasma membrane that are approximately 50-100 nm in diameter and they are intimately involved in molecular trafficking (1). Caveolae are highly ubiquitous and they can be found in most differentiated cell types ranging from smooth muscle cells to adipocytes. They are particularly abundant in adipocytes where they shuttle lipids and other signaling molecules across the plasma membrane (2, 3). Aside from lipid transport caveolae are also involved in calcium signaling and cell-cell communication (4, 5, 6, 7, 8, 9). Caveolae are comprised of a myriad of proteins and other biomolecules, and they are enriched with cholesterol and sphingolipids, which makes their composition unique from the bulk plasma membrane (10, 11). Although they have been compared to lipid rafts, caveolae are unique and often differentiated from lipid rafts by their ability to endocytose into cells. One of the first studies investigating mechanisms of caveolae transport uncovered the presence of one particularly abundant protein which became known as caveolin (12). Caveolin is the most important protein found in caveolae and it is vital to the creation of caveolae. When caveolin expression is silenced, caveolae are completely abolished from the surface of cells (13, 14). Caveolae can also be induced *de novo* in lymphocytes when non-native caveolin expression is introduced, which suggests that caveolin is necessary and sufficient for the formation of caveolae (15). Three isoforms of caveolin have been identified: 1, 2, 3, yet caveolin-1 is by far the most ubiquitous and it, alone, is sufficient to form caveolae. Caveolin-2 is not as abundant as caveolin-1 and its role in caveolae formation is much less understood than caveolin-1, though, it has been suggested that both isoforms hetero-oligomerize. Caveolin-3 is commonly referred to as "muscle specific" caveolin and it is found in high abundance in

30

skeletal muscle cells (14). All three caveolin isoforms show a high degree of sequence homology with caveolin-1 and -3 having the highest degree of homology. The soluble region of each caveolin protein varies in length; however, the membrane interacting regions of all three proteins are highly conserved.

Caveolin oligomerization is thought to contribute to caveolae formation by inducing and stabilizing the curvature of the plasma membrane. When isolated in vivo from a sucrose density gradient containing a mild detergent like Triton X-100 caveolin migrates with the Triton X-100 insoluble material. By isolating the Triton X-100 insoluble fractions from whole cell lysates, and using a combination of SDS-PAGE and western blot analysis to probe for the presence of caveolin, it was found that caveolin could be isolated in 200, 400, and 600 kD molecular weight complexes by SDS-PAGE (16). Chemical cross-linking studies further reveal that caveolin self-associates into dimers, trimers and tetramers in addition to the high-molecular weight complexes that were previously observed (16). From these results it is believed that the extreme curvature of caveolae may be a direct consequence of high-order homo-oligomer formation of caveolin. Furthermore, the membrane curvature is thought to be stabilized by these large caveolin complexes. The precise characterization of the oligomeric state of caveolin in these complexes is difficult to achieve because it is unclear if other biomolecules are present. Attempts to characterize the oligomeric state using biophysical methods have focused on soluble pieces of the protein. For example, residues 1-62 do not have any oligomeric properties, yet residues 1-82 oligomerize into a heptameric complex (17). This data led to the conclusion that residues 82-101, also called the "scaffolding domain", were responsible for the oligomerization of caveolin-1. Other studies suggest that the C-terminal region of the protein contains elements involved in oligomerization as well. When a GST fusion of the C-terminal domain of

31

caveolin-1 (residues 135-178) was co-expressed with the full-length protein, the C-terminal domain co-immunoprecipitates, indicating that it may bind to or oligomerize with the full-length caveolin protein. Based on the results of this study, the C-terminal region of caveolin-1 influences oligomerization (18). Although work in the area of caveolin-1 oligomerization has offered useful insight into caveolin behavior, a direct and precise characterization of caveolin oligomerization is lacking which leaves the answer to this question ambiguous and unclear. The goal of this study is to characterize the homo-oligomeric interaction of caveolin-1 in a biologically relevant medium using a combination of gel filtration chromatography and sedimentation equilibrium analytical ultracentrifugation. Further, the goal is to assess the strength of the observed interactions from the data.

Caveolin has been closely linked to a number of disease states including heart disease, Alzheimer's, and cancer. A naturally occurring point mutation (P132L) in the caveolin-1 gene is present in approximately 16% of breast cancers, and has been closely linked to increased recurrence and metastasis (19, 20). In addition, this mutant appears to be functionally different from the wild-type as it is retained in the Golgi apparatus of cells and does not get transported to its final destination in the plasma membrane resulting in the elimination of caveolae from the surface of cells (21). Interestingly, the P132L mutant appears to behave in a dominant negative manner: When both the P132L mutant and wild-type caveolin are co-expressed, both become localized to the Golgi, which is a fate common to misfolded proteins (21). Furthermore, a study by Bonuccelli et al demonstrates that when caveolin-1 P132L is expressed in Met-1 cells, it acts as a loss-of-function mutation and promotes recurrence of breast cancer (19). The second goal of this study is characterize the oligomeric state of the caveolin-1 P132L mutant and determine if the wild-type and mutants show differences in

their behavior at the atomic level.

MATERIALS AND METHODS

Protein Expression and Purification

The DNA for Cav1(62-178) was synthesized by Genscript Corporation (Piscataway, NJ). Caveolin-1 has three sites of cysteine palmitoylation (C133, C143, C156) that have been shown to be nonessential for proper caveolin-1 folding and trafficking (22, 23, 24). Therefore, each cysteine was mutated to serine to avoid unwanted and biologically irrelevant disulfide bonding. The Cav1(62-178) gene was cloned, over-expressed, and purified as described in Diefenderfer et al (25). After HPLC purification, 30 mg of dried Cav1(62-178) was dissolved in 3 mL of hexafluoroisopropanol followed by the addition of 7 mL of deionized water. The solution was flash frozen and lyophilized. MALDI-TOF analysis confirmed the identity of the final protein product. Truncated and mutant constructs were prepared using the same procedure described above. The truncated wild-type and P132L mutant constructs prepared were residues: 82-178, 82-136, 96-178, 96-136, 62-136. The mutant constructs prepared were Cav1(62-178): P132L, P132A, P132G, P132W, P132F, P132V, P132I.

Gel Filtration Chromatography

To 0.8 mg of lyophilized Cav1(62-178), 1.0 mL of buffer (20 mM HEPES pH 7.4, 150 mM NaCl, and 50 mM DPC (Anatrace, Maumee, OH)) was added followed by three minutes of vigorous vortexing. Next, the resultant clear solution was filtered through a 0.2 µm spin filter and injected onto a Sephacryl-300HR 16/60 column (GE Healthcare, Piscataway, NJ) equilibrated with buffer (20 mM HEPES pH = 7.4, 150 mM NaCl and 5 mM DPC). The column was calibrated using alcohol dehydrogenase, carbonic anhydrase, α-amylase, bovine serum albumin, and cytochrome c oxidase, and the elution profile was monitored at 280 nm. All truncated and mutant constructs were run in an identical fashion.

34

Analytical Ultracentrifugation

0.8 mg of lyophilized Cav1(62-178) was reconstituted into a density-matched buffer comprised of 20 mM HEPES pH 7.4, 100 mM NaCl, 50 mM DPC and 52.5 % (v/v) D_2O. DPC micelles were matched using a D_2O concentration of 52.5% (v/v) in a solution of 20 mM HEPES 100 mMNaCl pH = 7.4 (26). Each protein sample was prepared at three concentrations (30 µM, 15 µM, and 7.5 µM), and verified using the BCA Assay (Pierce Protein Research Products, Rockford IL). The samples were loaded into a six-sector charcoal-filled epon centerpiece (path length 1.2 cm) using the DPC buffer solution above without protein as the reference solution. The volume of sample per sector was 120 µL. The cells were loaded in a Beckman Ti-60 4-hole rotor. Equilibrium absorbance measurements were taken at three speeds, and the data were analyzed by global nonlinear least squares fitting using the computer program "HeteroAnalysis Version 1.1.0.44 - beta" (University of Connecticut) (27). Cav1(62-178) was fit to the ideal model to obtain the weight-averaged molecular weight of the protein. During fits, all parameters (molecular weight, baseline, and reference concentration) were allowed to float. The partial specific volume of the protein (0.7603 mL/g) was calculated using established methodology (28). The density of the buffer (1.0592 g/mL) was determined using a Kyoto Electronics Density/Specific Gravity Meter (model #DA-210). Mutant Cav1(62-178)_P132L was fit to a monomer-nmer model (where n was fixed to a value of 2). During fits, all parameters (molecular weight, baseline, and reference concentration) were allowed to float. The partial specific volumes of the proteins (0.7603 mL/g wild-type, 0.7615 mL/g mutant) were calculated using established methodology (28). The density of the buffer (1.0592 g/mL) was determined using a Kyoto Electronics Density/Specific Gravity Meter (model #DA-210).

RESULTS AND DISCUSSION

For studies of caveolin oligomerization we chose a construct that encompasses residues 62-178 (Cav1(62-178)). *In vivo* studies have shown that when the first 65 amino acids were deleted from caveolin-1, it had a behavior that was indistinguishable from that of the full-length protein (29). This strongly indicates that Cav1(62-178) retains the crucial structural elements necessary for full caveolin-1 function.

Wild-type Cav1(62-178) was reconstituted into a buffer containing dodecylphosphocholine (DPC) micelles. DPC micelles are a very native-like membrane mimic that is used widely in a variety of biophysical membrane protein studies (30, 31, 32). When the reconstituted protein was subjected to gel filtration analysis in the same buffer, a single symmetrical peak was observed (Figure 2 – solid line). The presence of a single symmetrical peak indicates that a homogenous population of species is present, and that Cav1(62-178) is *not* forming multiple oligomeric states, which had been previously reported. In addition, Cav1(62-178) did not elute in the void volume, 40 mL, revealing that caveolin-1 is not present in a high oligomeric state. When the gel filtration column was calibrated with known globular protein standards, the Cav1(62-178) fraction had an apparent molecular weight of 115 kDa. Based on these results, there is no evidence that caveolin-1 forms multiple oligomeric states which were reported previously. Upon further examination, it is unclear whether the observed high-order oligomeric complexes in the previous study contained only the caveolin-1 protein and no other biomolecules such as cholesterol. In fact, caveolin-1 has been described as a cholesterol binding protein (33). Also, in the previous study, the presence of caveolin-1 was the only protein that was probed for, so it is unclear whether other proteins may have been associated with these high molecular weight complexes as well.

Next, mutant Cav1(62-178)_P132L was subjected to gel filtration analysis. The

mutant also elutes as a single, symmetrical, non-voided peak indicating that a homogenous population of species is present (Figure 2-1 – dashed line). However, the mutant eluted before the wild-type, indicating that it was present as larger species. In contrast to the wild-type, the mutant had an apparent molecular weight of 190 kDa. However, the gel filtration analysis does not give us definitive information about the oligomeric state of wild-type and mutant Cav1(62-178). This is due to the fact that DPC molecules bound to Cav1(62-178) and the presence of a non-globular protein structure can dramatically inflate the apparent molecular weight.

To overcome the limitations of gel filtration analysis, wild-type and mutant Cav1(62-178) were subjected to analysis by analytical ultracentrifugation. The method of sedimentation equilibrium was employed because it is a very powerful approach for determining the molecular weight of proteins. Importantly, sedimentation equilibrium experiments give molecular weight information that is independent of molecular shape. In addition, sedimentation equilibrium experiments can be run under density-matched conditions, which allows for the detergent contribution to the observed molecular weight to be eliminated (34, 35, 36). Therefore, using this method, the exact oligomeric state of wild-type and mutant Cav1(62-178) can be characterized.

Figure 2-2 summarizes the data from the analytical ultracentrifugation experiments of both the wild-type and P132L mutant. For wild-type Cav1(62-178) (Figure 2-2, A-C), the data were fit to the ideal species model. This model gives a weight-averaged molecular weight of all species present. However, it was clear from the gel filtration experiments that a homogenous population of species was present. After fitting, the observed molecular weight was determined to be 14,606 Da. This agrees very well with the calculated molecular weight of the wild-type monomer which is 13,450 Da (The ~1 kDa discrepancy is most likely due to the inaccuracy of predicting partial specific volumes of

proteins in detergent solutions). Based on these results it is clear that caveolin-1 is a monomer, and does not homo-oligomerize. Importantly, this result helps to clarify the role of caveolin-1 in caveolae. As stated previously, *in vivo*, caveolin-1 is isolated as a high molecular weight complex that is SDS resistant (16, 37). However, it is unclear from this study as to whether caveolin-1 *itself* is responsible for the observed oligomeric behavior. For example, caveolin-1 has been shown to closely associate with cholesterol *in vivo*; therefore the appearance of these high molecular weight complexes may be due to the presence of SDS resistant caveolin-cholesterol aggregates. It is important to note that SDS is a much more powerful detergent towards protein deaggregation than DPC, which is much milder. Considering this, it is highly unlikely that DPC would interfere with caveolin-1 oligomerization. Additionally studies suggesting caveolin-1 oligomerizes have relied heavily on fragments of caveolin based on the N-terminal and scaffolding domains (16, 17, 29). However, it is not clear from these studies whether the fragments were representative of the native caveolin-1 protein, and in one case the studies were performed in the absence of a membrane mimic which is not representative of caveolin-1's membrane environment. Our studies reveal that when a *fully-functional* construct of Cav1(62-178) is analyzed in a membrane environment it does not form high-order oligomers and is in fact monomeric.

Next, mutant Cav1(62-178) was subjected to analysis by analytical ultracentrifugation (Figure 2-2, D-F). Initially, the data were fitted to the ideal species model. The resulting observed molecular weight was 28,282 Da. This value is approximately twice the molecular weight of the P132L monomer, 13,465 Da, showing a dimeric species was forming. Next, we explored the possibility of a monomer-dimer equilibrium by fitting the data to a monomer-dimer model. After doing so, the resulting observed molecular weight of the monomer was 14,079 Da. This corresponds very well

to the calculated molecular weight of the P132L monomer (13,465 Da). In addition, the model yielded a dissociation constant of approximately 15 nM which shows that the dimer is remarkably stable. From these results, we conclude that the P132L mutant is dimeric in a membrane-like environment unlike the wild-type which is monomeric.

After determining that the oligomeric state of P132L was dimeric, we turned our attention to determining the region of Cav1(62-178) P132L that was responsible for the observed dimerization. Caveolin-1 is generally divided into 4 domains: an N-terminal domain (residues 62-81), scaffolding domain (residues 82-95), transmembrane domain (residues 96-136), and C-terminal domain (residues 137-178). Therefore, truncated constructs of both wild-type and mutant caveolin-1 were generated: residues 62-136, 82-136, 82-178, 96-136, and 96-178. Importantly, all constructs contained the intact transmembrane domain. Each of the 5 constructs was run on gel filtration and the elution profiles of both wild-type and P132L were compared (Figure 2-3, B-F). In all five cases, the P132L mutant elutes before the wild-type indicating that a larger species was forming. Since all of the truncation constructs contained the intact transmembrane domain, these results indicated that the dimerization region is in the transmembrane domain of caveolin-1 where the P132L mutation is found.

Next, NMR structural studies were undertaken to observe the changes that were occurring in the transmembrane domain of wild-type versus mutant caveolin. Figure 2-4 shows an ^{15}N-^{1}H TROSY HSQC spectrum of mutant Cav1(96-136)_P132L. Linewidths are larger when compared to the wild-type spectrum (Figure 2-5) indicating the presence of oligomers. Chemical shift indexing (Figure 2-6) reveals that the transmembrane domain still retains the four distinct regions previously observed for the caveolin transmembrane domain: There is an α-helix from residues 97-107 (helix 1), a break from residues 108-110, another α-helix from residues 111-129 (helix 2), and an

39

unstructured region from residues 130-136 (38). Consistent with the horseshoe topology model of caveolin, the break at residues 108-110 is likely where the turn occurs so that the polypeptide chain can return to the membrane surface. Clearly in the case of the mutant, the break is not being lost so it is unlikely that this mutant disrupts the proposed horseshoe topology. In addition, helix 1 is unaffected as well. However, helix 2 is extended 4 residues to encompass residues 111-133. Therefore there is approximately one extra helical turn in the mutant. The unstructured region now does not begin until residue 134. This increased helicity is likely forming a dimerization domain in the transmembrane domain around position 132 (Figure 2-8). In the native protein, P132 acts to end the helix at residue 129 which prevents the dimerization from occurring. Therefore the helix-breaking tendency of proline is used to prevent the dimerization of caveolin.

Next, specific hydrophobic amino acid substitutions were made at position 132 to determine whether the other amino acids could substitute for proline at the 132 position. We chose to substitute the following residues: isoleucine, valine, alanine, glycine, tryptophan, and phenylalanine. Each residue is non-polar so it should not affect the structure by limiting the integration into the micelle. Each of these mutants were examined by gel filtration and compared to wild-type and mutant Cav1(62-178). Based on the elution profiles of the mutants, we can see that all of them elute before the wild-type (Figure 2-7) showing that all of the mutants retain dimerization capabilities. Retention times increased slightly from that of the P132L mutant indicating that the dimerization may be somewhat weaker for some of the mutants. Clearly it appears that proline is the only amino acid that is tolerated at position 132 and it explains why this mutant is conserved in all of the three caveolin isoforms.

As stated in the Introduction, the mutation of P132L in caveolin-1 can result in a

variety of disease states. However there has been little characterization of the differences between the wild-type and the mutant. Importantly, our data show that wild-type caveolin is monomeric and does not form high-order oligomers. Therefore, the high order oligomers observed for caveolin are likely due to other proteins/factors that are present *in vivo*. In contrast, the P132L mutant is a dimer. This dimerization could explain why the mutant is retained in the Golgi apparatus and does not reach its final destination in the plasma membrane. Furthermore, it is reasonable that other factors are responsible for the caveolin oligomers observed *in vivo* which would allow the cell to control when the oligomerization occurs. For example caveolin could be transported to the plasma membrane as a monomer, and then once in place other factors such as cholesterol, or the protein PTRF/cavin could trigger the oligomerization. Recent studies have shown that caveolin closely associates with the protein, PTRF/cavin. In fact, when the PTRF/cavin gene is silenced, the number of caveolae in the plasma membrane diminishes (39). The mutant, on the other hand, is a dimer which is not the proper oligomeric state for trafficking to the plasma membrane. Proline is a very unique amino acid because it is conformationally rigid. Because of this rigidity proline is known to be helix breaking. This could be critical for caveolin as P132 is located towards the end of the transmembrane domain where the protein is transitioning from a near-vertical helix in the membrane to the C-terminal domain which is an amphipathic helix which is predicted to reside horizontally on the membrane surface. When the proline is removed, the second helix of the transmembrane domain is extended by one turn. This small change is significant enough to open up a dimerization domain in the helix (Figure 2-8). No other non-polar amino acids can be substituted for proline, indicating how critical this residue is for caveolin structure. Therefore, P132 is critical for proper caveolin-1 structure and behavior.

41

CONCLUSIONS

Caveolae are flask-like invaginations in the plasma membrane of cells that serve as signaling platforms. The principle protein that is found in caveolae is caveolin. Caveolin has three isoforms: 1, 2, and 3. Caveolin-1 is the most ubiquitous and it is necessary and sufficient to induce caveolae formation. Caveolin-1 was thought to form high-order oligomers, which was believed to lead to the creation of caveolae (37). A direct observation of caveolin-1 oligomerization has been lacking and most studies which set out to characterize caveolin-1 oligomerization were either biological in nature or they utilized small pieces of the protein in their studies to address this question. The biology studies probed caveolae which were isolated from whole cell lysates for the presence of the caveolin-1 protein. Caveolin was indeed found isolated to caveolae, but they were isolated in high molecular weight complexes. The presence of other artifacts was not probed for in these complexes making it difficult to conclude that caveolin-1 forms high order oligomers. Other studies which sought to measure caveolin-1 oligomerization directly used similar method, but they focused on evaluating small pieces of the caveolin-1 protein which may not accurately reflect the true behavior of the caveolin protein. From the studies presented in Chapter 2 we can conclude that the protein is not oligomeric. These studies focus on using a construct of caveolin-1 that is fully functional and contains an intact intramembrane region of the protein. Further, the oligomeric state of the P132L mutant of caveolin-1 is dimeric. This contrast in the oligomeric states of the wild-type and mutant proteins may help to explain why the P132L protein does not traffic properly *in vivo* (21). The nature of the P132L dimerization has not been fully elucidated; however, from these studies is appears that the intramembrane region may

42

be responsible for this interaction.   Further studies are necessary to uncover the

chemical nature of the P132L dimerization.
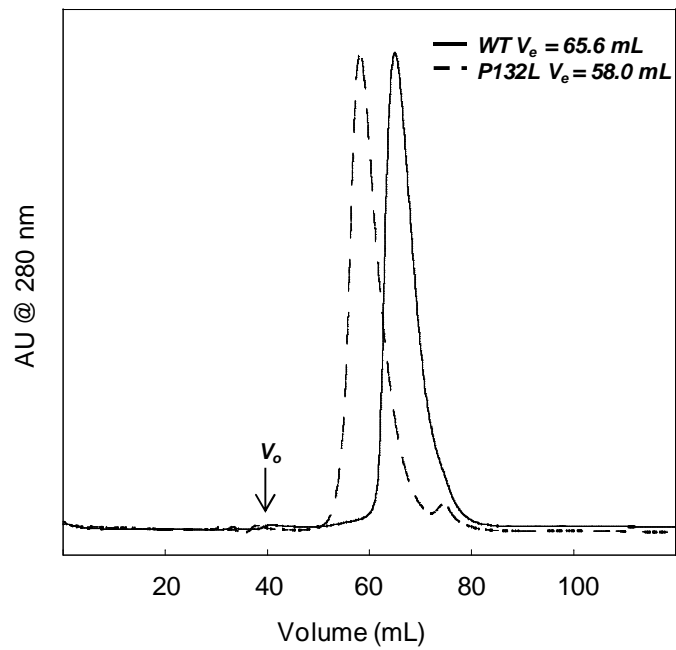
Figure 2-1. Elution profile of Cav1(62-178)_WT
(solid black) and Cav1(62-178)_P132L

43
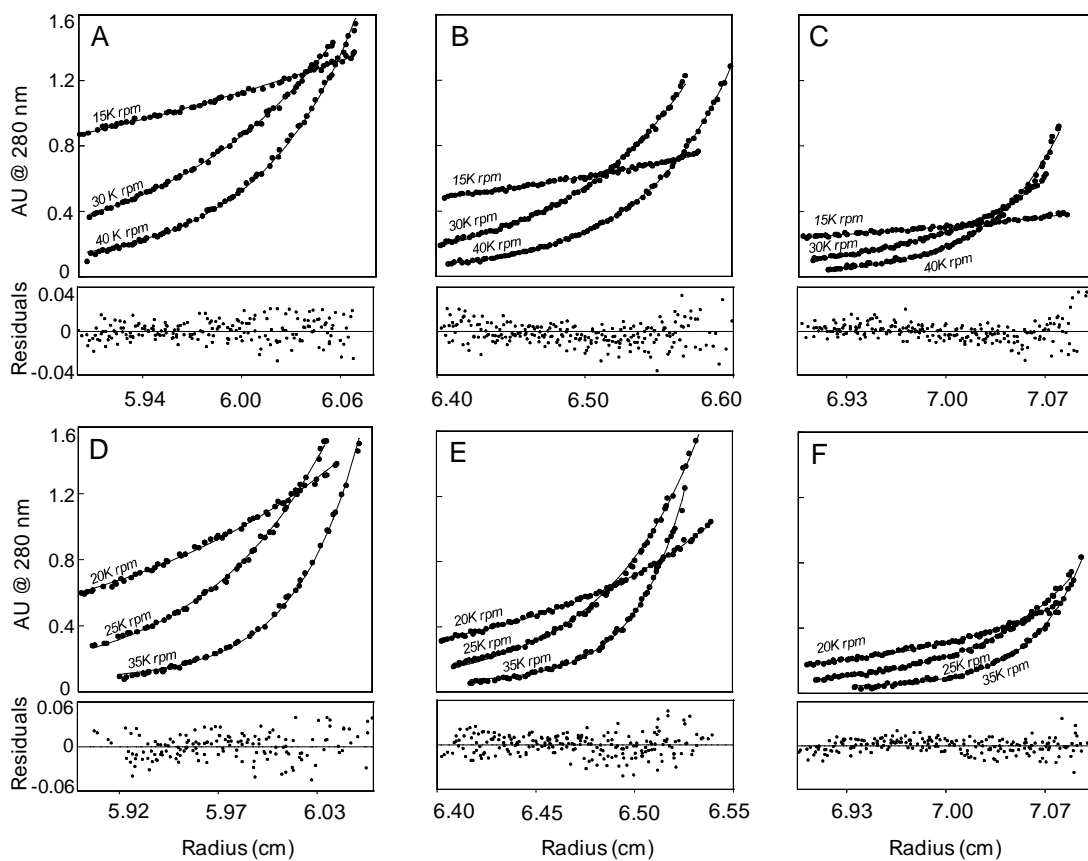
Figure 2-2. Sedimentation equilibrium results of caveolin-1 in DPC micelles. Panels A-C represent Cav1(62-178)_WT at A) 30 µM B) 15 µM C) 7.5 µM and three speeds denoted in each panel. Panels D-F represent Cav1(62-178)_P132L at A)30 µM B) 15 µM C)7.5 µM and three speeds.
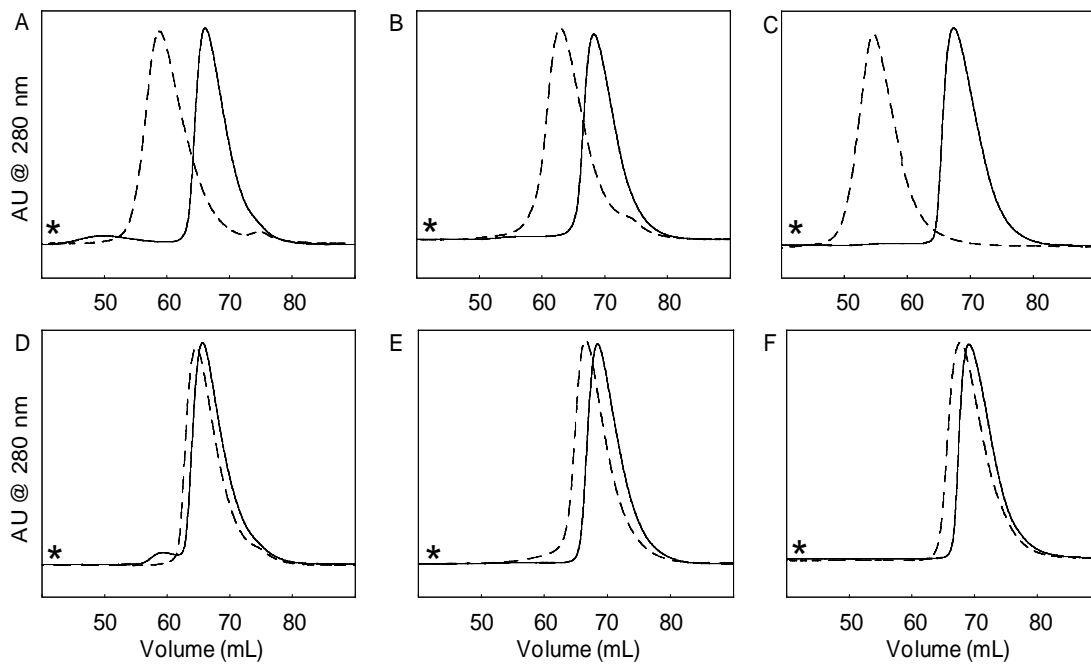
Figure 2-3. Gel filtration chromatograms of caveolin-1 constructs. A) Cav1(62-178) B) Cav1(82-178) C) Cav1(96-178) D) Cav1(62-136) E) Cav1(82-136) F) Cav1(96-136). The solid line represents wild type caveolin-1, the dashed line represents the P132L mutant.
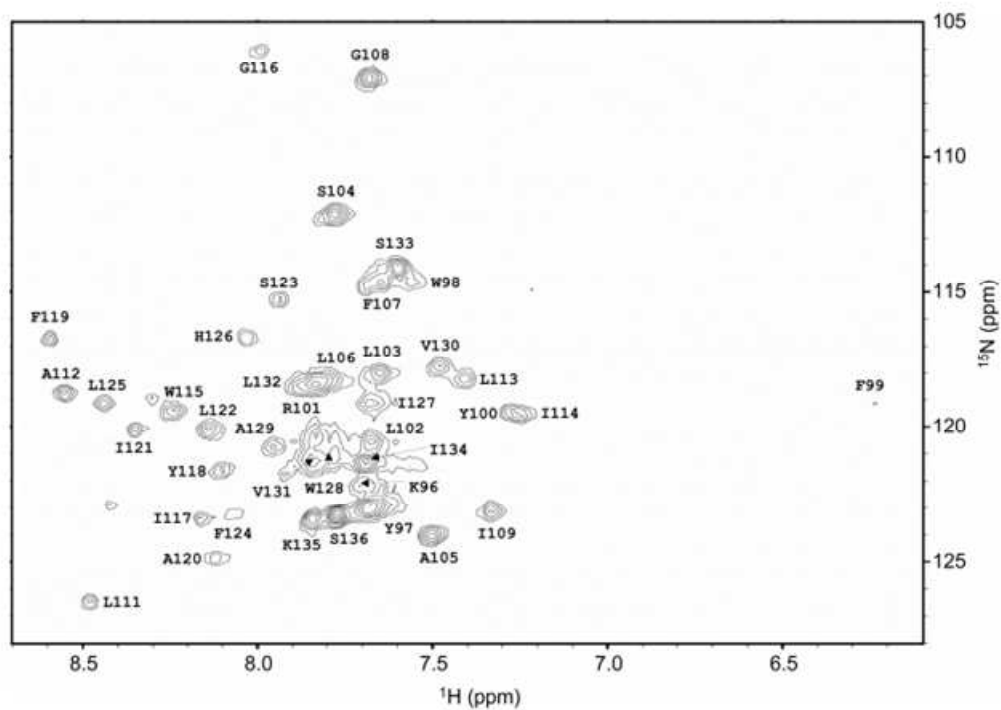
Figure 2-4. ^{1}H-^{15}N TROSY HSQC spectrum of Cav1(96-136)_P132L. The spectrum was acquired with 256 complex points in t1 (^{15}N) and 2048 complex points in t2 (^{1}H).
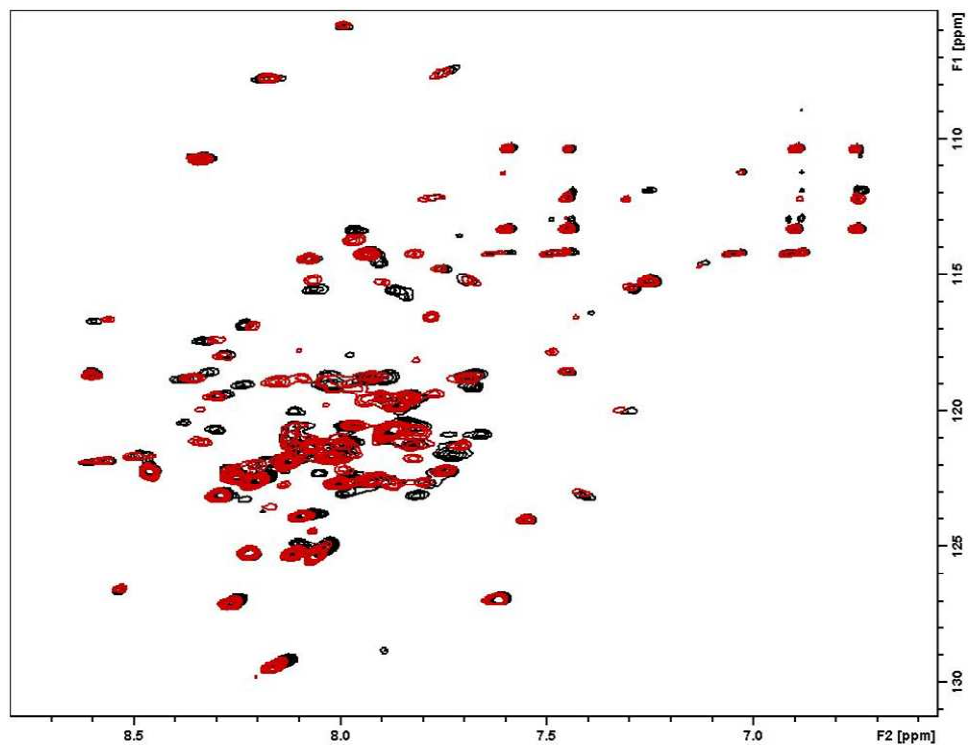
Figure 2-5. Overlay of ^{1}H-^{15}N TROSY HSQC spectra of Cav1(96-136)_WT (black) and Cav1(96-136)_P132L (red). The P132L mutant displays a high degree of overlap with wild type caveolin-1 which shows that the mutant does not introduce global changes to caveolin-1. Slight line broadening of the mutant can be seen indicating a small change in oligomeric state from the wild type.
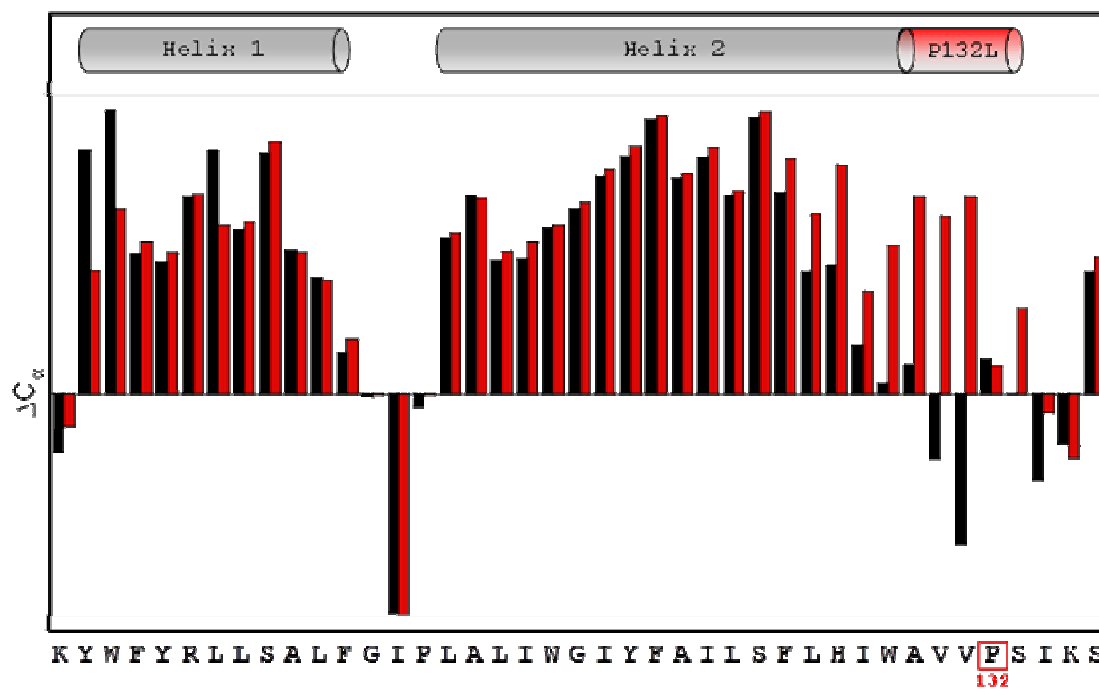
Figure 2-6. Chemical shift analysis of Cav1(96-136)_WT (black) and Cav1(96-136)_P132L (red). The P132L mutant shows an extension of helix 2 by four residues.
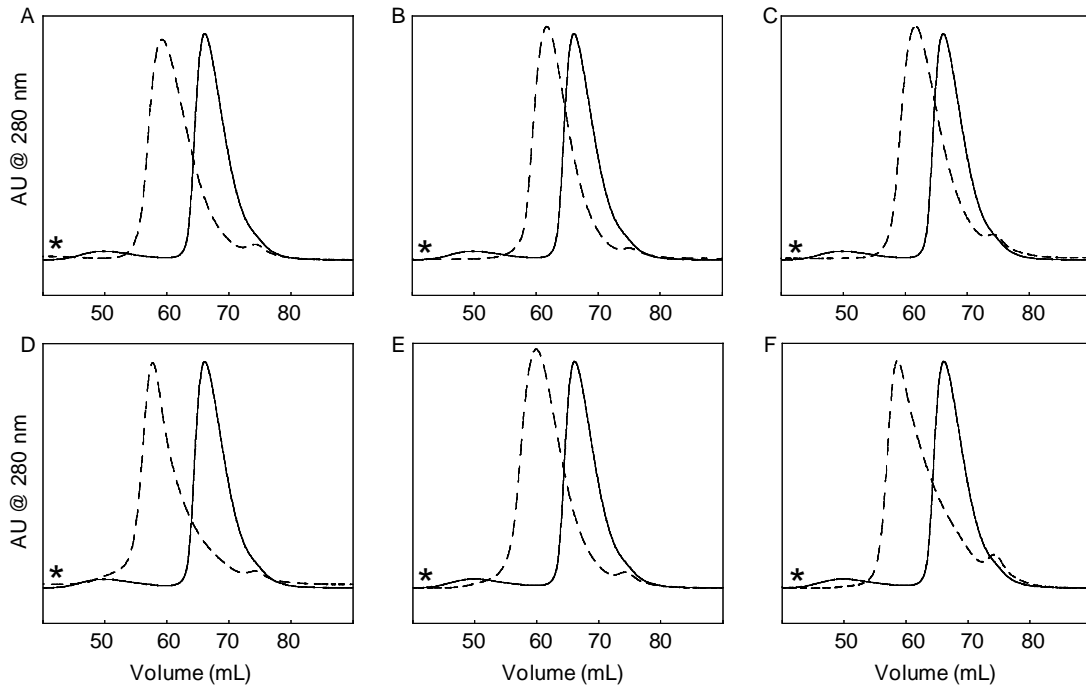
Figure 2-7. Gel filtration chromatograms of Cav1(62-178)_P132X mutants. A) P132I B) P132G C)P132A D) P132F E)P132V F) P132W. The solid line represents wild type caveolin-1, the dashed line represents each P132X mutant.
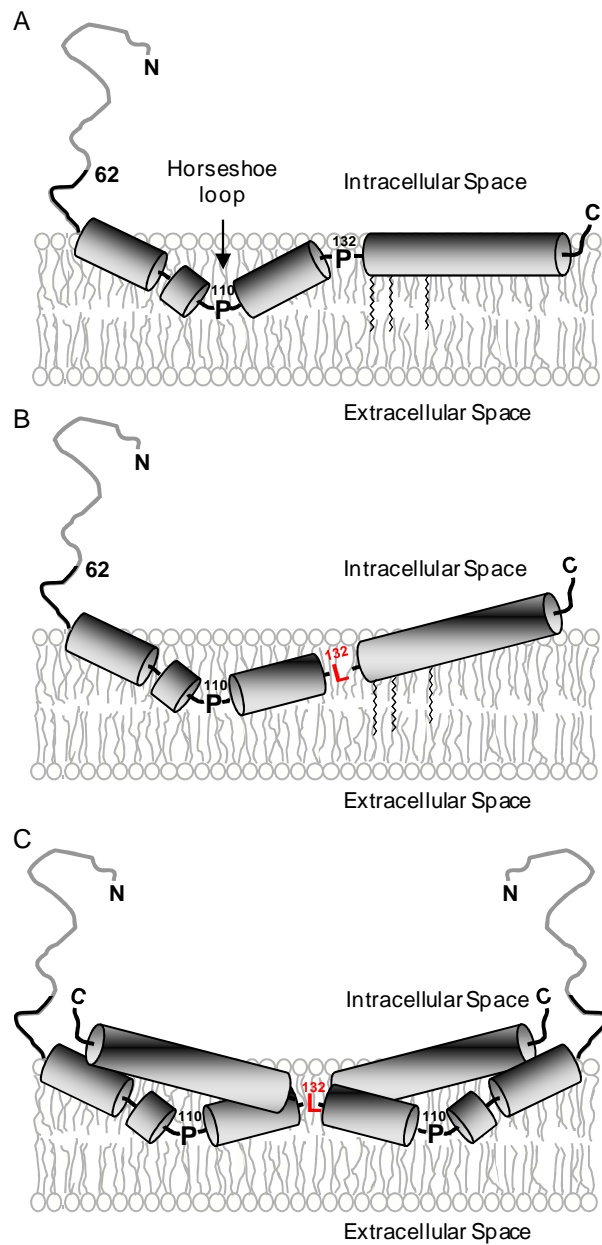
Figure 2-8. A) Schematic diagram of caveolin-1_WT (A) and P132L (B) in the plasma membrane. C) A proposed schematic depiction of the P132L dimer.

REFERENCES

1. Lisanti, M. P., and Williams, T. M. (2004) The Caveolin Genes: From Biology to Medicine. *Ann Med. 36*, 584-595.

2. Thorn, H., Stenkula, K. G., Karlsson, M., Ortegren, U., Nystrom, F. H., Gustavsson, J., and Stralfors, P. (2003) Cell Surface Orifices of Caveolae and Localization of Caveolin to the Necks of Caveolae in Adipocytes. *Mol. Biol. Cell. 14*, 3967-3976.

3. Spisni, E., Tomasi, V., Cestaro, A., and Tosatto, S. C. (2005) Structural Insights into the Function of Human Caveolin 1. *Biochem. Biophys. Res. Commun. 338*, 1383-1390.

4. Luoma, J. I., Boulware, M. I., and Mermelstein, P. G. (2008) Caveolin Proteins and Estrogen Signaling in the Brain. *Mol Cell Endocrinol.* 290. 8-13.

5. Awasthi, V., Mandal, S. K., Papanna, V., Rao, L. V. M., and Pendurthi, U. R. (2007) Modulation of Tissue Factor-Factor VIIa Signaling by Lipid Rafts and Caveolae. *Arterioscler. Thromb. Vasc. Biol. 27*, 1447-1455.

6. Callera, G. E., Montezano, A. C. I., Yogi, A., Tostes, R. C. A., and Touyz, R. M. (2007) Vascular Signaling through Cholesterol-Rich Domains: Implications in Hypertension. *Curr Opin Nephrol Hypertens. 16*, 90-104.

7. Balijepalli, R. C., Foell, J. D., Hall, D. D., Hell, J. W., and Kamp, T. J. (2006) Localization of Cardiac L-Type Ca2+ Channels to a Caveolar Macromolecular Signaling Complex is Required for Beta(2)-Adrenergic Regulation. *Proc. Natl. Acad. Sci. U.S.A. 103*, 7500-7505.

8. Bauer, P. M., Wertz, J. W., and Billiar, T. R. (2006) Reciprocal Regulation of Caveolin-1 Expression and Bone Morphogenetic Protein Signaling in Mouse Aortic Smooth Muscle Cells. *Circulation. 114*, 179-179.

9. Weerth, S. H., Holtzclaw, L. A., and Russell, J. T. (2007) Signaling Proteins in Raft-Like Microdomains are Essential for Ca2+ Wave Propagation in Glial Cells. *Cell Calcium. 41*, 155-167.

10. Sonnino, S., and Prinetti, A. (2009) Sphingolipids and Membrane Environments for Caveolin. *FEBS Lett. 583*, 597-606.

11. Briand, N., Dugail, I., and Le Lay, S. (2011) Cavin Proteins: New Players in the Caveolae Field. *Biochimie. 93*, 71-77.

12. Rothberg, K. G., Heuser, J. E., Donzell, W. C., Ying, Y. S., Glenney, J. R., and Anderson, R. G. (1992) Caveolin, a Protein Component of Caveolae Membrane Coats. *Cell. 68*, 673-682.

13. Drab, M., Verkade, P., Elger, M., Kasper, M., Lohn, M., Lauterbach, B., Menne, J., Lindschau, C., Mende, F., Luft, F. C., Schedl, A., Haller, H., and Kurzchalia, T. V. (2001) Loss of Caveolae, Vascular Dysfunction, and Pulmonary Defects in Caveolin-1 Gene-Disrupted Mice. *Science. 293*, 2449-2452.

14. Parton, R. G., Hanzal-Bayer, M., and Hancock, J. F. (2006) Biogenesis of Caveolae: A Structural Model for Caveolin-Induced Domain Formation. *J. Cell. Sci. 119*, 787-796.

15. Fra, A. M., Williamson, E., Simons, K., and Parton, R. G. (1995) De Novo Formation of Caveolae in Lymphocytes by Expression of VIP21-Caveolin. *Proc. Natl. Acad. Sci. U.S.A. 92*, 8655-8659.

16. Sargiacomo, M., Scherer, P. E., Tang, Z., Kubler, E., Song, K. S., Sanders, M. C., and Lisanti, M. P. (1995) Oligomeric Structure of Caveolin: Implications for Caveolae Membrane Organization. *Proc. Natl. Acad. Sci. U. S. A. 92*, 9407-9411.

17. Fernandez, I., Ying, Y., Albanesi, J., and Anderson, R. G. (2002) Mechanism of Caveolin Filament Assembly. *Proc. Natl. Acad. Sci. U. S. A. 99*, 11193-11198.

18. Schlegel, A., and Lisanti, M. P. (2000) A Molecular Dissection of Caveolin-1 Membrane Attachment and Oligomerization. Two Separate Regions of the Caveolin-1 C-Terminal Domain Mediate Membrane Binding and oligomer/oligomer Interactions in Vivo. *J. Biol. Chem. 275*, 21605-21617.

19. Bonuccelli, G., Casimiro, M. C., Sotgia, F., Wang, C., Liu, M., Katiyar, S., Zhou, J., Dew, E., Capozza, F., Daumer, K. M., Minetti, C., Milliman, J. N., Alpy, F., Rio, M. C., Tomasetto, C., Mercier, I., Flomenberg, N., Frank, P. G., Pestell, R. G., and Lisanti, M. P. (2009) Caveolin-1 (P132L), a Common Breast Cancer Mutation, Confers Mammary Cell Invasiveness and Defines a Novel Stem cell/metastasis-Associated Gene Signature. *Am. J. Pathol. 174*, 1650-1662.

20. Williams, T. M., and Lisanti, M. P. (2005) Caveolin-1 in Oncogenic Transformation, Cancer, and Metastasis. *Am J of Physiol-Cell Physiol. 288*, C494-C506.

21. Lee, H., Park, D. S., Razani, B., Russell, R. G., Pestell, R. G., and Lisanti, M. P. (2002) Caveolin-1 Mutations (P132L and Null) and the Pathogenesis of Breast Cancer - Caveolin-1 (P132L) Behaves in a Dominant-Negative Manner and Caveolin-1 (-/-) Null Mice show Mammary Epithelial Cell Hyperplasia. *Am J Pathol. 161*, 1357-1369.

22. Uittenbogaard, A., and Smart, E. J. (2000) Palmitoylation of Caveolin-1 is Required for Cholesterol Binding, Chaperone Complex Formation, and Rapid Transport of Cholesterol to Caveolae. *J. Biol. Chem. 275*, 25595-25599.

23. Dietzen, D. J., Hastings, W. R., and Lublin, D. M. (1995) Caveolin is Palmitoylated on Multiple Cysteine Residues. Palmitoylation is Not Necessary for Localization of Caveolin to Caveolae. *J. Biol. Chem. 270*, 6838-6842.

24. Sotgia, F., Razani, B., Bonuccelli, G., Schubert, W., Battista, M., Lee, H., Capozza, F., Schubert, A. L., Minetti, C., Buckley, J. T., and Lisanti, M. P. (2002) Intracellular Retention of Glycosylphosphatidyl Inositol-Linked Proteins in Caveolin-Deficient Cells. *Mol. Cell. Biol. 22*, 3905-3926.

25. Diefenderfer, C., Lee, J., Mlyanarski, S., Guo, Y., and Glover, K. J. (2009) Reliable Expression and Purification of Highly Insoluble Transmembrane Domains. *Anal Biochem. 384*, 274-8.

26. Losonczi, J. A., Olejniczak, E. T., Betz, S. F., Harlan, J. E., Mack, J., and Fesik, S. W. (2000) NMR Studies of the Anti-Apoptotic Protein Bcl-xL in Micelles. *Biochemistry. 39*, 11024-11033.

27. Cole, J. L. (2004) Analysis of Heterogeneous Interactions. *Methods Enzymol. 384*, 212-232.

28. Cohn E.J. & Edsall J.J. (1943) *Proteins, Amino Acids, and Peptides as Ions and Dipolar Ions.* , 375.

29. Machleidt, T., Li, W. P., Liu, P., and Anderson, R. G. (2000) Multiple Domains in Caveolin-1 Control its Intracellular Traffic. *J. Cell Biol. 148*, 17-28.

30. Neumoin, A., Arshava, B., Becker, J., Zerbe, O., and Naider, F. (2007) NMR Studies in Dodecylphosphocholine of a Fragment Containing the Seventh Transmembrane Helix of a G-Protein-Coupled Receptor from Saccharomyces Cerevisiae. *Biophys. J. 93*, 467-482.

31. Zamoon, J., Mascioni, A., Thomas, D. D., and Veglia, G. (2003) NMR Solution Structure and Topological Orientation of Monomeric Phospholamban in Dodecylphosphocholine Micelles. *Biophys. J. 85*, 2589-2598.

32. Beswick, V., Guerois, R., Cordier-Ochsenbein, F., Coic, Y. M., Tam, H. D., Tostain, J., Noel, J. P., Sanson, A., and Neumann, J. M. (1999) Dodecylphosphocholine Micelles as a Membrane-Like Environment: New Results from NMR Relaxation and Paramagnetic Relaxation Enhancement Analysis. *Eur. Biophys. J. 28*, 48-58.

33. Murata, M., Peranen, J., Schreiner, R., Wieland, F., Kurzchalia, T. V., and Simons, K. (1995) Vip21/Caveolin is a Cholesterol-Binding Protein. *Proc Natl Acad Sci U S A. 92*, 10339-10343.

34. Fleming, K. G. (2008) Determination of Membrane Protein Molecular Weight using Sedimentation Equilibrium Analytical Ultracentrifugation. *Curr. Protoc. Protein Sci. Chapter 7*, Unit 7.12.1-7.12.13.

35. Reynolds, J., and Tanford, C. (1976) Determination of Molecular Weight of the Protein Moiety in Protein-Detergent Complexes without Direct Knowledge of Detergent Binding. *Proc. Natl. Acad. Sci. 73*, 4467-4470.

36. Mayer, G., Ludwig, B., Muller, H. -., van den Brook, J. A., Friesen, R. H. E., and Schubert, D. (1999) Studying Membrane Proteins in Detergent Solution by Analytical Ultracentrifugation: Different Methods for Density Matching. *Progr Colloid Polym Sci. 113*, 176-181.

37. Monier, S., Parton, R. G., Vogel, F., Behlke, J., Henske, A., and Kurzchalia, T. V. (1995) VIP21-Caveolin, a Membrane Protein Constituent of the Caveolar Coat, Oligomerizes in Vivo and in Vitro. *Mol. Biol. Cell. 6*, 911-927.

38. Lee, J., and Glover, K. J. (2012) The Transmembrane Domain of Caveolin-1 Exhibits a Helix-Break-Helix Structure. *Biochim. Biophys. Acta.*

39. Liu, L., Brown, D., McKee, M., Lebrasseur, N. K., Yang, D., Albrecht, K. H., Ravid, K., and Pilch, P. F. (2008) Deletion of Cavin/PTRF Causes Global Loss of Caveolae, Dyslipidemia, and Glucose Intolerance. *Cell. Metab. 8*, 310-317.

Chapter 3. Evaluating Caveolin-1 Oligomerization in a Bilayer

ABSTRACT

Caveolin-1 is the most important protein found in caveolae, which are invaginations of the plasma membrane. It was once thought that caveolin-1 had the ability to form high-order oligomers which stabilizes the curvature of caveolae. It was shown that in DPC micelles, caveolin is a monomer and does not have the ability to oligomerize by itself at all. This result contradicts the initial belief that caveolin oligomerizes on its own thereby creating caveolae. Although this was not observed in DPC micelles, it is important to consider the influence of a micelle environment on caveolin behavior. To evaluate the oligomerization of caveolin in a true bilayer, bicelles were employed in the following study to determine if the oligomeric state of caveolin-1 depends on the detergent / lipid environment. Bicelles were first density matched using the density modifiers D_2O, glycerol and sucrose. D_2O was chosen as the density modifier for subsequent caveolin-1 studies. Cav1(62-178) was incorporated into bicelles using detergent dialysis to form DMPC vesicles from which bicelles were formed by subsequently adding the detergent, DHPC. Results of the sedimentation equilibrium studies show that caveolin-1 remains monomeric in bicelles and its oligomeric state is not influenced by its lipid environment.

INTRODUCTION

The bicelle system has emerged as a lipid system in which to study membrane protein structure and protein interactions. Bicelles are a better membrane mimic than micelles because they provide a true bilayer which reflects the natural protein environment in the cell. Bicelles are comprised of two types of phospholipids, a long-chain lipid and a short-chain lipid (Figure 1-3b). When mixed together, the two lipids spontaneously organize in such a way that a discoidal-shaped aggregate assembles with the long-chain lipid comprising the planar region of the bicelle and the short-chain lipid assembles to form the rim of the bicelle. Like, micelles, bicelles are also dynamic, therefore, they do not inhibit protein interactions. Most commonly, dimyristoyl-3-phosphatidylcholine (DMPC) is used as the long-chain lipid (Figure 1-3b) and dihexanoyl-3-phosphatidylcholine (DHPC) is used as the short-chain lipid (Figure 1-3b). However, bile salts such as CHAPSO can be used instead of the short-chain lipid. The long chain lipid can vary in length, which effectively changes the thickness of the bilayer. The length of the bicelles can be tailored as well by changing the q value or the mole ratio of DMPC to DHPC. Bicelles with a q of 0.5 and 1.0 were chosen for these studies because q = 0.5 bicelle have been well characterized and they support membrane protein structure and q = 1.0 bicelles provide an effective bilayer region in which to evaluate membrane proteins (1, 2, 3). Bicelles have not yet been used in the analytical ultracentrifuge to evaluate the oligomeric properties of proteins. The first step was to prepare bicelle solutions at varying densities in order to determine the density at which bicelles no longer sediment down a solution column, or where M_{eff} = 0. These studies also allow the density of q = 1.0 bicelles to be determined. Three different density modifiers were used to adjust the density of the bicelle solutions: D_2O, glycerol, and sucrose. These density modifiers are biocompatible and do not substantially alter the

behavior of proteins and lipids in solution. It was found that bicelles at a q=1.0 could be density matched using a D_2O concentration of 74.5 % (v/v), a glycerol concentration of 37.5 % (v/v), and sucrose concentration of 0.418 M. The results of this study also show that the choice of density modifier has a small effect on the density of bicelles.

The results of the caveolin oligomerization studies carried out in DPC micelles reveal that caveolin is a monomer and does not have the ability to interact with itself. This begs the question, are micelles sufficient to support caveolin interactions? Micelles have inherent limitations in that their extreme curvature may affect protein structure enough to influence the self-association of membrane proteins. Also, micelles, while useful in the study of membrane proteins, do not provide a true bilayer environment where membrane proteins are natively found. In order to understand if the micelle environment is influencing caveolin self-association it is necessary to study caveolin interactions in a bilayer environment. Bicelles are well-suited to this goal because they are dynamic like micelles, which means they are equilibrium structures that will support the self-association of membrane proteins. Also, bicelles provide a true bilayer environment where protein interactions can be more accurately assessed. Lastly, bicelles have now been density matched using three different density modifiers; D_2O, sucrose, and glycerol. For these studies, D_2O was chosen as the density modifier because it is most similar to water and it does not preferentially interact with bicelles in the way that sucrose and glycerol do. The results of the study presented show that caveolin is also a monomer in bicelles, and further supports the use of bicelles as a medium in which to study membrane protein interactions.

MATERIALS AND METHODS

Density matching bicelles

All sedimentation equilibrium density matching experiments were performed at 25°C using a Beckman XL-A analytical ultracentrifuge. To 3.58 mg of lyophilized dimyristoyl-3-glycero phosphatidylcholine (DMPC) containing a 1:10,000 ratio of DMPC to 1,2-dimyristoyl-glycero-3-phosphoethanolamine-*N*-(7-nitro-2-1,3-benzoxadiazol-4-yl) (Avanti Polar Lipids, Alabaster, AL) 300 µL of buffer containing 10 mM HEPES, 100 mM NaCl pH 7.4 and various amounts of either D_2O (0, 10, 25, 40, 50 , 60, 70, 80, 90 % (v/v)) , glycerol (0, 2, 5, 10, 15, 20, 25, 30, 35 %(v/v)) or sucrose (0, 0.1, 0.2, 0.3, 0.4, 0.5, 0.6, 0.7, 0.8 M) was added. Next, the samples were vigorously vortexed until a homogeneous milk-like suspension was obtained. 13.03 µL of 25% (w/w) dihexanol-3-glycero phosphatidylcholine (DHPC) solution was added to the DMPC to give a final DMPC : DHPC mole ratio of 1.0 (q = 1.0). After adding the DHPC, the solution became clear. The samples were loaded into a 6-sector charcoal filled epon centerpiece (pathlength 1.2 cm) using a reference solution that did not contain bicelles. The volume of sample per sector was 120 µL, and the cells were loaded in a Beckman Ti-60 4-hole rotor. Equilibrium absorbance measurments (468 nm) were taken at 10,000 rpm to 35,000 rpm in 1,000 rpm increments. Data was collected at each incremental speed. Initial equilibration was done at 10,000 rpm for 24 hours. At each 1,000 rpm increment the equilibration time was 4 hours. For each concentration of additive a plot of the natural log of the absorbance versus the square of the radius was generated. This plot was fitted to a linear function and the buoyant molecular weight was extracted from the slope. For each concentration the buoyant molecular weight was averaged over all speeds. A total of nine data points were generated for each buffer additive (D_2O,

glycerol, sucrose). The density of the bicellar solutions were measured using a Kyoto Electronics Density/Specific Gravity Meter (model #DA-210).

Incorporation of caveolin-1(62-178) into bicelles

Caveolin was incorporated into bicelles using the detergent dialysis method presented in Mimms et al. (4). 0.25 mg of caveolin-1(62-178) was co-dissolved with 5.96 mg of DMPC (1:500 protein:lipid mole ratio) in 500 µL of HFIP. The sample was flash frozen in liquid nitrogen and lyophilized to a powder for a minimum of 16 hours. This lyophilized material was used to prepare 500 µL of a caveolin bicelle sample with a calculated absorbance of 1.0. To the lyophilized lipid and protein, 440 µL of a 300 mM PFO, 10 mM Tris pH 8 solution is added. This volume ensures a lipid concentration of 20 mM, which is crucial to forming vesicles. To the lyophilized powder 358.5 µL of D_2O (density matched volume of 71.7%), 95.8 µL of water, 12.5 µL of 40X concentrated buffer (0.4 M HEPES, 4 M NaCl pH 7.4) and 21.7 µL of 25% DHPC (w/w) were added and the sample was left to mix on the rotating mixer until clear. The sample was centrifuged at 15,000 x g for 2 hours and the presence or absence of a white pellet was monitored at the bottom of the tube. The absence of a pellet confirms that most of the caveolin material has been incorporated into bicelles. Next, an "empty bicelle" solution is prepared without caveolin. To prepare 1.0 mL of a control or "empty bicelle" sample, 11.92 mg of DMPC are weighed out in a 1.5 mL Eppendorf tube. 717.0 µL D_2O is added to the DMPC powder in the tube followed by 25.0 µL of 40X concentrated HEPES; NaCl pH 7.4 buffer solution to give a final concentration of 10 mM HEPES, 100 mM NaCl pH 7.4. The DMPC was vortexed for several seconds to suspend the powder (17.6 mM final concentration) and 43.4 µL of a 25% (w/w) DHPC solution was added to a final concentration 24.4 mM. The ratio of DMPC to DHPC yields an effective q-value of 1.0. The solution turns clear upon addition of the DHPC solution. The empty bicelle solution

is used to prepare dilutions of the most concentrated caveolin-1(62-178) bicelle solution to give three protein concentrations, which represents the minimum data required to give an accurate estimate of the oligomeric state of caveolin.

RESULTS AND DISCUSSION

The goal of this study was to evaluate the oligomeric state of caveolin-1 in a lipid bilayer medium. Previous results in DPC micelles show that caveolin-1 (62-178) is monomeric, however, it is unclear if the extreme curvature of micelles is influencing the conformation and consequently biasing any preferential interactions of caveolin-1 with itself. Membrane protein structure and function can be influenced by the lipid medium in which it resides, therefore, the goal of this study was to compare the oligomeric state of caveolin in micelles to the oligomeric state in a true bilayer environment. Bicelles were chosen as the medium in these studies primarily because they are well-characterized, dynamic system. They are equilibrium structures as well, which makes them conducive to sedimentation equilibrium studies in the analytical ultracentrifuge as well. Bicelles with a q = 1.0 were chosen for the caveolin studies because they were best suited to the incorporation of caveolin-1 (62-178) and they provide a larger bilayer area in which oligomerization can be better evaluated.

Choice of Caveolin-1 Construct

For these studies a construct of caveolin-1 was chosen that encompasses residues 62-178. This construct contains the intact intramembrane region of caveolin (96-136). *In vivo* studies have shown that when the first 65 amino acids were deleted from the caveolin-1, it had a behavior that was indistinguishable from that of the full-length protein (5). This strongly indicates that Cav1(62-178) retains the crucial structural elements necessary for full caveolin-1 function, specifically, the full transmembrane region (approximately 96-136).

Density Matching Experiments

To characterize the precise oligomeric state of caveolin, we used sedimentation equilibrium analytical ultracentrifugation. The method of sedimentation equilibrium was employed because it is a very powerful approach for determining the precise molecular weight of Cav1(62-178), in the presence of bicelles. To determine the molecular weight of Cav1(62-178) it is necessary to subtract out the molecular weight of the bicelles first. The method of density matching was employed to accomplish this task. Density matching is often used in membrane protein experiments where detergents and lipids are present, and this approach allows us to eliminate the molecular weight contribution of the detergent to the molecular weight of the protein (6, 7, 8). Density matching of the bicelles was carried out using D_2O, sucrose and glycerol, which are three commonly used density additives that are compatible with proteins and do not cause them to denature. Bicelles with a *q* = 1.0 have not been density-matched in the analytical ultracentrifuge. By adapting the method of sedimentation equilibrium to bicelles a more accurate depiction of membrane protein interactions can be evaluated since bicelles provide a true bilayer environment. Cav1(62-178) oligomerization was also assessed in bicelles using sedimentation equilibrium. A total of nine bicelle solutions were prepared for each of the three density- matching experiments using the different density modifiers. The number of bicelle samples is consistent with the maximum number of samples that can be run in a 4-hole rotor at one time. The density of each of the prepared bicelle solutions was measured using a density meter and summarized in Table 3.1. Each of the bicelle solutions was subjected to sedimentation equilibrium analysis and the data were treated with the Lamm equation. From the Lamm equation, the effective molecular weight of the bicelles in each of the nine solutions was determined. A plot of the effective molecular weight of the bicelle solutions versus the buffer density was

generated for each density modifier as shown in Figures 3-1, 3-2, 3-3. From these results, we determined the point at which the effective molecular weight of the bicelles is zero for each additive, thereby establishing the density matched concentration of each additive required (Figure 3-4). The results are summarized in Table 3.2 where we can see that the partial specific volume of the bicelles is dependent on the density modifier used. For example, in D_2O, the bicelles have a partial specific volume of 0.923 mL / g versus 0.943 mL / g in sucrose. This suggests that the lipids in the D_2O bicelles may be packed more closely compared to the lipids in bicelles prepared with sucrose. This data represents, to our knowledge, the first instance where q = 1.0 bicelles have been successfully density-matched and their partial specific volume determined.

Caveolin-1 Incorporation into Bicelles

Several approaches were investigated to incorporate Cav1(62-178) into q = 1.0 bicelles. The method that was most effective was detergent dialysis. Cav1(62-178) has a strong tendency to irreversibly aggregate; therefore, it was necessary to ensure that Cav1(62-178) was monomeric prior to dialyzing into DMPC bilayers to form vesicles. Previous experiments show that Cav1(62-178) is monomeric in DPC micelles. DPC was chosen initially as the detergent from which to dialyze; however due to the low critical micelle concentration (CMC) DPC proved to be particularly challenging to remove completely by dialysis and consistent results were difficult to produce. The fluorinated detergent, PFOA, was superior to most detergents because it was powerful enough to solubilize Cav1(62-178) and DMPC, and it dialyzed more efficiently. It also provided more reproducible dialysis results compared to DPC. The temperature of the dialysis is an important factor and is critical to the quality of Cav1(62-178) bicelles that are formed. PFOA does not dialyze efficiently at temperatures below 21 ℃, yet lower temperatures

are effective at preventing undesirable Cav1(62-178) aggregation. The best results were obtained when the temperature was held constant during dialysis by incubating at 21 °C.

Caveolin-1 Oligomerization in Bicelles

The sedimentation profile of Cav1(62-178) was obtained at three different speeds and using *"Heteroanalysis Version 1.1.0.44 - beta"*, the data were fit globally to a single species model. This model provides an average molecular weight of all oligomeric populations present in solution. However, based on the gel filtration analysis, it is clear that caveolin-1 only exists in one oligomeric state. Figure 3-6 shows the fitted data from the analytical ultracentrifugation experiments of Cav1(62-178) in q = 1.0 bicelles. Cav1(62-178) was analyzed at concentrations of 30 µM, 15 µM, and 7.5 µM at 25,000, 30,000, and 35,000 rpm. After fitting the sedimentation equilibrium data to the single species model, the observed molecular weight was determined to be 14,650 Da. This agrees very well with the calculated molecular weight of the caveolin-1 monomer which is 13,450 Da (calculated from the amino acid sequence). The ~1 kDa discrepancy can be attributed to the inherent error of predicting the partial specific volume of membrane proteins in detergent solutions (9). From this data it is clear that when a fully-functional construct of Cav1(62-178) is analyzed in a membrane environment it does not form high-order oligomers, but instead is monomeric. These results are similar to the results obtained for the investigation of caveolin in DPC micelles. This indicates that DPC is not responsible for the observed monomeric state of caveolin in previous studies.

CONCLUSIONS

There has been skepticism surrounding the hypothesis that caveolin-1 has the ability to form high-order oligomers, which drives and/or stabilizes the caveolae invaginations on the surface of the plasma membrane in mammalian cells. This study set out to address the question, does caveolin-1 have the ability to form high-order oligomers on its own or could there be other biomolecules involved in the creation of the observed high-order complexes that were previously characterized by SDS-PAGE. A previous study presented in this thesis shows that in DPC micelles, caveolin-1 is monomeric while a naturally occurring mutant, P132L is dimeric. This study provides evidence that even in a bilayer, which is more native-like than a micelle, caveolin-1 is still monomeric and does not oligomerize. For the first time, we also show that q = 1.0 bicelles can be successfully density matched, and this medium is conducive to studies of membrane protein interactions in the analytical ultracentrifuge. Bicelles are ideal for studying membrane protein interactions compared to micelles because the extreme curvature introduced by the latter can bias protein conformation resulting in changes in protein behavior.

Table 3.1. Density measurements of bicelle solutions with density modifiers

Sample #	1	2	3	4	5	6	7	8	9
D_2O	0%	10%	25%	40%	50%	60%	70%	80%	90%
	1.0060	1.0169	1.0332	1.0495	1.0604	1.0713	1.0822	1.0931	1.1039
glycerol	0%	2%	5%	10%	15%	20%	25%	30%	35%
	1.0056	1.0114	1.0201	1.0346	1.0490	1.0635	1.0780	1.0925	1.1070
sucrose	0 M	0.1 M	0.2 M	0.3 M	0.4 M	0.5 M	0.6 M	0.7 M	0.8 M
	1.0059	1.0192	1.0325	1.0458	1.0590	1.0723	1.0856	1.0990	1.1122

Table 3.2. Partial specific volume of q = 1.0 bicelles determined from density matching experiments

Density Modifier	Partial specific volume (mL / g)	% (v/v) or Molarity	Buffer Density (g / cm^3)
D$_2$O	0.923	71.7	1.084
Glycerol	0.932	23.4	1.073
Sucrose	0.942	0.418	1.061
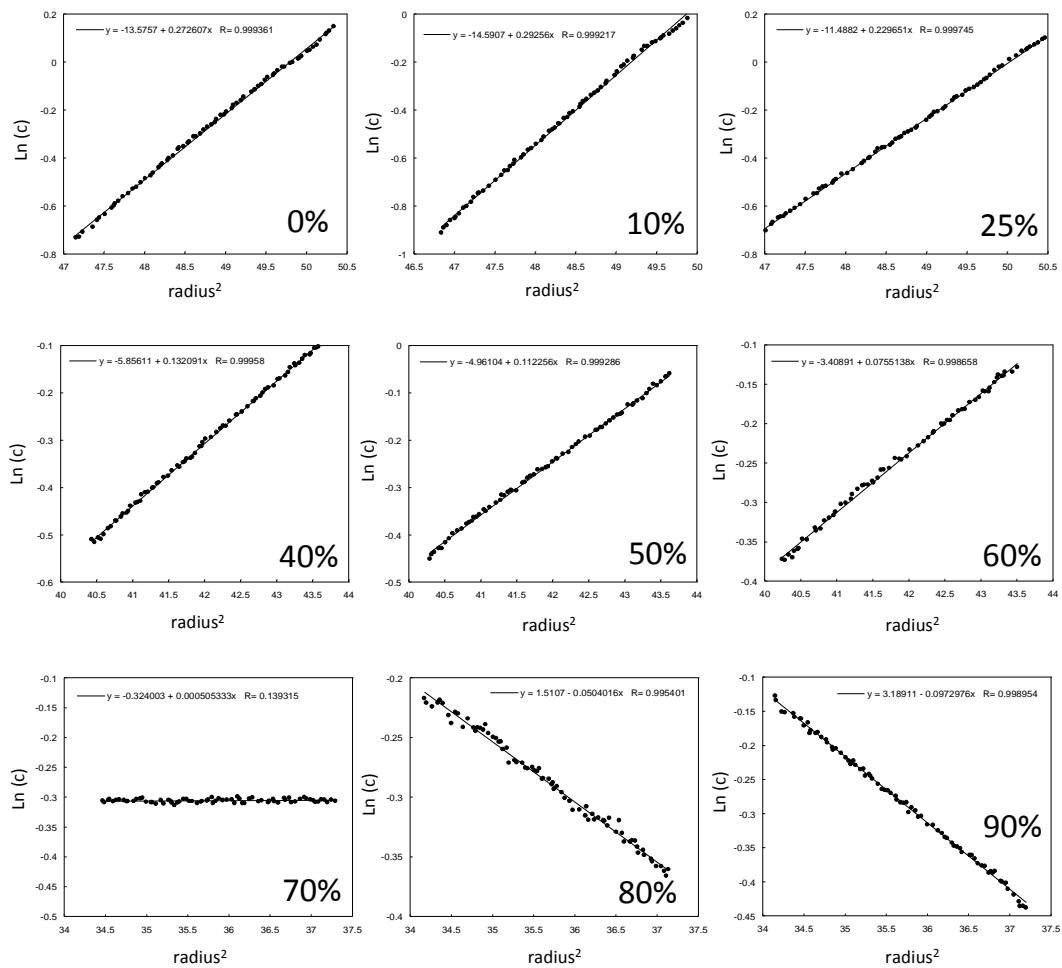
Figure 3-1. Ln (c) versus radius^2 of bicelle solutions with varying concentrations of D$_2$O. Concentrations of D$_2$O are expressed in % v/v and are denoted in each of the figure panels. The slope of the lines represents M$_{eff}$ at different concentrations of D$_2$O. A slope of zero represents the point at which M$_{eff}$ = 0 and the bicelles are matched, approximately 70% (v/v) D$_2$O.

.
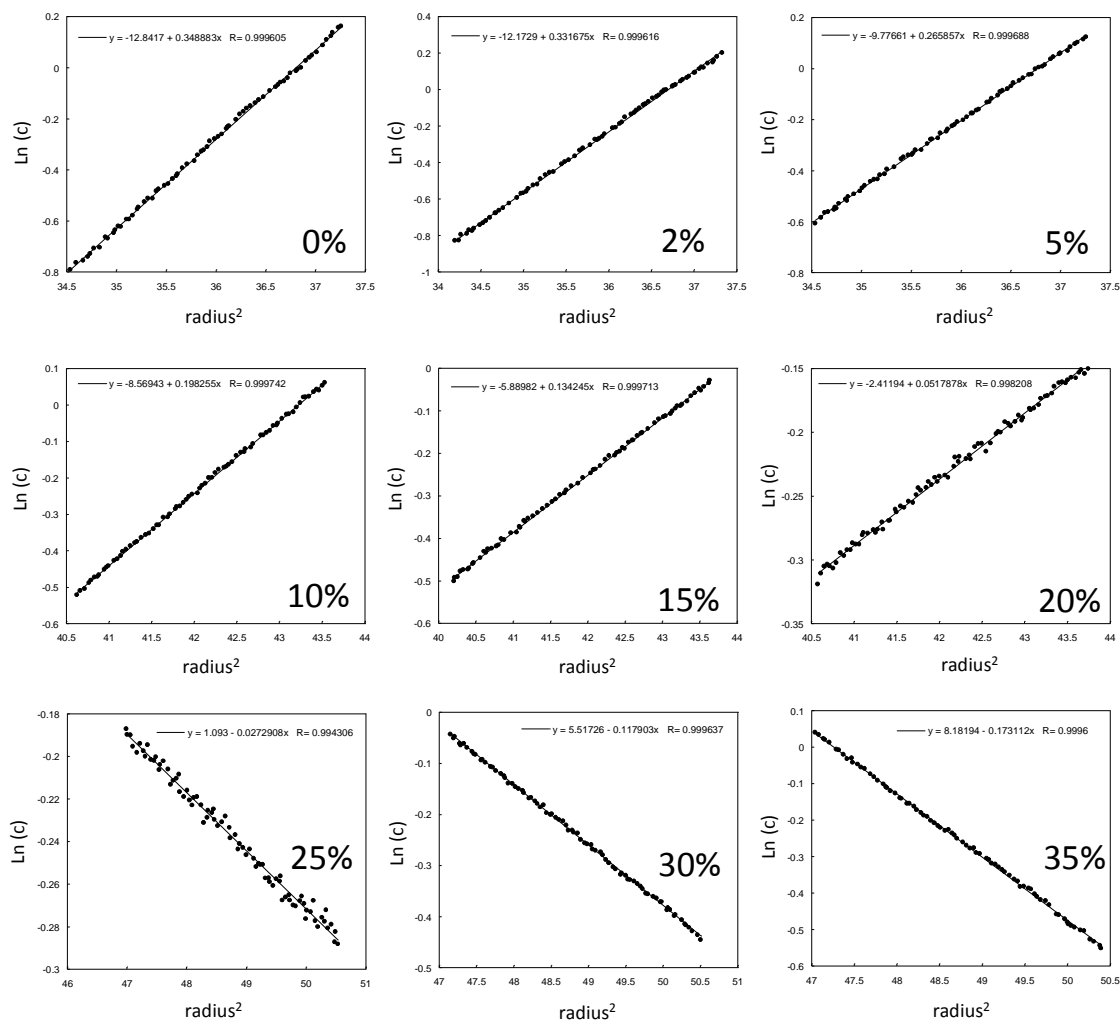
Figure 3-2. Ln (c) versus radius^2 of bicelle solutions with varying concentrations of glycerol. Concentrations of glycerol are expressed in % v/v and are denoted in each of the figure panels. The slope of the lines represents M_{eff} at different concentrations of glycerol. A slope of zero represents the point at which $M_{eff} = 0$ and the bicelles are matched, approximately 23.4% (v/v) glycerol.
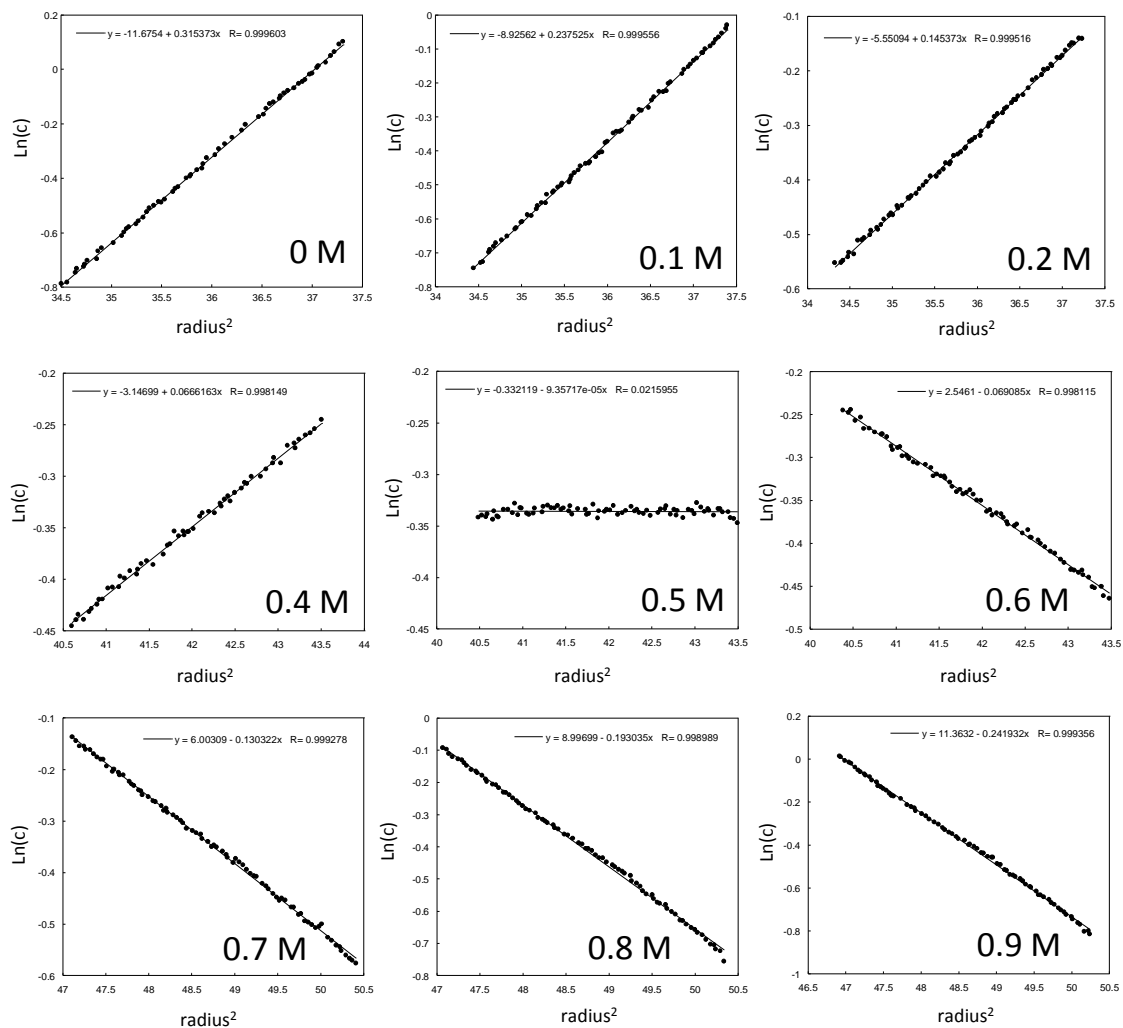
Figure 3-3. Ln (c) versus radius^2 of bicelle solutions with varying concentrations of sucrose. Concentrations of sucrose are expressed in Molarity and are denoted in each of the figure panels. The slope of the lines represents M_{eff} at different concentrations of D_2O. A slope of zero represents the point at which $M_{eff} = 0$ and the bicelles are matched, approximately 0.5 M sucrose.
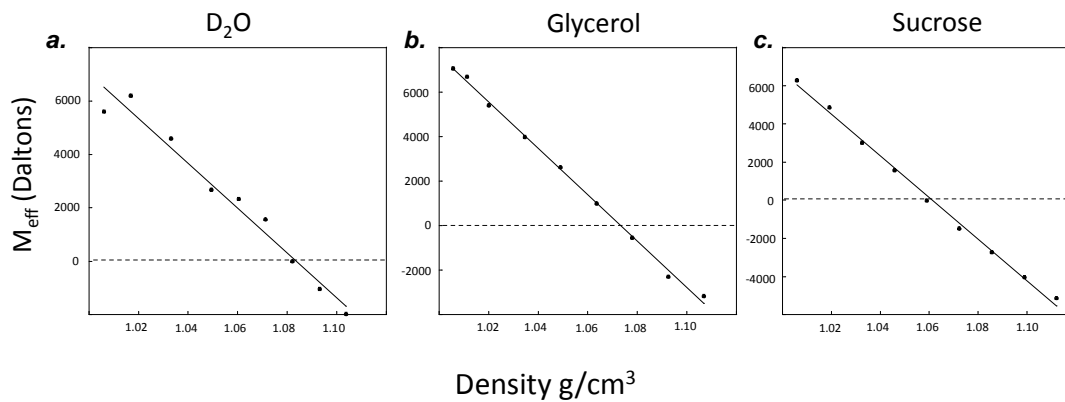
Figure 3-4. M_{eff} versus buffer density. The dotted line indicates the point at which M_{eff} of bicelles equals zero, which corresponds to a specific buffer density for each different density modifier tested. The buffer density required to density match bicelles is slightly dependent on the density modifier used in each experiment indicating a small, but noticeable change in the partial specific volume of bicelles for each density modifier used. a) D_2O b) glycerol c) sucrose
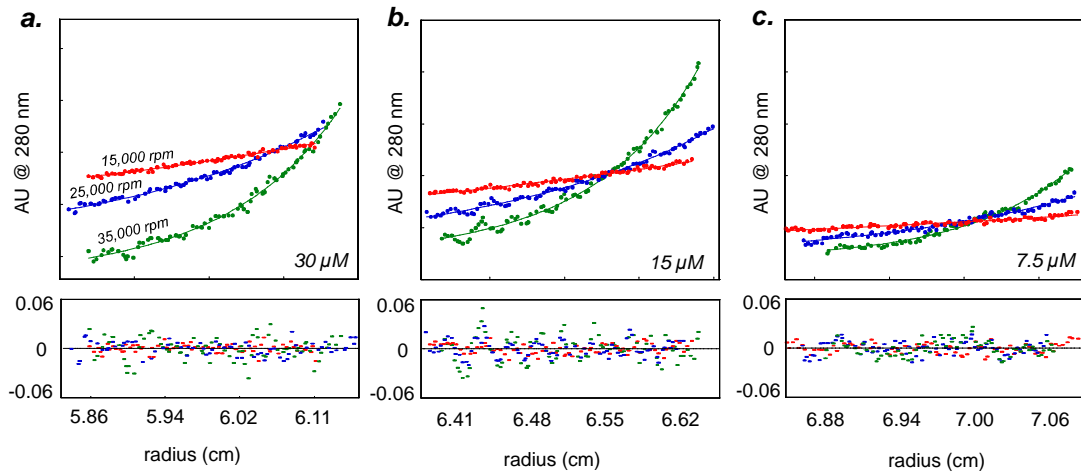
Figure 3-5. Sedimentation equilibrium data of caveolin-1 (62-178) in q = 1.0 bicelles at three different speeds and concentrations. The different speeds are highlighted in colors. Red represents the data collected at 15,000 rpm, blue represents the data collected at 25,000 rpm, and green represents the data collected at 35,000 rpm. a) 30 µM protein concentration b) 15 µM protein concentration c) 7.5 µM protein concentration.

REFERENCES

1. Glover, K. J., Whiles, J. A., Wu, G., Yu, N., Deems, R., Struppe, J. O., Stark, R. E., Komives, E. A., and Vold, R. R. (2001) Structural Evaluation of Phospholipid Bicelles for Solution-State Studies of Membrane-Associated Biomolecules. *Biophys. J. 81*, 2163-71.

2. Whiles, J. A., Deems, R., Vold, R. R., and Dennis, E. A. (2002) Bicelles in Structure-Function Studies of Membrane-Associated Proteins. *Bioorganic Chemistry. 30*, 431-442.

3. McKibbin, C., Farmer, N. A., Jeans, C., Reeves, P. J., Khorana, H. G., Wallace, B. A., Edwards, P. C., Villa, C., and Booth, P. J. (2007) Opsin Stability and Folding: Modulation by Phospholipid Bicelles. *J. Mol. Biol. 374*, 1319-1332.

4. Mimms, L. T., Zampighi, G., Nozaki, Y., Tanford, C., and Reynolds, J. A. (1981) Phospholipid Vesicle Formation and Transmembrane Protein Incorporation using Octyl Glucoside. *Biochemistry. 20*, 833-40.

5. Machleidt, T., Li, W. P., Liu, P., and Anderson, R. G. (2000) Multiple Domains in Caveolin-1 Control its Intracellular Traffic. *J. Cell Biol. 148*, 17-28.

6. Losonczi, J. A., Olejniczak, E. T., Betz, S. F., Harlan, J. E., Mack, J., and Fesik, S. W. (2000) NMR Studies of the Anti-Apoptotic Protein Bcl-xL in Micelles. *Biochemistry. 39*, 11024-11033.

7. Mayer, G., Ludwig, B., Muller, H. -., van den Brook, J. A., Friesen, R. H. E., and Schubert, D. (1999) Studying Membrane Proteins in Detergent Solution by Analytical Ultracentrifugation: Different Methods for Density Matching. *Progr Colloid Polym Sci. 113*, 176-181.

8. Fleming, K. G. (2000) Probing Stability of Helical Transmembrane Proteins. *Methods Enzymol. 323*, 63-77.

9. Noy, D., Calhoun, J. R., and Lear, J. D. (2003) Direct Analysis of Protein Sedimentation Equilibrium in Detergent Solutions without Density Matching. *Anal. Biochem. 320*, 185-192.

Chapter 4. Investigating LMPG and LMPC micelles for the study of membrane protein interactions in the AUC

ABSTRACT

It is often useful to employ several techniques to study membrane protein structure and function. For example, in studies of the caveolin-1 protein information can be gleaned from both NMR and analytical ultracentrifuge analysis. However, the detergents used in each of these studies were not the same because it is difficult to obtain highly resolved structural data in DPC micelles. On the other hand, DPC micelles have been used successfully in AUC studies to characterize the oligomeric state of caveolin-1 and a P132L mutant (Chapter 2). NMR analysis of the P132L mutant showed a possible explanation for the dimerization of mutant caveolin-1, but these studies were carried out in different detergents which is not ideal when drawing conclusions about membrane protein structure and function. The detergent, LMPG, has proven useful in acquiring structural data of the intramembrane region of caveolin-1, but LMPG has not been density matched or used in studies of membrane protein oligomerization. The goal of this study was to determine if LMPG micelles can be density matched in the AUC so that the oligomerization of caveolin-1 can be investigated in LMPG and compared to structural NMR studies. LMPG micelles are very dense and were not able to be density matched using D_2O or 100 % D_2O^{18}. The detergent, LMPC, was also investigated to determine if a mixed micelle system of LMPG and LMPC could be density matched and translated to structural NMR studies. Although LMPC and LMPG mixed micelles looked promising for AUC studies, structural NMR data of caveolin-1(96-136) showed that only a small amount of LMPC (25 mM) was tolerated before the resolution collapsed. At 25 mM; however, LMPC / LMPG micelles are still too dense to be matched in the AUC.

INTRODUCTION

Although detergent and lipid molecules have the same general properties in that they are amphipathic, they also vary in their ability to solubilize and preserve native protein structure. For this reason, it is difficult to find a universal detergent or lipid system that is optimal to study membrane protein structure and behavior. Often times a rigorous screening is required to find the appropriate detergent or lipid for each application. Not only does the choice of detergent or lipid depend on the protein being studied, it also depends on the analytical method that is employed because not all detergents and lipids are conducive to all analytical methods. For example, dodecylphosphocholine (DPC) is a very native-like detergent that is often used in the study of membrane proteins (1). Specifically, DPC has allowed the oligomeric state of caveolin to be characterized in the AUC. However, this detergent is not always conducive to structural studies using solution NMR. For example, caveolin-1 is soluble in DPC micelles, but it does not allow useful NMR data to be obtained. The chemical shifts of most amino acid residues are not able to be resolved using this detergent. The lipid, LMPG, has been particularly useful in acquiring interpretable NMR data. In order to compare structural studies of caveolin with oligomeric studies obtained from AUC experiments, it is best if this can be accomplished using the same detergent or lipid system. Studies of membrane protein oligomerization have not been accomplished using LMPG in the AUC; therefore, in this chapter the utility of LMPG as a lipid system in which to study membrane protein interactions in the AUC will be explored. In order to begin these studies, it is necessary to density match LMPG micelles using the same approach that was used to density match bicelles (Chapter 3) where the density of LMPG micelles will first be determined. Subsequently, the LMPG micelles will be subjected to sedimentation equilibrium studies using varying amounts of a density

modifier present in the sample. The density of the LMPG micelles at each concentration of density modifier will be graphed versus the measured buffer density to determine the amount of density modifier required for the effective molecular weight of the micelles to be zero. Once the density matched conditions for LMPG have been established, caveolin-1(62-178) will be incorporated into LMPG micelles and the molecular weight will be evaluated in order to compare the oligomeric state of caveolin-1 in LMPG micelles versus DPC micelles. This study will reveal any dependence of the observed oligomeric state of caveolin on the detergent or lipid system used in our studies. It will further reveal any dependence of caveolin oligomerization on the lipid environment in which it resides.

MATERIALS AND METHODS

Measuring the density of LMPG and LMPC lipid solutions

Solutions of LMPG were prepared separately at different concentrations in a buffer containing 10 mM HEPES, 100 mM NaCl pH 7.5: 400 mM, 350 mM, 300 mM, 250 mM, 200 mM, 175 mM, 150 mM, 100 mM, 50 mM, 20 mM, 0 mM. The final volume prepared for each solution was 1.8 mL which is the minimum volume required to fill the sample loop of the density meter. Due to the extensive amount of lipid required for these measurements the 400 mM LMPG solution was diluted for each subsequent measurement down to 10 mM LMPG. The density measurements of each sample were obtained using a Kyoto Electronics Density/Specific Gravity Meter (model #DA-210).

Preparation of LMPG samples for analytical ultracentrifugation

A solution of 0.5 mg / mL diphenylhexatriene (DPH) was prepared in toluene. In a separate eppendorf tube a 100 mg / mL solution of LMPG in HFIP was prepared. To each of nine eppendorf tubes, 2.39 mg of LMPG (23.9 µL) was added followed by 2 µL (2 µg) of DPH solution. The amount of DPH was determined by calculating the desired molarity based on a target absorbance of 0.5, the extinction coefficient of DPH (88,000 $M^{-1}cm^{-1}$), path length of 1.2 cm, and sample volume of 100 µL. The samples were frozen and lyophilized overnight to create a homogeneous mixture of lipid and DPH. Water was added to each sample (500µL) in order to facilitate freezing and lyophilization.

The lyophilized samples were rehydrated in 100 µL of 10 mM HEPES; 100 mM NaCl pH 7.4 buffer with gentle heating (42 °C water bath) and vortexing until the samples were clear. Samples were loaded into sedimentation equilibrium 6-channel epoxy coated centerpiece and spun at increments of 1000 rpm beginning at 10,000 rpm

77

and increasing to 40,000 rpm. Samples were left to equilibrate at 10,000 rpm for 20 hours before measuring the absorbance profile and 4 hours thereafter at each subsequent speed before measuring the absorbance. The data were treated with the Lamm equation and M_{eff} was measured from the slope of the ln(c) vs. the square of the radius from the center of rotation:

$$\frac{\ln(c_r)}{r^2} = \frac{M(1-\bar{v}\rho)\omega^2}{2RT}$$

Preparation of caveolin-1(96-136) NMR samples in LMPG / LMPC lipid mixtures

Uniformly ^{15}N-labeled Cav1(96-178) was prepared by overexpressing in *E. coli* grown in auto-induction media supplemented with ^{15}NH$_4$Cl salt according to the method of Lee et al. (Appendix II – N-5052 Media) (5). Lyophilized caveolin-1(96-136) protein was reconstituted into three different solutions containing varying ratios of LMPG and LMPC but not exceeding a total lipid concentration of 100 mM: 1) 100 mM LMPG, 2) 75 mM LMPG / 25 mM LMPC, 3) 50 mM LMPG / 50 mM LMPC, 4) 25 mM LMPG / 75 mM LMPC, 5) 100 mM LMPC. The caveolin-1(96-136) protein-lipid solutions were buffered with 20 mM phosphate, 150 mM NaCl pH 7.5 containing 10% D$_2$O (v/v).   The solutions were vortexed vigorously for several minutes, immersed in a hot water bath (95 °C) for one minute, and centrifuged for 10 minutes at 20,000 x g at room temperature. A clear solution was obtained with no visible precipitate.

NMR data was acquired at 25 °C on a 600 MHz Bruke r Advance II spectrometer (Billerica, MA) equipped with a cryoprobe. TROSY-HSQC data was obtained for ^{15}N-labeled Cav1(96-136) in different LMPG / LMPC solutions. The spectra were processed using NMRPipe and Sparky (2, 3).

RESULTS AND DISCUSSION

The density of LMPG was determined by measuring solutions of LMPG that were prepared in a 10 mM HEPES; 100 mM NaCl buffered solution at pH 7.4. The results of the LMPG density measurements are summarized in Table 4.1. Densities were plotted against the concentration of each LMPG solution in order to determine the slope of the linear relationship between lipid concentration and density (Figure 4-1). From these results the density of the LMPG lipid can be calculated based on the method of Durchschlag (4).

$$\varphi_2 = \frac{1}{\rho_s} \left[1 - \left(\frac{\rho - \rho_s}{c_2} \right)_m \right]$$

From this equation, the density of LMPG was calculated to be 1.21 g / mL. This density is significantly higher than water (1.0 g / mL) and requires a large quantity of a density modifier present in the sample to be matched. Based on the density matching study of bicelles in Chapter 3 a 1.08 g / mL density is required to match the density of q = 1.0 bicelles. This corresponds to 71.7% D_2O required in the sample. Using the program, *Sednterp, version 1.0, U. of New Hampshire*, to calculate the density of a 100% D_2O solution buffered with 10 mM HEPES, 100 mM NaCl pH 7.4, it was found that the density of 100% D_2O is 1.107 g / mL. This density is not high enough to match LMPG micelles based on the calculated density. As an alternative, D_2O^{18} was investigated as a density modifier as well. Using *Sednterp, version 1.0, U. of New Hampshire* to calculate the density of 100% D_2O^{18} it was found to be 1.21623 g / mL, which is suitable to completely match the density of LMPG micelles.

Sedimentation equilibrium (AUC) experiments were carried out to experimentally determine the partial specific volume of LMPG micelles. 50 μL samples containing 50

mM LMPG doped with DPH at a ratio of 1:10,500 (DPH : LMPG) were initially spun at 10,000 rpm (8050 x g) for 16 hours until equilibrium was reached. The LMPG micelles were measured at a wavelength of 352 nm, which corresponds to the λ_{max} absorbance of DPH. After spinning for 16 hours at 10,000 rpm, the speed was increased by 1000 rpm, the samples were left to equilibrate for 6 hours (determined empirically) and the absorbance profiles were recorded. The speed of the analytical ultracentrifuge was increased to a maximum of 40,000 x g. The M_{eff} of each sample was calculated using the Lamm equation (Materials and Methods) to determine the concentration of D_2O^{18} required for $M_{eff} = 0$ for LMPG micelles. Preliminary results show that at all concentrations of D_2O^{18} that were sampled in the AUC, LMPG was more dense than the buffer (Figure 4-2). By extrapolating the M_{eff} data we can see that the amount of D_2O^{18} required to achieve M_{eff} of zero for LMPG is 103% (v/v). Therefore, it is not possible to completely density match LMPG micelles using heavy water. It is clear from the sedimentation equilibrium experiments that LMPG creates very dense lipid micelles making it difficult to adapt to sedimentation equilibrium experiments. However, it may be possible to mix LMPG with a similar lipid such as LMPC in order to attenuate the density of the LMPG. LMPC has the same lipid chain length as LMPG and a choline head group instead of the glycerol head group of LMPG. LMPC has also been used successfully in NMR to obtain structural information about membrane proteins. The density of this lipid was also measured at various concentrations of LMPC, and the data were tabulated (Table 4.2) and plotted against lipid concentration (Figure 4-3). By treating the slope of the line in Figure 4-3 with the Durchschlag equation the density of LMPC was calculated to be 1.086 g / mL, which still exceeds the density of 100% D_2O, but does not exceed the density of D_2O^{18} (1.25 g / mL). A 50 / 50 mixture of the two lipids reveals that the density of the mixed lipid solutions is lower than the LMPG solutions, which indicates

80

that a mixture of these two lipids may be more amenable to sedimentation equilibrium studies (Table 4.3). The density data for the lipid mixture was also plotted as a function of total lipid concentration in order to quantitate the density of the 50 / 50 LMPG / LMPC mixture (Figure 4-4). The density was calculated to be 1.15 g / mL, which is approximately equivalent to the average of the densities of LMPG and LMPC. The minimum amount of LMPG required to achieve a target density of 1.15 g / mL in a mixture of both lipids was calculated to be 37.5 % (w/w). The calculated value differs slightly from the density that was measured for the 50 / 50 mixtures of the two lipids. However, it is clear that at least 50% LMPC lipid is required to lower the density to where sedimentation equilibrium can be carried out.

LMPG is a powerful lipid that has been used with success to obtain structural information about the caveolin-1 protein (5). Few lipids are able to provide such valuable information about caveolin structure. The goal of these experiments was to adapt LMPG to sedimentation equilibrium studies in the AUC so that both structural and behavioral information can be obtained for caveolin using the same lipid system. Membrane protein structure and function can be influenced by the lipid medium in which it resides, therefore, it is ideal to study caveolin in the same lipid system. In order to proceed using a mixture of LMPG and LMPC, it is important to evaluate the ability of this lipid mixture to support caveolin-1 structure, which can be determined using solution NMR. To evaluate the utility of the LMPG / LMPC lipid mixture, the intramembrane region of caveolin-1 (96-136) was labeled with ^{15}N and reconstituted into mixtures of LMPG / LMPC. HSQC spectra were obtained for each sample and compared to the structure of caveolin-1(96-136) in 100% LMPG. We can see from Figures 4-5, 4-6, 4-7, 4-8, and 4-9 that as LMPC is added to the samples, the resolution of the peaks begins to diminish. This indicates that LMPC does not have the ability to provide clearly resolved

81

structural data compared to LMPG. The presence of LMPC is tolerated up to a concentration of 25 mM (Figure 4-6), which shows that most of the signals from each residue are clearly resolved and well-dispersed in the spectrum. However, at 50 mM LMPC the peaks begin to collapse and overlap significantly, which indicates that this lipid mixture is not suitable to acquire structural data. From the sedimentation equilibrium studies and the density meter studies we know that a minimum of 50 mM LMPC is desirable for density matching to be achieved, but if the presence of LMPC cannot support caveolin structure then it is not possible to use this lipid system to evaluate oligomerization in the analytical ultracentrifuge.

CONCLUSIONS

LMPG is an anionic detergent phospholipid that has been used successfully to solve membrane protein structure using solution NMR. It has been used to elucidate important structural information about the integral membrane protein, caveolin-1. Aside from structural information we wanted to probe the utility of LMPG in evaluating protein interactions in the analytical ultracentrifuge. By using the same lipid in which to evaluate membrane protein structure and function we can better compare this data in order to learn how this protein is able to curve the plasma membrane *in vivo*. The lipid system in which membrane proteins are studied can have a significant effect on their structure and function. Therefore, it is desirable to use the same lipid in multiple studies. In this study we attempted to adapt LMPG to sedimentation equilibrium experiments in the AUC. LMPG is a very dense lipid and alone cannot be density matched. However, LMPC is a similar lipid that has been used with some success in membrane protein NMR studies. It has a significantly lower density than LMPG and we show that a 50 / 50 mixture of the two lipids has a density closer to 1.0 g /mL, which is more conducive to density matching. HSQC NMR data of caveolin-1(96-136) in LMPG / LMPC mixtures shows that LMPC is not amenable to NMR studies of caveolin because the signals from the amino acid residues collapse in the presence of LMPC. The collapse of the HSQC NMR signal from caveolin intramembrane domain residues may be due to two reasons: LMPC creates a highly dynamic environment for protein structure causing peak broadening, or LMPC is zwitterionic and the lack of net charge (like LMPG) may not be strong enough to prevent caveolin from aggregating. Although LMPC can be density matched in the AUC, it is not suitable for NMR studies of caveolin, therefore, it offers no advantages over other detergents such as DPC, which has been both successfully density matched and used to obtain oligomeric information about membrane proteins.

Table 4.1. Density measurements of LMPG solutions.

LMPG concentration (mM)	Density (mL)	LMPG concentration (mg / mL)
400.	1.03122	191.4
350.	1.02748	167.5
300.	1.02367	143.6
250.	1.01996	119.6
200.	1.01616	95.7
175	1.01425	83.7
150.	1.01205	71.8
100.	1.00848	47.9
50.0	1.00470	23.9
20.0	1.00239	9.57
0.00	1.00044	0.00

Table 4.2. Density measurements of LMPC solutions

LMPC concentration (mM)	Density (mL)	LMPC concentration (mg / mL)
400.	1.01507	187.0
350.	1.01422	164.0
300.	1.01233	141.0
250.	1.01045	117.0
200.	1.00856	93.5
175	1.00761	82.0
150.	1.00662	70.0
100.	1.00455	46.8
50.0	1.00275	23.4
20.0	1.00161	9.35
0.00	1.00074	0.00
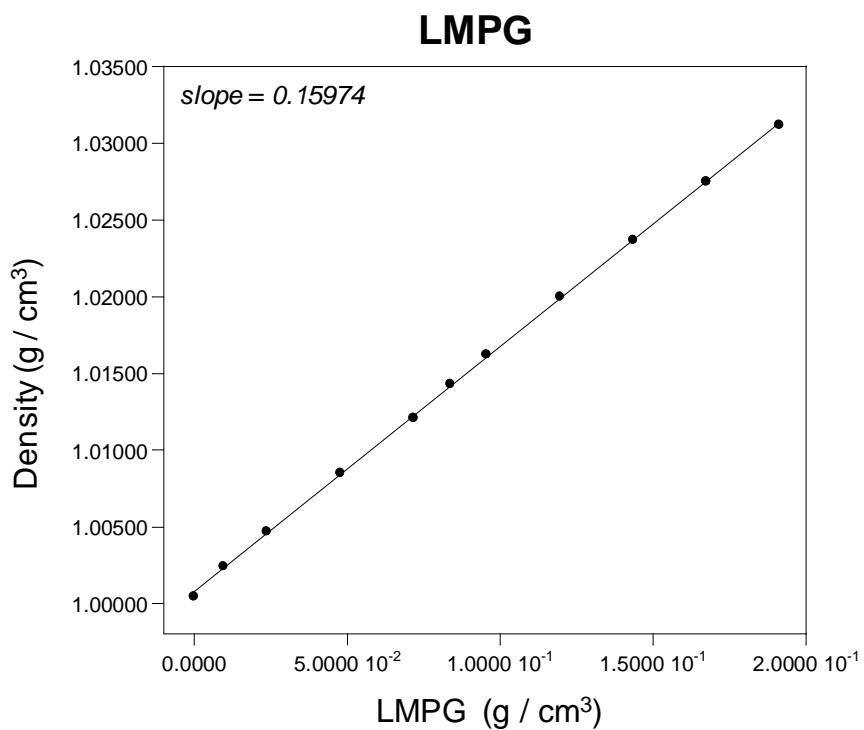
Figure 4-1. Measured LMPG density versus LMPG concentration plotted from Table 4.1. The slope of the line is used to determine the partial specific volume of LMPG micelles, which was found to be 0.83989 cm^3 / g using the Durchschlag equation.
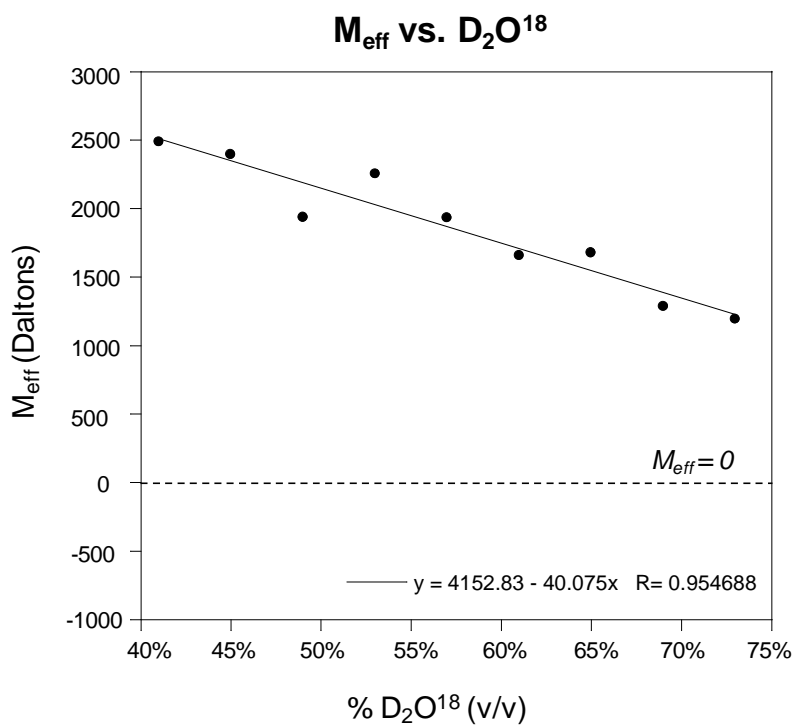
Figure 4-2. M_{eff} determination of LMPG micelles at various D_2O^{18} concentrations. LMPG micelles are not able to be density matched using D_2O^{18}. Using the equation of the line, the amount of D_2O^{18} required to reach $M_{eff} = 0$ is 103% (v/v).
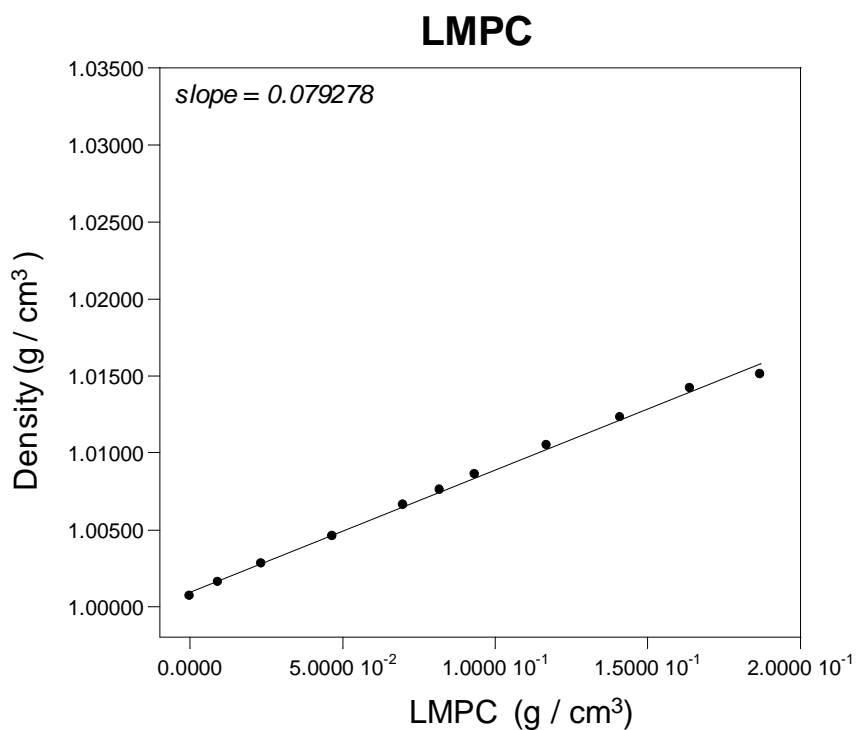
Figure 4-3. Measured LMPC density versus LMPC concentration plotted from Table 4.2. The slope of the line is used to determine the partial specific volume of LMPC micelles, which was found to be 0.92004 cm^3 / g using the Durchschlag equation.

Table 4.3. Density measurements of LMPC and LMPG mixtures.

LMPC concentration (mM)	LMPG concentration (mM)	Density (g /mL)
200.	0.00	1.00856
140.	60.0	1.01465
100.	100.	1.01547
40.0	160.	1.01740
0.00	200.	1.01661
0.00	0.00	0.99990

Density of 50 / 50 LMPG-LMPC Solutions vs. Total Lipid Concentration

y = 0.9972 + 0.13296x   R= 0.99999

$\bar{v} = 0.87020\ cm^3 / g\ or$
$approx.\ 1.150\ g / cm^3$

Y-axis: Density (g / cm^3)

X-axis: Total Lipid Concentration (mM)
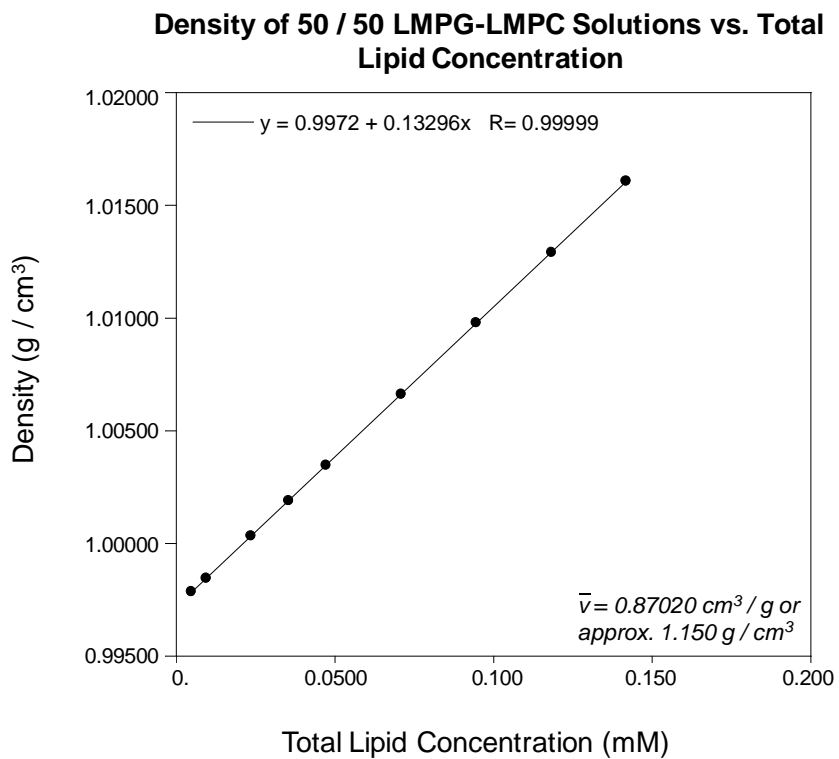
Figure 4-4. Density measurements of 50 / 50 LMPG / LMPC solutions versus total lipid concentration. The slope of this line was used to determine the partial specific volume of a 50/50 LMPG / LMPC micelle mixture, which was found to be 0.87020 cm^3 / g or 1.15 g / cm^3 using the Durchschlag equation.
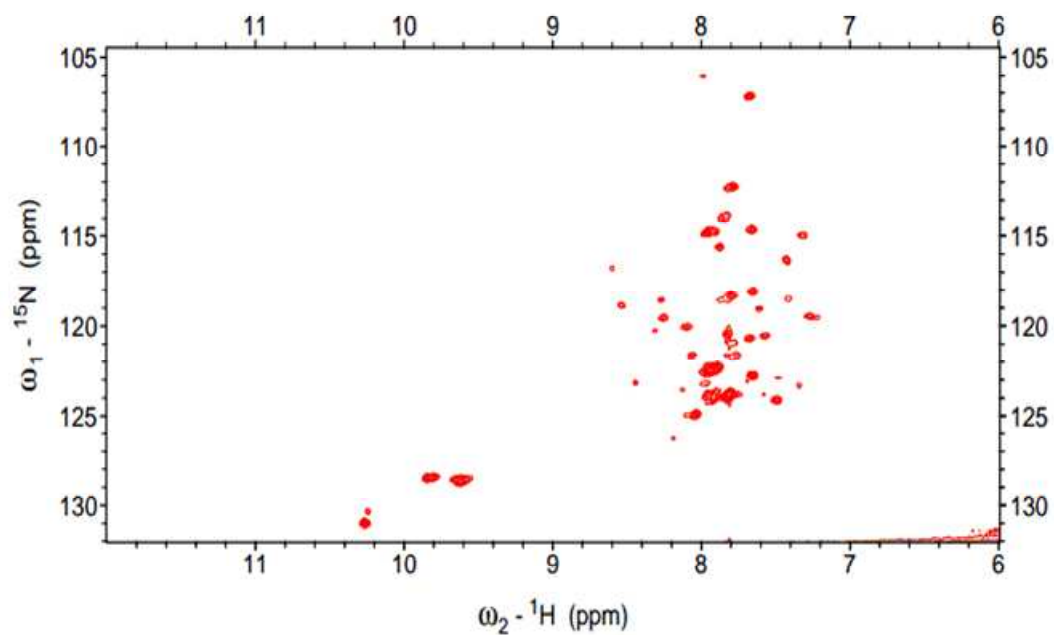
Figure 4-5. ^{1}H-^{15}N HSQC spectrum of Cav1(96-136) in 100 mM LMPG. The signals from all amino acid residues are resolved and peaks are well-dispersed.
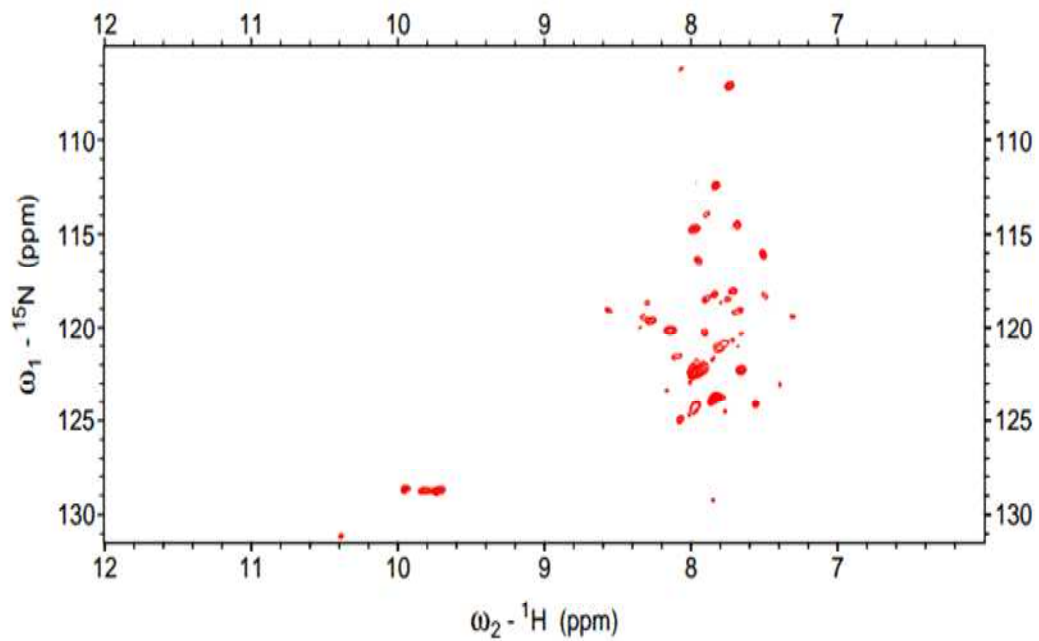
Figure 4-6. ^{1}H-^{15}N HSQC spectrum of Cav1(96-136) in 75 mM LMPG, 25 mM LMPC. The signals from most amino acid residues are resolved and they are still relatively well-dispersed.
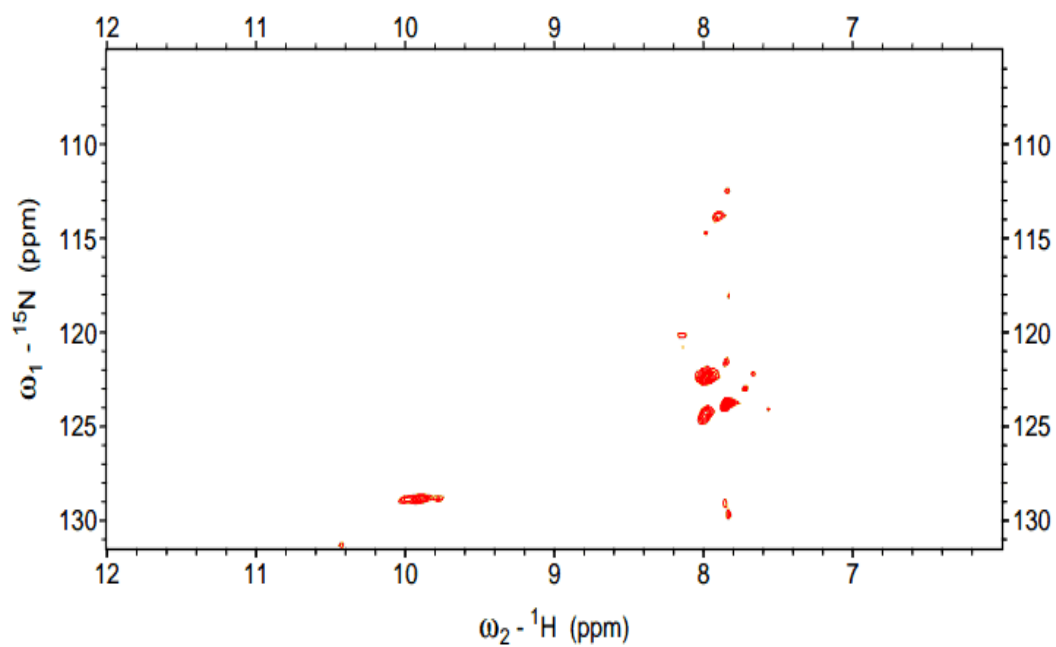
Figure 4-7. ^{1}H-^{15}N HSQC spectrum of Cav1(96-136) in 50 mM LMPG, 50 mM LMPC. Signals from amino acid residues have disappeared and there is significant peak broadening. The signal is no longer well-dispersed.
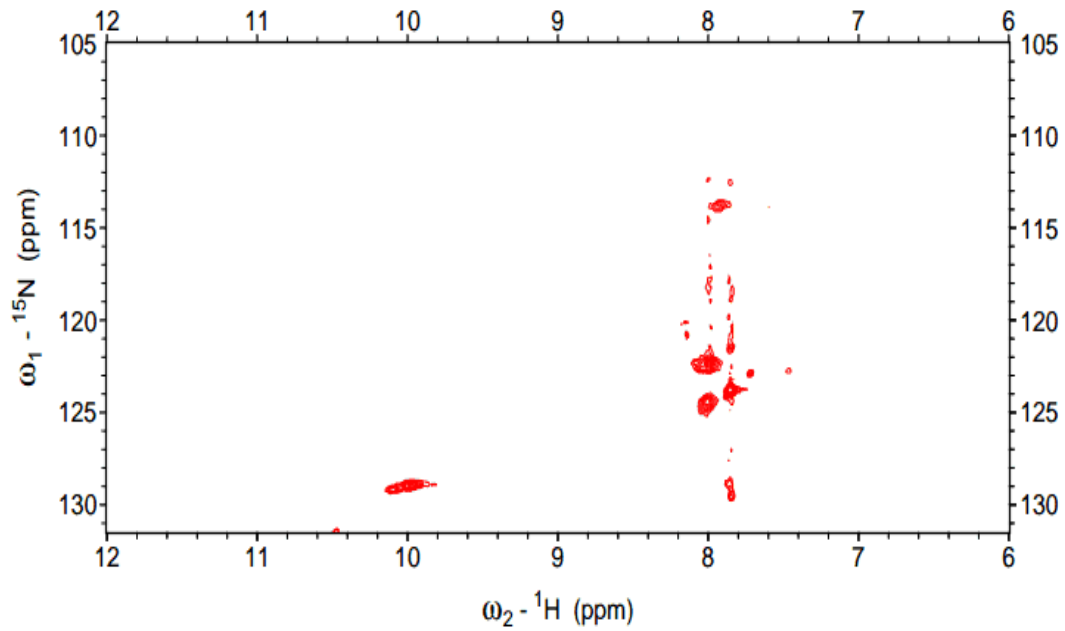
Figure 4-8. ^{1}H-^{15}N HSQC spectrum of Cav1(96-136) in 25 mM LMPG, 75 mM LMPC. Signals from amino acid residues have disappeared and there is significant peak broadening. The signal is no longer well-dispersed.
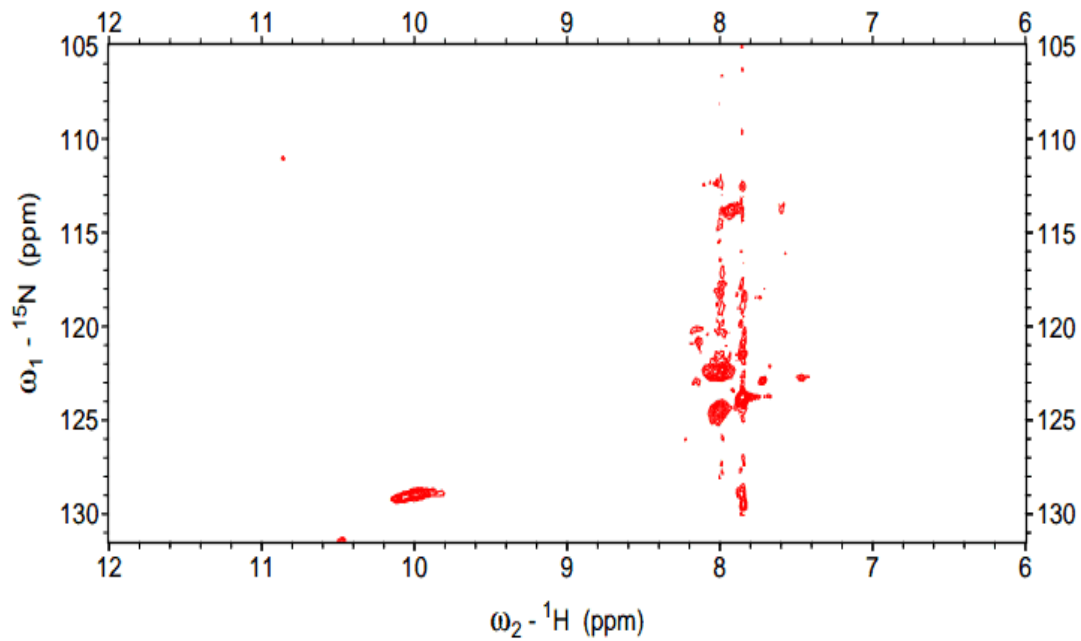
Figure 4-9. ^{1}H-^{15}N HSQC spectrum of Cav1(96-136) in 100 mM LMPC. Signals from amino acid residues have disappeared and there is significant peak broadening. The signal is no longer well-dispersed.

REFERENCES

1. Tamm, L. K., Abildgaard, F., Arora, A., Blad, H., and Bushweller, J. H. (2003) Structure, Dynamics and Function of the Outer Membrane Protein A (OmpA) and Influenza Hemagglutinin Fusion Domain in Detergent Micelles by Solution NMR. *FEBS Lett. 555*, 139-143.

2. Delaglio, F., Grzesiek, S., Vuister, G. W., Zhu, G., Pfeifer, J., and Bax, A. (1995) NMRPipe: A Multidimensional Spectral Processing System Based on UNIX Pipes. *J. Biomol. NMR. 6*, 277-293.

3. Goddard, T. D., and Kneller, D. G. *Sparky 3.* University of California, San Francisco.

4. Durchschlag, H. (1986) Specific Volumes of Biological Macromolecules and some Other Molecules of Biological Interest, in *Thermodynamic Data for Biochemistry and Biotechnology* (H. Hinz, Ed.) pp 46, Springer-Verlag, .

5. Lee, J., and Glover, K. J. (2012) The Transmembrane Domain of Caveolin-1 Exhibits a Helix-Break-Helix Structure. *Biochim. Biophys. Acta.*

Chapter 5. Investigation of C8E5 / DMPC Lipid Aggregates

ABSTRACT

Lipids and detergents can have a significant impact on membrane protein structure and function. When studying membrane protein oligomerization it is important to consider the lipid or detergent system in which these studies are carried out. Bicelles are unique in that they provide a lipid bilayer region that can support membrane protein structure and function. Also, bicelles are dynamic and allow proteins and other molecules to freely associate and dissociate. In traditional bicelles the two most commonly used phospholipids are DMPC, used as the long-chain lipid, and DHPC, used as the short-chain lipid. These bicelles were previously density matched in the analytical ultracentrifuge using 71.7% D_2O so that caveolin oligomerization could be carried out. The bicelles proved to be a very valuable tool in caveolin oligomerization experiments, but with 71.7% D_2O present in the sample, meaningful data could only be achieved at exceptionally high speeds (above 50,000 x g). The goal of this study was to investigate a new lipid aggregate system where pentaethylene glycol monooctyl ether (C8E5) was used as the short-chain, rim-capping detergent instead of DHPC. C8E5 has a density of 1.007 g /cm^3 making it very similar to water. This is expected to lower the density of DMPC / C8E5 lipid aggregates such that they will not require density matching or the use of a density modifier. By avoiding the use of density modifiers like D_2O, higher speeds will not have to be sampled in order to sediment proteins in oligomerization studies.

INTRODUCTION

In the study of membrane protein interactions many detergents and lipids that are effective at solubilizing membrane proteins are not always conducive to biophysical studies. In analytical ultracentrifugation it is often necessary to perform a technique called density matching to subtract out the molecular weight contribution of the surrounding lipids when investigating the oligomeric state of membrane proteins. This technique is necessary to avoid inflating the calculated molecular weight of the sedimenting species when the lipid and / or detergent is more dense than the buffer. Micellar systems have been density matched in the past and used successfully to assess membrane protein oligomerization. More recently, this technique has been used to density match bicelles (Chapter 3); however, the high levels of density modifier required (e.g. 71.7 % D_2O) can be problematic. When attempting to study low molecular weight peptides and proteins high speeds are required to sediment these species. When high amounts of density modifier are present it can be difficult to achieve the speeds necessary to sediment small peptides or proteins. DMPC and C8E5 both have densities that are similar to water, 1.0381 g / cm^3 and 1.0071, respectively (1, 2). Therefore, it may not be necessary to density match these detergents when using them to study membrane protein interactions in the analytical ultracentrifuge. It is unclear whether mixtures of DMPC / C8E5 form a mixed micelle system or a bicelle system like the DMPC / DHPC system. We hypothesize that the C8E5 / DMPC lipid / detergent system forms a bicellar lipid / detergent aggregate similar to the DMPC / DHPC system previously observed. To answer this question, ^{31}P-phosphorus NMR experiments were carried out to compare the chemical shift of DMPC in both a DMPC / DHPC bicelle sample and a DMPC / C8E5 sample. Lipids that are organized heterogeneously as in the case of the DMPC / DHPC bicelle system experience different lipid environments

98

giving rise to two distinct chemical shifts in the NMR arising from the phosphorous headgroup on the short-chain lipid (DHPC) versus the phosphorus group on the long-chain lipid (DMPC). The presence of two distinct environments is indicative of a heterogenouse bicelle-like organization of the lipids. Although, C8E5 does not contain a phosphorus headgroup, the chemical shift of DMPC in the C8E5 / DMPC sample is expected to produce a similar chemical shift to that of the DMPC / DHPC sample if it is experiencing a bicelle-like environment. A lanthanide shift reagent will be added to the lipid samples to enhance the resolution between the signal from DMPC and DHPC in the control bicelle sample. It will be included in the DMPC / C8E5 solutions as well. Praseodymium (III) chloride has been used successfully to differentiate the signal from DMPC and DHPC in ^{31}P-NMR (3).

Dynamic light scattering experiments were also carried out at theoretical q values based on previous studies that were carried out on DMPC / DHPC lipid systems (4). The diffusion of small particles or lipid aggregates to their hydrodynamic radius can be determined using the Stokes-Einstein equation where D is the diffusion coefficient of the fluctuating particles, k is the Boltzmann constant, T is the absolute temperature (K) and is held constant, η is the measured viscosity (cP), and the hydrodynamic radius, R_h (nm) is then calculated (5):

$$D = \frac{kT}{6\pi\eta R_h}$$

The goal of the light scattering experiments was to determine if the morphology and size of the C8E5 / DMPC aggregates changed relative to the theoretical q value or the ratio of C8E5 to DMPC. Last, the total lipid concentration was varied in order to determine if the lipid aggregate size and morphology vary depending on the total lipid concentration,

a characteristic that has been seen in DMPC / DHPC bicelle systems at different lipid concentrations (4).

The DMPC / C8E5 lipid solutions were evaluated in the analytical ultracentrifuge using sedimentation equilibrium to determine if these aggregates sediment in the absence of a density modifier. Three different theoretical bicelle q values were evaluated: 0.1, 0.25, and 0.5 where q was determined by the moles of DMPC / moles of C8E5.

MATERIALS AND METHODS

^{31}P-phosphorus NMR Experiments

Samples with a 25% (w/w) total lipid composition, and q = 1.0 were prepared for ^{31}P-phosphorus NMR experiments. To a 1.5 mL Eppendorf tube, 129.59 mg DMPC was added. The DMPC powder was reconstituted into bicelles to a final volume of 1.0 mL with 254.30 µL of 25% (w/w) DHPC () or 101.25 µL of C8E5 (143mM), D_2O, H_2O, 3 M sodium acetate (pH 5.6) with a final composition of 10% (v/v) D_2O, 90% H_2O, and 20 mM sodium acetate. Praeseodymium chloride powder was added to a final concentration of 197 mM as per Glover et al. (4). This concentration was previously determined to saturate the lanthanide-phospholipid interaction (3).

NMR experiments were carried out on a Bruker DRX500 spectrometer equipped with a BBI probe. One dimensional ^{31}P spectra were recorded at 25, 27, 29, 31, 35, 37 °C using a proton-decoupled single-pulse experiment with a minimum of 16 scans and a 100 ppm sweep width. The experiments were processed in TopSpin v. 1.3 (Bruker Corp.).

Dynamic Light Scattering Experiments

C8E5 / DMPC lipid / detergent samples were prepared at different q values and different lipid concentrations. In the first set of samples, the lipid concentration was held constant at 5% (w/w) while q varied from 0.05 to 0.5. Samples were prepared on a 12 mL volume scale:

q	5% lipid sample		40 X HEPES buffer (0.4 M HEPES; 4 M NaCl pH 7.4)	ddH$_2$O
	DMPC (mg)	C8E5 (µL)		
0.05	52.91	552.62	300 µL	11.100 mL
0.10	97.24	507.83	300 µL	11.100 mL
0.15	134.93	469.77	300 µL	11.100 mL
0.20	167.36	437.01	300 µL	11.100 mL
0.25	195.57	408.52	300 µL	11.100 mL
0.30	220.32	383.52	300 µL	11.100 mL
0.35	242.21	361.40	300 µL	11.100 mL
0.40	261.72	341.69	300 µL	11.100 mL
0.45	279.21	324.03	300 µL	11.100 mL
0.50	294.99	308.10	300 µL	11.100 mL

In the second set of samples, the lipid concentration was varied between 1% and 25% (w/w). *q* was held constant at 0.25. Samples were prepared on a 12 mL volume scale:

% lipid concentration (w/w)	DMPC (mg)	C8E5 (µL)	40 X HEPES buffer (0.4 M HEPES; 4 M NaCl pH 7.4)	ddH$_2$O
1	39.11	81.70	300 µL	11.580 mL
5	195.57	408.52	300 µL	11.100 mL
10	391.13	817.04	300 µL	10.500 mL
15	586.70	1225.55	300 µL	9.900 mL
20	782.27	1634.07	300 µL	9.300 mL
25	977.84	2042.59	300 µL	8.700 mL

Viscosity measurements were carried out on a Cannon Fenske viscometer and light scattering experiments were carried out on an ALV-CGS3 compact goniometer

equipped with a 22 mW HeNe laser at a wavelength of 632.8 nm. The autocorrelation function of scattered light intensity was acquired at 90 °C. The intensity weighted hydrodynamic radius was determined for each DMPC / C8E5 lipid solution using the Cumulants algorithm provided by the ALV software.

Sedimentation Equilibrium (AUC)

Three DMPC / C8E5 lipid solutions were evaluated at three theoretical q values: 0.1, 0.25, and 0.5 and a total lipid composition of 5 % (w/w). A small amount of NBD-labeled DMPE was incorporated into DMPC / C8E5 samples to allow the lipid aggregates to be monitored using absorption optics. The ratio of NBD-labeled lipid to unlabeled lipid was kept sufficiently high so that the label did not influence the physical properties of the aggregates (1:500 mole ratio of NBD-DMPE:DMPC). Samples were prepared by lyophilizing appropriate amounts of DMPC and DMPE-NBD together. The final sample volume was 150 μL:

q value	DMPC (mg)	NBD-DMPE (mg)	C8E5 (mg)	ddH$_2$O (μL)	40X HEPES buffer (μL)
0.1	1.216	0.003650	6.35	138.75	4.0
0.25	2.436	0.003650	5.11	138.75	4.0
0.5	3.686	0.003650	3.85	138.75	4.0

All sedimentation equilibrium studies were carried out at 25 °C using a 6-channel equilibrium charcoal-filled epon centerpiece with a pathlength of 1.2 cm. Samples were initially equilibrated at 10,000 rpm for 16 hours to allow equilibrium to be reached. Equilibrium measurements were evaluated using Match in the program, HeteroAnalysis (University of Connecticut, Storrs CT). Thereafter speeds were increased by 5,000 rpm and samples were left to equilibrate for 4 hours before acquiring data. A flat line with a zero slope indicates no sedimentation has occurred and M$_{eff}$ = 0 for the lipid aggregates.

RESULTS AND DISCUSSION

^{31}P-phosphorus NMR experiments reveal that the chemical shift of DMPC in bicelle and DMPC / C8E5 lipid solutions is very similar (Figures 5-1 and 5-2). Experiments were run at several temperatures to determine if the slight change in the DMPC chemical shift was enhanced with temperature. Although, the chemical shift appears to fluctuate slightly in both solutions with changes in temperature, we would expect DMPC to have a significantly different chemical shift if it were not associated with C8E5 in a bicelle-like environment. The peak for DMPC in C8E5 is shifted slightly downfield which is not completely surprising given the presence of oxygen atoms in the hydrocarbon tail of the C8E5 detergent whereas there are no oxygen atoms present in the hydrocarbon tail of DHPC. The chemical shift data indicates that DMPC may be in a bicelle-like arrangement similar to what was previously observed by Glover et al (4). This study supports the hypothesis that DMPC / C8E5 associates in a bicelle-like manner. To further characterize these lipid aggregates, dynamic light scattering experiments were carried out to measure the hydrodynamic radius as a function of theoretical *q*, moles of DMPC / moles of C8E5.

Results of the dynamic light scattering experiments reveal that as the theoretical *q* value of the C8E5 bicelles increases the hydrodynamic radius of the lipid aggregates increases significantly (Figure 5-3). A lipid aggregate that contains a planar region, as in the case of bicelles, could carve out a large radius as it tumbles in solution giving rise to a sharp increase in the hydrodynamic radius as *q* gets larger. A mixed micelle solution would not be expected to give rise to such a large increase in the hydrodynamic radius as **q** increases. In general, the DMPC / C8E5 lipid aggregates are much larger compared to DMPC / DHPC bicelles (4). In Figure 5-4 the affect of the total lipid concentration (% w/w) on the hydrodynamic radius of the aggregates was plotted. As

the lipid concentration increases, the hydrodynamic radius of the aggregates approaches zero. Data at a lipid concentration of 25% (w/w) could not be collected, which may be attributed to the apparent decrease in size with increasing lipid concentration. The size of the lipid aggregates decreases with increasing lipid concentration even when q is held constant at 0.25.

Figure 5-5 shows the results of the sedimentation equilibrium experiment. Experiments show that DMPC / C8E5 lipid aggregates are not as dense as traditional DMPC / DHPC bicelles, but they still migrate down the solution column at modest speeds indicating that they have a density that is significantly higher than water. Without the use of a density modifier, it is not possible to completely density match the DMPC / C8E5 lipid-detergent aggregates.

CONCLUSIONS

The goal of this study was to find an alternative bicelle-like lipid aggregate that would provide a bilayer environment in which to characterize protein oligomerization. Ideally, the new bilayered lipid aggregate would have a density that was equal to the density of water so that density matching sedimentation equilibrium experiments would not have to be carried out. By avoiding the need to add a density modifier such as D_2O, excessive speeds can be avoided in sedimentation equilibrium experiments so that smaller proteins can be evaluated for their oligomeric activity. Although the data suggest that DMPC / C8E5 aggregates form a bicelle-like arrangement similar to traditional DMPC / DHPC bicelles, preliminary density matching experiments show that these lipid aggregates are slightly more dense than water and require the need for density matching much like DMPC / DHPC bicelles.

Table 5.1 Viscosity measurements of DMPC / C8E5 samples at various theoretical *q* values.

q value, 5% lipid (w/w)	*Dynamic Viscosity (Pa * s)*	*Viscosity (cP)*
0.05	0.00128	1.27659
0.10	0.00130	1.29977
0.15	0.00129	1.29047
0.20	0.00130	1.29959
0.25	0.00129	1.29459
0.30	0.00131	1.31296
0.35	0.00135	1.35020
0.40	0.00132	1.32339
0.45	0.00150	1.50336
0.50	0.00151	1.51056

Table 5.2 Viscosity measurements of DMPC / C8E5 samples at various lipid concentrations.

q = 0.25, % lipid (w/w)	Dynamic Viscosity (Pa*s)	Viscosity (cP)	R_h (nm)
1	0.00109	1.09144	8.69
5	0.00129	1.28765	4.84
10	0.00182	1.82314	2.22
15	0.00286	2.85859	1.33
20	0.00441	4.41406	0.82
25	0.00674	6.73514	N/A
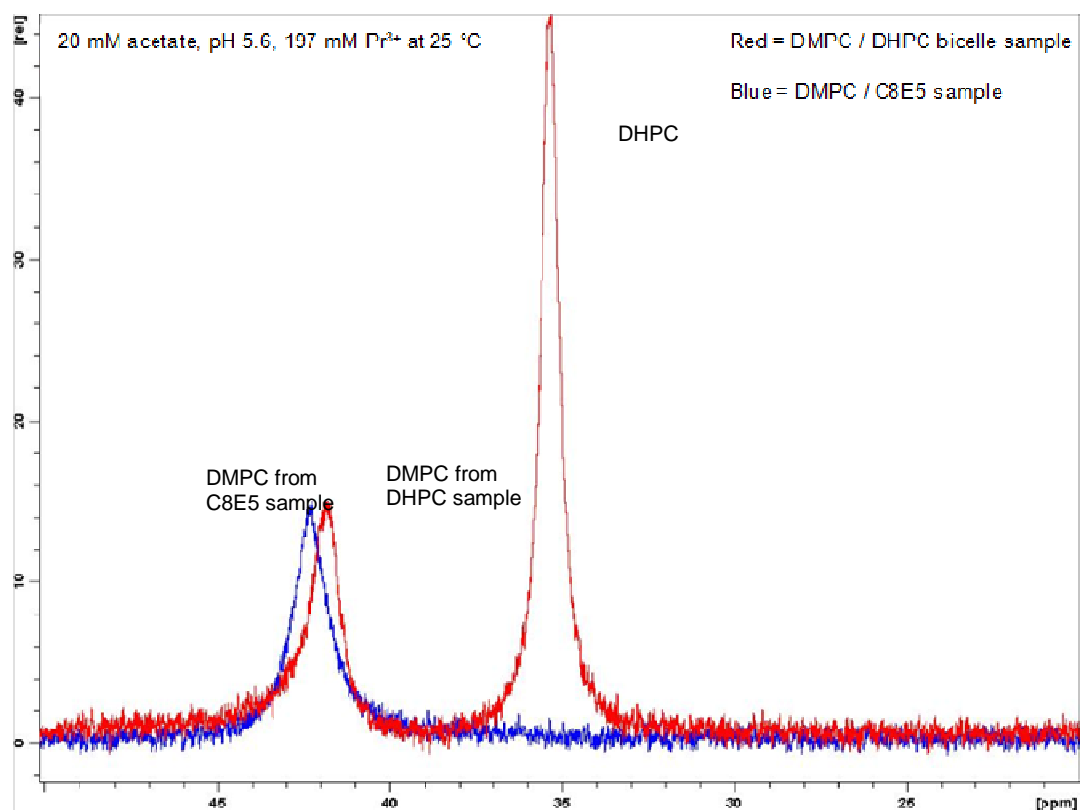
Figure 5-1. Overlay of 1-D ^{31}P-phosphorus NMR spectra of DMPC / DHPC bicelles with DMPC / C8E5 lipid aggregates at 25 °C. The chemical shift of DMPC is highly similar in both lipid samples.
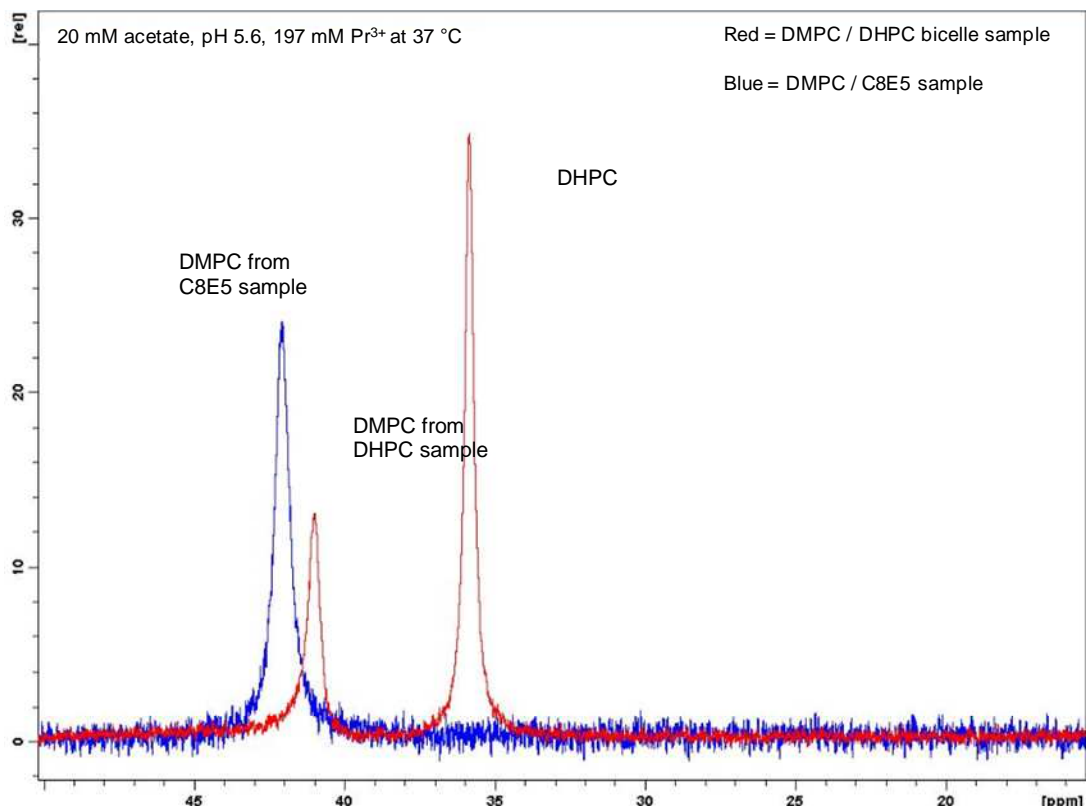
Figure 5-2. Overlay of 1-D ^{31}P-phosphorus NMR spectra of DMPC / DHPC bicelles with DMPC / C8E5 lipid aggregates at 37 °C. The chemical shift of DMPC is highly similar in both lipid samples.
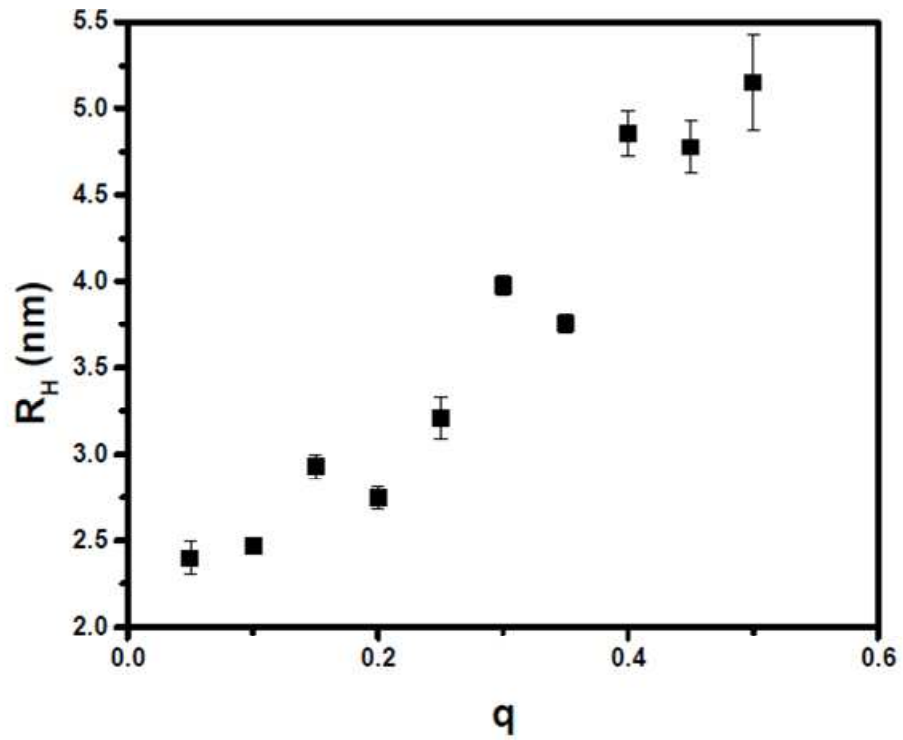
Figure 5-3. Hydrodynamic radius, R_h, versus theoretical **q** values of DMPC / C8E5 solutions.

R_h versus % total lipid concentration
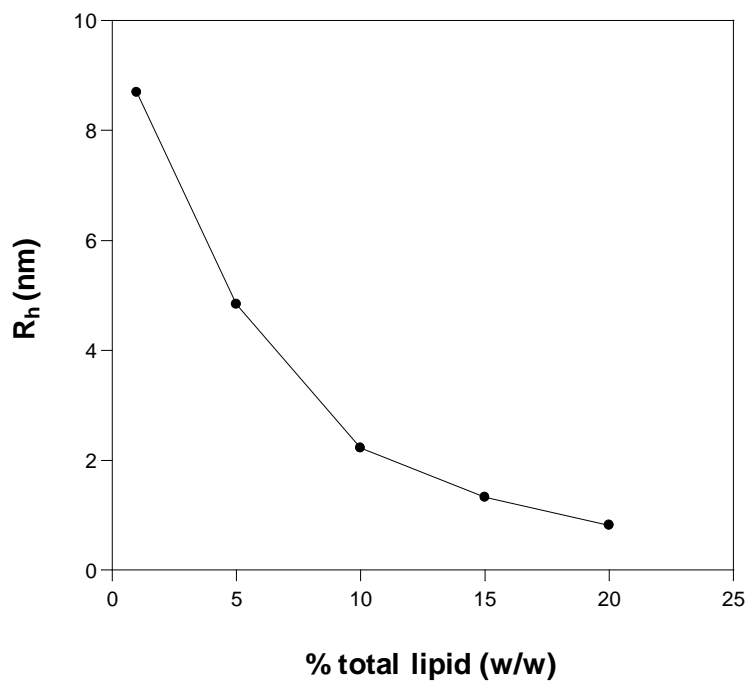
Figure 5-4. Hydrodynamic radius, R_h, versus % lipid concentration (w/w) of DMPC / C8E5 solutions.
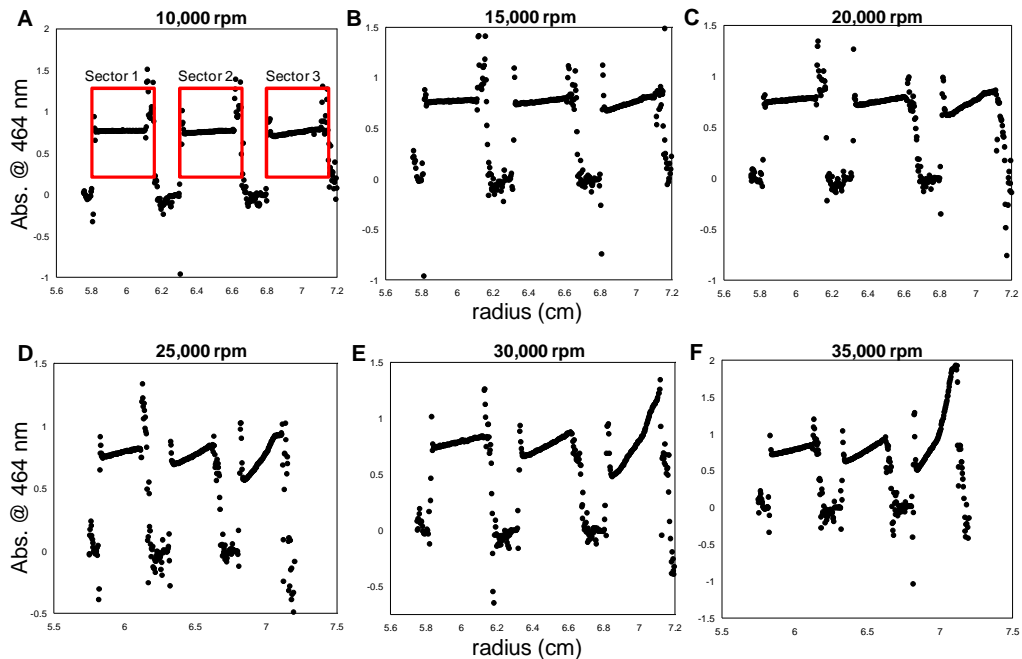
Figure 5-5. Preliminary sedimentation equilibrium (SE) data of DMPC / C8E5 lipid aggregates doped with NBD-labeled DMPE to allow aggregates to be monitored at 464 nm. Sector 1 of the SE centerpiece contains q = 0.1 lipid aggregates, sector 2 contains q = 0.25 lipid aggregates, and sector 3 contains q =0.5 lipid aggregates. Each panel shows the results acquired at different speeds: A) 10,000 rpm B) 15,000 rpm C) 20,000 rpm D) 25,000 rpm E) 30,000 rpm F) 35,000 rpm.

REFERENCES

1. Durchschlag, H. (1986) Specific Volumes of Biological Macromolecules and some Other Molecules of Biological Interest, in *Thermodynamic Data for Biochemistry and Biotechnology* (H. Hinz, Ed.) pp 46, Springer-Verlag, .

2. le Maire, M., Champeil, P., and Moller, J. V. (2000) Interaction of Membrane Proteins and Lipids with Solubilizing Detergents. *Biochim. Biophys. Acta. 1508*, 86-111.

3. Kumar, V. V., and Baumann, W. J. (1991) Lanthanide-Induced Phosphorus-31 NMR Downfield Chemical Shifts of Lysophosphatidylcholines are Sensitive to Lysophospholipid Critical Micelle Concentration. *Biophys. J. 59*, 103-107.

4. Glover, K. J., Whiles, J. A., Wu, G., Yu, N., Deems, R., Struppe, J. O., Stark, R. E., Komives, E. A., and Vold, R. R. (2001) Structural Evaluation of Phospholipid Bicelles for Solution-State Studies of Membrane-Associated Biomolecules. *Biophys. J. 81*, 2163-71.

5. Chu, B. (1991) *Laser Light Scattering: Basic Principles and Practice.* Academic Press, New York.

Chapter 6. Expression and Purification of Membrane Proteins

ABSTRACT

Expression of membrane proteins in bacteria has proven to be a very useful tool in which to acquire useful quantities of membrane protein for biophysical studies. Membrane proteins are extremely toxic to the organisms from which they are expressed and achieving high yields is cumbersome. Ideal expression conditions vary from protein to protein and often expression methods must be determined empirically. In these studies, E. coli was used to express different proteins ranging from small peptides (2 kD) up to fully active proteins with native enzymatic activity (23 kD). To mitigate the toxic effects of membrane protein expression to the E. coli host, most of the proteins were expressed as fusions to a Trp Leader peptide sequence. Trp Leader (tryptophan operon) is native to E. coli and expresses very readily compared to non-native mammalian proteins. This sequence also directs protein expression into inclusion bodies which protects the host organism from the toxic effects of membrane protein expression. Ultimately by expressing proteins into inclusion bodies, large quantities can be achieved. In the following chapter, the Trp Leader expression system proved successful at expressing the desired constructs. Further, E. coli was able to express a full-length protein as well; however, it was not able to produce enzymatically active protein.

INTRODUCTION

In the field of membrane protein biophysics new methodologies are continuously explored to facilitate and enhance the study of these proteins. To assess the utility of new biochemical and biophysical methods it is often advantageous to employ model peptides whose properties have been well-characterized in order to assess the value of a new method. One peptide that is commonly used is a synthetic peptide called "WALP". The WALP peptide is comprised of leucine and alanine repeats flanked on both ends by either tryptophan (W) or lysine (K) residues which help to anchor the peptide in lipid bilayers (1, 2, 3). The WALP peptide can vary in length from 16 up to 31 residues long and can be tailored to the needs of the experiment in which it will be used. WALP was chosen as a model peptide in order to evaluate the utility of bicelles in the analytical ultracentrifuge. The goal was to express and purify the WALP peptide from E. coli so that it can be reconstituted into bicelles and its molecular weight calculated from sedimentation equilibrium experiments in the AUC. WALP is known to be monomeric; therefore, this peptide is a suitable model for which the bicelle system can be evaluated before investigating proteins whose oligomeric nature is unknown. Although micelles have been successfully used to study membrane protein oligomerization, discretion must be used when interpreting the data because micelles have properties that are different from the lipid bilayer where membrane proteins reside. For example, the extreme curvature of micelles has the potential to influence the tertiary structure of proteins which can affect oligomerization. Another membrane protein that was expressed and purified for the purposes of evaluating bicelles in the AUC was the E. coli outer membrane protein (OmpX). OmpX has been well characterized structurally and functionally and has been shown to be readily incorporated into lipid bilayers (4, 5, 6, 7, 8, 9). OmpX

116

also has a higher molecular weight which is expected to allow for adequate sedimentation in bicelles under density matched conditions (71.7% D_2O).

Other sections of this chapter describe, in detail, the expression and purification of caveolin-1(62-178) (referred to as Cav1(62-178)) constructs including wild type and the many mutants that were used for the oligomerization studies executed in Chapter 2. The details of the expression and purification of WALP and the caveolin constructs are presented together in this chapter because their preparation follows the same procedure.

The last section of this chapter describes the expression and purification of a membrane associating protein called phosphatidylethanolamine methyltransferase A (PmtA). PmtA is responsible for transferring a methyl group from an S-adenosylmethionine to the plasma membrane lipid, phosphatidylethanolamine (PE). This process occurs three times in order to convert phosphtidylethanolamine to phosphatidylcholine (PC) in the bacterial species, *R. sphaeroides*. PmtA was expressed and purified from E. coli in order to study the nature of its interaction with the lipid bilayer (10).

MATERIALS AND METHODS

WALP, Cav1(62-178), and Cav1 Mutants (P132L, Truncated and Point Mutants)

Preparation of WALP Gene

The WALP peptide sequence that was chosen for this study was based on a study carried out by Whiles et al., NH$_2$-**MAKKLLLALLLALLLLALLLWKK**-COOH (11). A tryptophan residue was included at the C-terminus of the construct to allow for an appreciable absorbance at 280 nm which will facilitate monitoring of the peptide during the purification process and in downstream studies. A methionine residue was also included so the peptide may be cleaved from its fusion partner after expression and purification using cyanogen bromide.

Primers for the full-length WALP sequence were ordered from Invitrogen Life Technologies (Grand Island, NY) and both primers included BamH1 and EcoR1 restriction sites for cloning:

5'-CGCGG ATCCA TGGCG AAAAA ACTGC TGCTG CGCGC TGCTG CTGGC GCTGC TGCTG CTGGC GCTGC TGCTG TGGAA AAAAT GAGAA TTCCG G-3'

3'- CCGGA ATTCT CATTT TTTCC ACAGC AGCAG CGCCA GCAGC AGCAG CGCCA GCAGC AGCGC CAGCA GCAGT TTTTT CGCCA TGGATC CGCG-5'

The gene was amplified using PCR. All reagents used for PCR except the primers were purchased from New England Biolabs (Ipswich, MA) unless otherwise specified. The reaction was set up on a 50 μL scale with reagents added in the following order to a sterile thin-walled PCR tube:

Sterile dH$_2$O	41.1 μL
10X ThermoPol buffer	5.0 μL
dNTPs (25 mM each)	0.4 μL

5' WALP primer (2 µg / µL)	1.0 µL
3' WALP primer (2 µg / µL)	1.0 µL
Taq Polymerase	1.0 µL

PCR Cycling Conditions:

1 cycle	X	94 ^{0}C	2 minutes
5 cycles	X	94 ^{0}C	15 seconds
		40 ^{0}C	15 seconds
		72 ^{0}C	1.0 minute
1 cycle	X	72 ^{0}C	5.0 minutes
Storage		4 ^{0}C	∞

After optimization of the PCR reaction, the presence of the PCR product was confirmed using a 1.5 % agarose gel. The agarose gel was prepared by dissolving 1.5 grams of agarose (EMD Millipore, Billerica, MA) in 100 mL 1 X Tris-acetate-EDTA, pH 8.0 buffer (Appendix I). The TAE buffer was prepared (Appendix I). The gel was cast into a horizontal mini-gel system from C.B.S. Scientific (Del Mar, CA). To 4 µL of the PCR product 1 µL of 5 X nucleic acid sample loading buffer (Biorad, Hercules, CA) was added. 2-log DNA ladder (NEB, Ipswich, MA) was run in parallel on the agarose gel at 140 Volts for 50 minutes using the Biorad PowerPac™ HC Power Supply for electrophoresis. The gel was stained in a 0.5 µg / mL ethidium bromide solution for 20 minutes and destained in dH$_2$O for 20 minutes. The presence of a 100 base pair band was assessed using a UV transilluminator at a wavelength of 365 nm.

Preparation of Cav1(62-178) Gene

The gene for caveolin-1(62-178) (referred to as Cav1(62-178)) was synthesized with BamH1 and EcoR1 restriction sites by Genscript (Piscataway, NJ). A methionine residue was incorporated at the beginning of the construct to allow chemical cleavage of Cav1(62-178) from its fusion partner in downstream studies (Figure 6-1). The synthesized gene was supplied in a pUC19 vector and was transformed into XL1-Blue cells, and a glycerol stock was prepared (Appendix I).

Ligation of WALP and Caveolin-1(62-178)

The WALP PCR product and Cav1(62-178) genes were ligated into a pET-TrpLE-Ubiquitin-24a or pET-nTrpLE-24a E. coli expression vector, respectively. These vectors were a gift from the E. Komives Lab at the University of California, San Diego (San Diego, CA). The vectors contain a Trp-Leader protein sequence which codes for the partial sequence of a native E.coli protein. The "n" in the pET-nTrpLE-24a vector represents a codon-optimized version of the original TrpLE sequence from the Komives Lab. Proteins that are expressed as fusions to the Trp-Leader sequence are often directed into inclusion bodies. Also, it is possible to obtain high-level protein expression using this vector. The WALP PCR product was gel purified on a 1.5% agarose gel and the 100 base pair band was excised from the gel and purified using the Qiagen Gel Extraction Kit (Valencia, CA). A 5 mL LB culture of E. coli containing the pET-TrpLE-Ubiquitin-24a or pET-nTrpLE-24a vector was grown overnight at 37 ^{0}C and pelleted using a benchtop microcentrifuge. The pET-TrpLE-Ubiquitin-24a or nTrpLE vectoral DNA was extracted from E. coli cells and purified using the Qiagen Miniprep kit (Valencia, CA). The WALP PCR product, Cav1(62-178), pET-TrpLE-Ubiquitin-24a, pET-nTrpLE-24a DNA were subjected to double digest with BamH1 and EcoR1 restriction

120

enzymes (New England Biolabs, Ipswich, MA). The reactions were set up in separate

sterile 1.5 mL Eppendorf tubes according to the conditions described below:

DNA (WALP, Cav1(62-178), pET-TrpLE-Ubiquitin-24a, pET-nTrpLE-24a)   42.5 µL

10X EcoR1 Buffer   5.0 µL

100X BSA   0.5 µL

BamH1 restriction enzyme   1.0 µL

EcoR1 restriction enzyme   1.0 µL

The reactions were left to proceed for at least 20 hours at room temperature. The

product of the digest reactions was purified using a 1.0% agarose gel (1.5% agarose gel

for WALP). The band corresponding to the expected DNA product size was excised

from the gel and purified using the QIAquick Gel Extraction kit (Qiagen, Valencia, CA).

The purified DNA was quantitated using a 1.0% agarose gel (1.5% for WALP). After the

DNA was quantitated, a ligation reaction was set up using 50 ng of vectoral DNA as the

limiting reagent and a 200-fold excess of WALP or Cav1(62-178) insert was added to the

reaction. 10X T4 ligase buffer was added to the reaction followed by 1.0 µL of T4 Ligase

enzyme (New England Biolabs, Ipswich, MA). A control was prepared in parallel to the

ligation reaction with sterile dH$_2$O used instead of the insert DNA. The control and

ligation reactions were allowed to proceed at room temperature for 16-20 hours.

The ligation and control reactions were transformed into either DH5α (Invitrogen

Life Technologies, Grand Island, NY) or XL1-Blue subcloning grade competent cells

purchased from Stratagene / Agilent (Santa Clara, CA) and test digests were performed

(Appendix I). To each of the reactions, 2.5 µL of 5X nucleic acid sample loading buffer

was added and the samples were run on a 1.5% agarose gel for 50 minutes at 140

Volts. The gel was stained in ethidium bromide and destained in dH_2O and the presence of the insert, 100 base pairs, and the vector, 5000 base pairs, were assessed. The correct DNA sequence from the picked colonies was confirmed by Jutta Marzillier, Ph.D in the Department of Biological Sciences (WALP) (Lehigh University, Bethlehem, PA) or Genewiz Corp.(Cav1(62-178)) (South Plainfield, NJ). The DNA that was extracted from the DH5α or XL1-Blue colony was transformed into BL21-DE3 competent cells purchased from Invitrogen Life Technologies (Grand Island, NY) following the procedure in Appendix I. 0.20 µL of DNA was used to transform BL21-DE3 cells. The SOC culture was plated on a MDAG agar plate containing kanamycin and incubated overnight at 37 ^{0}C. The following day 3-5 colonies were picked from the plate and grown in 5 mL of MDAG broth containing kanamycin. Glycerol freezes were prepared for each of the colonies.

Preparation of Caveolin-1 P132L, Truncated and Point Mutant Genes

Mutagenesis primers were designed using the PrimerX web program (Carlo Lapid and Yimin Gao; hosted by Bioinformatics.org) and the original nucleotide sequence for Cav1(62-178). The desired mutations were introduced into the primers and PCR was carried out using Cav1(62-178) as the template DNA:

Site-directed Mutagenesis PCR Reaction:

Sterile ddH_2O 15.3 µL

10X Pfu AD buffer   2.5 µL

10X 9°N Ligase buffer   2.5 µL

DMSO   0.2 µL

dNTPs (100 mM)   1.0 µL

template DNA (10 ng / μL)	0.5 μL
FOR 5' quikchange primer (125 ng / μL)	1.0 μL
Pfu Turbo polymerase	1.0 μL
9°N Ligase	1.0 μL

PCR Cycling Conditions:

1 cycle	x	95 ℃	30 seconds
30	x	95 ℃	30 seconds
	x	55 ℃	1 minute
	x	68 ℃	6 minutes
Storage	x	4 ℃	∞

To the PCR reaction was added 1 μL of Dpn I endonuclease to digest the methylated parental DNA strand. The Dpn I reaction was left to proceed overnight at 37 ℃. 1 μL of the Dpn I reaction was used to transform a 50 μL aliquot of XL1-Blue subcloning grade E. coli cells (Appendix I). Colonies were picked from the LB agar plates and grown in 5 mL of LB-KAN broth for 12-16 hours. The cells were pelleted and DNA extracted using the QIAprep Miniprep Kit (Qiagen, Valencia, CA). The DNA was sequenced to confirm the presence of the desired mutation (Genewiz, South Plainfield, NJ).

Expression and Purification of WALP, Caveolin-1(62-178), and Caveolin-1 P132L, Truncated and Point Mutants

Each of the picked BL21-DE3 colonies was tested for the expression of the WALP, Cav1(62-178), or Cav1(62-178) mutants (Appendix I). The growths from which the glycerol freezes were made were propagated by adding 50 μL of the culture to 5 mL

of fresh MDAG media containing kanamycin. The growths were incubated at 37 ^{0}C with shaking at 225 rpm for 3 hours. After 3 hours, 100 µL of the culture was transferred to a 1.5 mL eppendorf tube and 100 µL of 2X SDS sample loading buffer (Laemmlli buffer) was added. The samples were heated in boiling water and vortexed. To the remainder of the growths 0.95 µL of 1 M isopropyl β-D-1-thiogalactopyranoside (IPTG) was added to induce the expression of the nTrpLE-WALP fusion protein. The growths were allowed to proceed for another 3 hours at 37 ^{0}C with shaking. Afterwards, 100 µL of the growths were transferred to a 1.5 mL eppendorf tube and 100 µL of 2X SDS buffer was added. The samples were boiled in a water bath and the "non-induced" and "induced samples" were loaded onto an SDS-PAGE gel: 5 %T stacking gel, 15 % T resolving gel and run in standard electrophoresis buffer at 150 V for 1 hour and 20 minutes. The ColorPlus pre-stained protein ladder (10-230 kDa) (NEB, Ipswich, MA) was included in lane 1 to evaluate the molecular weight of the protein bands. The gel was stained for 30 minutes in Coomassie Brilliant Blue R-250 and destained for several hours until the bands could be visualized. The presence of the fusion protein on the gel was assessed and the intensity of the stained band determined which colony best expressed the desired protein.

Once the best expressing colony was determined, a large scale growth was performed using a 6-liter shaker flask using the auto-induction method for high-density cultures (12). First, a starter culture was prepared by adding 5 mL of MDAG media (Appendix II) to a 10 mL culture tube followed by the addition of 5 µL of 30 mg / mL kanamycin to the media. The media was inoculated using the BL21-DE3 WALP / Cav1(62-178) glycerol stock by poking the freeze with a micropipette tip to obtain an ice chip. The tip was ejected into the 10 mL culture and incubated at 37 ^{0}C overnight (minimum 16 hours) with shaking at 225-250 rpm. The following day, 2 mL of the starter

124

growth was added to 2 liters of pre-warmed ZYM-5052 sterile media (Appendix II). The 2-liter growth was incubated at 37 ^{0}C with shaking at 225-250 rpm. Progress of the growth was monitored by measuring the OD_{600nm} of the culture every hour and plotting the growth profile of the protein. Once the density of the growth leveled off, the cells were harvested in 1-liter aliquots by centrifugation at 5,000 x g at 4 ^{0}C for 30 minutes. The supernatant was discarded and each cell pellet was washed by re-suspending the cell pellets in 80 mL of ice-cold 0.9% NaCl solution. The cells were spun again at 5,000 x g for 30 minutes at 4 ^{0}C. The supernatant was discarded from the second spin and the remaining cell pellets could be stored at -80 ^{0}C for several months.

A series of selective wash steps was performed to purify the protein from the harvested cell pellets. The desired protein was expressed in highly insoluble inclusion bodies, which facilitates the partial purification of the desired protein using several wash steps that are designed to remove unwanted proteins. To a 1-liter cell pellet, approximately 200 mL of 20 mM Tris buffer pH 8.0 containing 20% sucrose (w/v) was added. The cell pellet and buffer were sonicated in a 600-mL beaker with stirring using a Branson sonifier with a flat tip head. Cells were ruptured using a 40% duty cycle, power level 9 with stirring. The sonication proceeded for 15 minutes in the cold room. The homogenized mixture was centrifuged in a JA-14 tube using a Beckman floor model preparative ultracentrifuge. The contents of the tube were spun at 27,500 x g for 2 hours at 8 ^{0}C. The pellet was retained and the supernatant was discarded. A second wash step was performed to remove broken pieces of cell membrane and membrane bound proteins. The pellet was resuspended in 200 mL of 20 mM Tris pH 8.0 buffer containing 1% Triton X-100 (v/v) in a 600-mL beaker. The mixture was sonicated again with stirring at a 40% duty cycle, power level 9 for 15 minutes in the cold room. The homogenized mixture was centrifuged again in a JA-14 tube at 27,500 x g for 45 minutes at 8 ^{0}C. The

supernatant was discarded and the pellet was retained and subjected to a second wash with the 1% Triton X-100 buffer. The supernatant was discarded and the pellet was subjected to one last wash step with 200 mL of 20 mM Tris buffer pH 8.0 containing 60% isopropyl alcohol (v/v) which was designed to remove traces of Triton X-100. The sonication and centrifugation steps were repeated from the Triton X-100 wash step. The supernatant was discarded and the grayish white pellet was retained and dried under a stream of nitrogen gas to remove traces of isopropyl alcohol. A sample of the pre-spun mixture was retained at all steps along with a sample of the supernatant when each spin was complete. The fusion protein was tracked through all wash steps to track the target protein. The pellet was dissolved in 40 mL of 88% formic acid and centrifuged in a JA-20 tube for 30 minutes at 21 ^{0}C. The supernatant was retained and subjected to cyanogen bromide in order to cleave the fusion protein and liberate the desired peptide. To the formic acid mixture, 0.2 g of cyanogen bromide crystalline powder was added. The solution was bubbled under a stream of nitrogen gas for 5 minutes. The reaction was covered with aluminum foil and allowed to rotate overnight for a minimum of 18 hours at room temperature (Figure 6-2). The reaction mixture was dried down in a Savant speed vacuum concentrator to remove the formic acid and cyanogen bromide. The dried film was re-dissolved in 88% formic acid to final concentration of approximately 5 mg / mL. The TrpLE-Ubiquitin or nTrpLE protein was separated from WALP or Cav1(62-178) and mutants, respectively, using a Phenomenex (Torrance, CA) Jupiter C4 reverse-phase HPLC column with a 15 μm particle size with a 300 Å pore size. A gradient elution was performed using a mobile phase consisting of 20% acetic acid / 80% dH$_2$O and changing over to 20% acetic acid / 80% butanol at a rate of 2.5% per minute. The identity of the peak is confirmed using MALDI-TOF mass spectrometry. The desired protein is collected and dried to a thin film using the speed vacuum

concentrator. The protein film is dissolved in HFIP to which dH_2O is added to a final concentration of 70% (v/v). Immediately after adding the dH_2O the solution is frozen in liquid nitrogen and lyophilized. The lyophilized protein is stored at -20 ^{0}C and is stable for several months.

OmpX

A pET-28a vector containing the OmpX gene was generously provided by the Berger Lab (Lehigh University, Bethlehem, PA). The DNA sequence of OmpX was verified (GENEWIZ, South Plainfield, NJ) and contained an N-terminal hexahistidine tag to facilitate purification. The DNA was transformed to XL1-Blue cells and plated on LB agar containing kanamycin. The plate was incubated overnight at 37 ℃ and three to five colonies were picked the following day. The picked colonies were grown in 5 mL of LB broth containing kanamycin overnight at 37 ℃ sh aking at 225-250 rpm on a platform shaker (New Brunswick Scientific, Edison, NJ). Glycerol freezes were prepared from each of the 5 mL cultures (Appendix I) and the remaining culture was pelleted. DNA from the XL1-Blue cells was extracted and purified using the QIAprep Miniprep Kit (Qiagen, Valencia, CA) and transformed into chemically competent E. coli BL21-DE3 cells purchased from Invitrogen Life Technologies (Grand Island, NY) (Appendix I). The SOC culture was plated on an MDAG agar plate containing kanamycin and incubated overnight at 37 ^{0}C. The following day 3-5 colonies were picked from the plate and grown in 5 mL of MDAG broth containing kanamycin. Glycerol freezes were prepared for each of the colonies (Appendix I).

<u>Expression and Purification of OmpX from E. coli</u>

To 5 mL of sterile MDAG-KAN, a chip of the OmpX glycerol freeze was added. The MDAG starter culture was incubated at 37 ℃ ove rnight (12-16 hours) with shaking at 250 rpm on a platform shaker (New Brunswick Scientific, Edison, NJ). The following morning 5 mL of MDAG starter culture was added to 2 liters of ZYM-5052 media. The growth was left to proceed at 37 ℃ with shaking at 220-250 rpm for 9 - 10 hours. The cells were harvested by centrifugation at 5000 x g for 30 minutes at 4 ℃ in two 1-liter centrifuge bottles. Each one-liter cell pellet was resuspended in 130 mL of ice cold 0.9% NaCl (w/v) solution and centrifuged at 5000 x g for 30 minutes at 4 ℃. The supernatant was poured off and the one-liter pellets were stored at 80 ℃.

A one-liter cell pellet was suspended in 240 mL of 50 mM phosphate buffer pH 7 containing 8 M urea. The cells were lysed by sonication using a Branson Sonifier at a 40% duty cycle, power level 9 while stirring for 15 minutes. Afterward, the lysate was spun at 27,500 x g for 2 hours at 8 ℃. The cleare d lysate was incubated with approximately 10 mL of Nickel-NTA resin (Qiagen, Valencia, CA) to bind hexahistidine-labeled OmpX to bind to the resin. The resin was washed with three column volumes (30 mL) of 50 mM phosphate buffer pH 7 containing 8 M urea and 20 mM imidazole. The column was batched eluted with 20 mL of 50 mM phosphate buffer pH 7 containing 8 M urea and 250 mM imidazole.

Phosphatidylethanolamine methyltransferase (PmtA)

Genomic DNA from *R. sphaeroides* was purchased from American Type Culture Collection (ATCC, Manassas, VA). Primers to the PmtA gene were designed and purchased from Invitrogen (Carlsbad, CA):

5' –GGTAT TCCAT ATGGA ACTTG ACGCG GTAAG CCGGA G – 3'

3' – CCGGA ATTCT CAGCG GCGCT GGAAG CGCAG GAAGG TGA – 5'

The gene was amplified using PCR. All reagents used for PCR except the primers were purchased from New England Biolabs (Ipswich, MA) unless otherwise specified. The reaction was set up on a 50 µL scale with reagents added in the following order to a sterile thin-walled PCR tube:

Genomic DNA from *R. sphaeroides* (100 ng / µL)	1.0 µL
FOR 5' primer (200 ng / µL)	2.0 µL
REV 3' primer (200 ng / µL)	2.0 µL
5 x Optimization Kit Buffer E	10.0 µL
PCR water from kit	29.8 µL
Taq Polymerase (5000 U / mL)	0.2 µL
dNTPs (2.5 mM each from kit)	5.0 µL

Cycling Conditions:

1 cycle	X	94 ℃	2 minutes
30 cycles	X	94 ℃	15 seconds
	X	55 ℃	15 seconds
	X	72 ℃	45 seconds
1 cycle	X	72 ℃	5 minutes
Storage		4 ℃	∞

The PCR product was verified on a 1% agarose gel (631 base pairs) and purified using the PCR Quick Cleanup from the QIAquick Gel Extraction Kit (Qiagen, Valencia, CA). A 5 mL LB culture of E. coli containing the pET-24a vector was grown overnight at

37 ^{0}C and pelleted using a benchtop microcentrifuge. The pET-24a vectoral DNA was extracted from E. coli cells and purified using the Qiagen Miniprep kit (Valencia, CA). The purified PmtA and pET-24a DNA was double digested in separate sterile 1.5 mL Eppendorf tubes:

DNA (PmtA insert or pET-24a)	43.0 µL
10 X EcoR1 buffer	5.0 µL
EcoR1 Endonuclease	1.0 µL
Nde1 Endonuclease	1.0 µL

Reactions were left to proceed for 20 hours at room temperature (overnight). The products of the double digest reactions were purified and quantitated on a 1.0% agarose DNA gel. After the DNA was quantitated, a ligation reaction was set up using 50 ng of vectoral DNA as the limiting reagent and a 200-fold excess of PmtA insert was added to the reaction. 10X T4 ligase buffer was added to the reaction followed by 1.0 µL of T4 Ligase enzyme (New England Biolabs, Ipswich, MA). A control was prepared in parallel to the ligation reaction with sterile dH$_2$O used instead of the insert DNA. The control and ligation reactions were allowed to proceed at room temperature for 16-20 hours.

The ligation and control reactions were transformed into DH5α subcloning grade E. coli cells (Invitrogen Life Technologies, Grand Island, NY) and test digests were performed (Appendix I). To each of the reactions, 2.5 µL of 5X nucleic acid sample loading buffer was added and the samples were run on a 1.0% agarose gel for 50 minutes at 140 Volts. The gel was stained in ethidium bromide and destained in dH$_2$O and the presence of the insert, 631 base pairs, and the vector, 5000 base pairs, were

assessed. The correct DNA sequence from the picked colonies was confirmed by Jutta

Marzillier, Ph.D in the Department of Biological Sciences (Lehigh University, Bethlehem,

PA). The DNA extracted from the DH5α E. coli cells was transformed into BL21-DE3

competent cells purchased from Invitrogen Life Technologies (Grand Island, NY)

following the procedure in Appendix I. 0.20 µL of DNA was used to transform BL21-DE3

cells. The SOC culture was plated on a MDAG agar plate containing kanamycin and

incubated overnight at 37 ^{0}C. The following day 3-5 colonies were picked from the plate

and grown in 5 mL of MDAG broth containing kanamycin.   Glycerol freezes were

prepared for each of the colonies.

Expression and Purification of PmtA in E. coli

Each of the picked BL21-DE3 colonies was tested for the expression of PmtA

(Appendix I). The growths from which the glycerol freezes were made were propagated

by adding 50 µL of the culture to 5 mL of fresh MDAG media containing kanamycin. The

growths were incubated at 37 ^{0}C with shaking at 225 rpm for 3 hours. After 3 hours, 100

µL of the culture was transferred to a 1.5 mL eppendorf tube and 100 µL of 2X SDS

sample loading buffer (Laemmlli buffer). The samples were heated in boiling water and

vortexed.   To the remainder of the growths 0.95 µL of 1 M isopropyl β-D-1-

thiogalactopyranoside (IPTG) was added to induce the expression of PmtA protein. The

growths were allowed to proceed for another 3 hours at 37 ^{0}C with shaking. Afterwards,

100 µL of the growths were transferred to a 1.5 mL eppendorf tube and 100 µL of 2X

SDS buffer was added. The samples were boiled in a water bath and the "non-induced"

and "induced samples" were loaded onto an SDS-PAGE gel: 5 %T stacking gel, 15 % T

resolving gel and run in standard electrophoresis buffer at 150 V for 1 hour and 20

minutes. The ColorPlus^{TM} pre-stained protein ladder (10-230 kDa) (NEB, Ipswich, MA)

131

was included in lane 1 to evaluate the molecular weight of the protein bands. The gel was stained for 30 minutes in Coomassie Brilliant Blue R-250 and destained for several hours until the bands could be visualized. The presence of the fusion protein on the gel was assessed and the intensity of the stained band determined which colony best expressed the desired protein.

Once the best expressing colony was determined, a large scale growth was performed using a 6-liter shaker flask using the auto-induction method for high-density cultures (12). First, a starter culture was prepared by adding 5 mL of MDAG media to a 10 mL culture tube followed by the addition of 5 µL of 30 mg / mL kanamycin to the media. The media was inoculated using the BL21-DE3 WALP / Cav1(62-178) glycerol stock by poking the freeze with a micropipette tip to obtain an ice chip. The tip was ejected into the 10 mL culture and incubated at 37 ^{0}C overnight (minimum 16 hours) with shaking at 225-250 rpm. The following day, 2 mL of the starter growth was added to 2 liters of pre-warmed ZYM-5052 sterile media. The 2-liter growth was incubated at 37 ^{0}C with shaking at 225-250 rpm. Progress of the growth was monitored by measuring the OD_{600nm} of the culture every hour and plotting the growth profile of the protein. Once the density of the growth leveled off, the cells were harvested in 250-500 mL aliquots by centrifugation at 5,000 x g at 4 ^{0}C for 30 minutes. The supernatant was discarded and each cell pellet was washed by re-suspending the cell pellets in 80 mL of ice-cold 0.9% NaCl solution. The cells were spun again at 5,000 x g for 30 minutes at 4 ^{0}C. The supernatant was discarded from the second spin and the remaining cell pellets could be stored at -80 ^{0}C for several months.

A 500 mL pellet was reconstituted into ice-cold 40-50 mL of 50 mM phosphate pH 8, 10 mM Imidazole, 300 mM NaCl buffer. The E. coli cells were lysed by sonication using a microtip sonifier on duty cycle 10%, power level 3. The material was kept on ice

and temperature did not exceed 16 °C. The lysate w as further purified by centrifuging at 4 °C for 30 minutes. The cleared lysate was filter ed through a 0.2 µm syringe filter and applied to 1 mL of Ni-NTA resin in a 4 °C cold room . The column was washed with two column volumes (10 mL) of 50 mM phosphate pH 8, 20 mM Imidazole, 300 mM NaCl (ice cold) and eluted in 1 mL fractions with 50 mM phosphate pH 8, 250 mM Imidazole, 300 mM NaCl. Fractions were evaluated in SDS-PAGE for the presence of PmtA, pooled and exchanged into 50 mM phosphate pH 8, 150 mM NaCl buffer. The purified PmtA was stored at 4 °C.

RESULTS AND DISCUSSION

WALP

The goal of cloning, expressing and purifying the WALP peptide was to use this peptide as a model that could be incorporated into bicelles and its oligomeric state evaluated in the analytical ultracentrifuge. WALP is known to be a monomer; therefore, its oligomeric state could be determined with confidence using density matched bicelles in the analytical ultracentrifuge. Initially, WALP was cloned into a pET-TrpLE-Ubiquitin-24a vector and expressed as a tandem fusion to TrpLE-Ubiquitin. TrpLE is known to promote protein expression into inclusion bodies, which is often desirable when expressing highly toxic membrane proteins. The TrpLE system has been used successfully to express large quantities of membrane proteins. WALP was found to be best expressed in a tandem fusion to both TrpLE and Ubiquitin. Figure 6-3 shows the results of the test expression performed on this construct. We can see from SDS-PAGE that a 25 kD band appears after protein production was initiated by the addition of IPTG. This band corresponds to the molecular weight of the TrpLE-Ubiquitin-WALP fusion. Next, a large-scale growth of TrpLE-Ubiquitin-WALP was performed to produce sufficient quantities of WALP for downstream studies. An inclusion body preparation was performed on the cells harvested from this large-scale growth. Next, the semi-pure inclusion bodies were dissolved in 88% formic acid and a cyanogen bromide reaction was carried out to chemically cleave TrpLE-Ubiquitin from WALP (Figure 6-2). The reaction was purified by reverse phase HPLC and fractions were collected. Figure 6-4 shows the results of HPLC. WALP is extremely hydrophobic compared to TrpLE-Ubiquitin and was expected to elute last from the HPLC column. The identity of the starred peak was confirmed to be WALP using MALDI-TOF mass spectrometry (Figure 6-5). The results of the MALDI-TOF analysis show that the cleavage product has a

monoisotopic molecular weight of 2.473 kDa, which coincides with the predicted molecular weight of the gene product that was created for this protein. Once the molecular weight of the cyanogen bromide cleavage product was confirmed, the lyophilized material could be used for analytical ultracentrifugation studies.

The purpose of this study was to express a small model peptide, WALP, which could be used to assess the utility of bicelles as a system to study membrane proteins in the analytical ultracentrifuge. The WALP peptide was successfully cloned, expressed and purified using the E. coli bacterial expression system. The TrpLE–Ubiquitin tandem fusion system gave the highest peptide yield. The Ubiquitin fusion system yielded truncated expression products with little to no detectable full-length protein, which was confirmed by western blot analysis. The TrpLE system did not yield appreciable amounts of the WALP peptide. Based on these results, it was concluded that the E. coli expression system is most effective at expressing larger proteins having a molecular weight close to approximately 25 kDa. Small peptides are best expressed as fusions yielding a final protein molecular weight close to 25 kDa. The WALP peptide was later incorporated into bicelles, however, under the density matched conditions of bicelles, it was found that the WALP peptide, with a calculated partial specific volume of 0.847 cm^3 / g, failed to sediment in the analytical ultracentrifuge under density matched conditions preventing a meaningful concentration profile from being achieved. Bicelles are relatively large, dense lipid aggregates and they require a D$_2$O concentration of approximately 75% (v/v) to be matched. While unsuitable for small, hydrophobic peptides, bicelles may be better suited to the analysis of larger membrane proteins.

It is clear from previous efforts to characterize the WALP peptide using bicelles in the analytical ultracentrifuge that the size of the peptide can pose problems in density matched systems. This is especially true in the case of DMPC / DHPC bicelles where

high amounts of D_2O must be used to match the bicelles (72.4% D_2O). Using small peptides in this system requires that extremely high speeds be achieved to generate sufficient curvature in the concentration profile of the peptide and this can cause leaking of the equilibrium centerpieces. To circumvent this problem, the use of a larger membrane protein will be explored. Outer membrane protein X (OmpX) is an integral membrane protein that is situated in the outer membrane of E. coli. It is a highly conserved bacterial membrane protein that belongs to a large family of outer membrane proteins and they are thought to enhance bacterial resistance to mammalian cells. Both the NMR and crystal structure of OmpX have been solved and it forms an eight strand β-barrel, which creates a pore that has been implicated in adhesion and mammalian cell invasion. OmpX has a molecular weight of 17.5 kDa, which is much higher than that of WALP, 2.47 kDa. Like WALP, OmpX is also monomeric in the lipid bilayer of the plasma membrane. This membrane protein may serve as a better candidate to evaluate the utility of bicelles in the analytical ultracentrifuge, since extreme speeds should not be required to sediment this protein under density matched conditions.

OmpX

OmpX was successfully expressed and isolated from E. coli cells using the inclusion body method previously established in the Kerney Jebrell Glover Lab (13). A small sample of prepared material was retained at each step of the inclusion body preparation in order to track the protein during this process. Figure 6-6 shows the results of the inclusion body prep. A strong 17.5 kD molecular weight band is observed in the pre-spun material for both the sucrose and Triton X-100 wash steps. OmpX is very hydrophobic and is expected to be relatively insoluble, traveling with the hydrophobic inclusion body-enriched material in the pre-spin samples. Lane 2 and 4 are

the pre-spun washes and we can see that a 17.5 kD band is present. In the supernatant from these washes (Lanes 3 and 5) the 17.5 kD band is no longer visible, indicating that this material is present in the inclusion bodies. Once the semi-pure inclusion bodies were obtained, OmpX was further purified on a Ni-NTA affinity chromatography column. The column was eluted and fractions were collected and run on an SDS-PAGE gel to confirm the presence of a 17.5 kD band. Figure 6-7 shows that there is a large quantity of material that elutes from the column at approximately 17.5 kD, which is evidence for the presence of OmpX. The OmpX enriched fractions were pooled and stored for bicelle reconstitution studies.
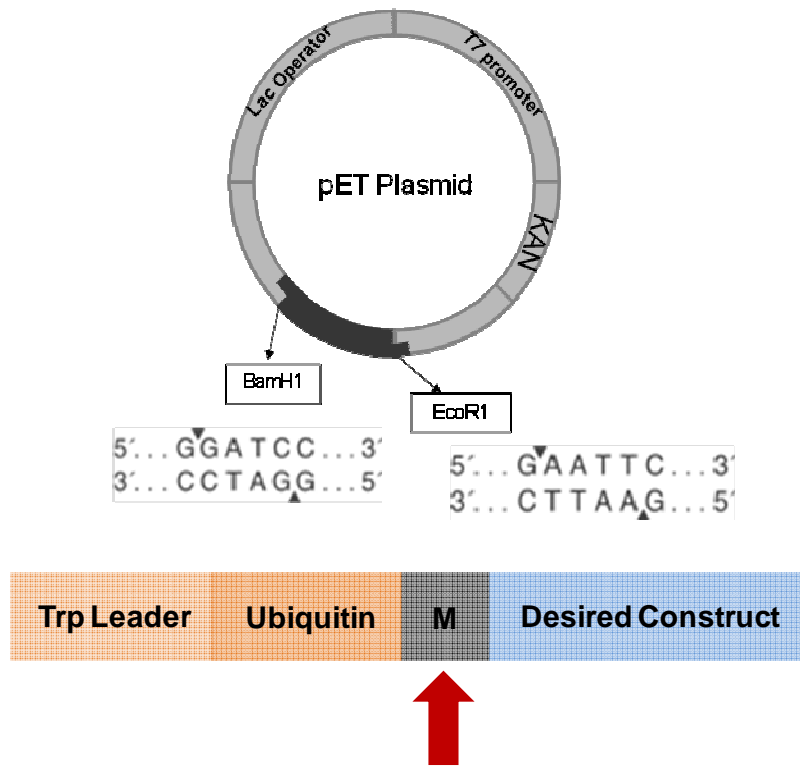
Cav1(62-178) and Cav1(62-178) Mutants

Cav1(62-178) and Cav1(62-178) mutants were expressed and purified using a similar approach to the TrpLE-Ubiquitin-WALP method. The constructs were overexpressed in E. coli and grown in ZYM-5052 media for approximately 9-10 hours or until the growth profile leveled off (Figure 6-8). After the cells were harvested, an inclusion body preparation was carried out to partially purify the overexpressed Cav1(62-178)_WT and Cav1(62-178) mutant constructs. After dissolving the inclusion bodies in 88 % formic acid, a cyanogen bromide reaction was carried out to liberate Cav1(62-178)_WT and Cav1(62-178) mutants from the Trp Leader protein. The cleavage products were separated using HPLC. Figure 6-10 shows representative trace from the HPLC purification of the Cav1(62-178) constructs. Because Cav1(62-178)_WT and the Cav1(62-178) mutants are highly hydrophobic, they are always the last to elute from the column. The red star above the peak in the HPLC trace notes Cav1(62-178)_WT. The identity of Cav1(62-178) along with the identity of the Cav1(62-178) mutants was confirmed by MALDI-TOF mass spectrometry (Figure 6-11).

137

PmtA

PmtA was transformed into E. coli BL21-DE3 cells and successfully expressed based on the results of the test expression (Figure 6-12). An inclusion body preparation reveals that PmtA expressed in inclusion bodies (Figure 6-13a). Ni-NTA affinity chromatography was carried out to purify PmtA (Figure 6-13b), and later gel filtration to remove all unwanted proteins. The purity of the final PmtA material was assessed by SDS-PAGE (Figure 6-14) and was shown to be pure. The enzyme was assayed for activity, but showed no level of activity. Other attempts to express PmtA at lower temperatures and in minimal media resulted in no appreciable enzyme activity. Although, PmtA was successfully expressed and purified, this method failed to produce active enzyme for downstream studies.

CONCLUSIONS

The expression methods presented in this chapter have proven useful in producing extremely hydrophobic proteins, which are otherwise toxic to bacterial host cells. Large quantities were achieved, however, using the inclusion body approach to express and purify small peptides and membrane proteins. E. coli is also useful for expressing higher level full-length proteins albeit without enzymatic activity. To produce enzymatically active protein the use of a higher level organism such as yeast may be necessary. Another approach could be to express full-length protein in E. coli and attempt to refold it in vitro.

Figure 6-1. Schematic diagram of pET-24a plasmid and the construct design of WALP, Cav1(62-178)_WT and Cav1(62-178) mutants. A methionine residue was incorporated before the desired protein sequence so that chemical cleavage could be carried out to separate the fusion.
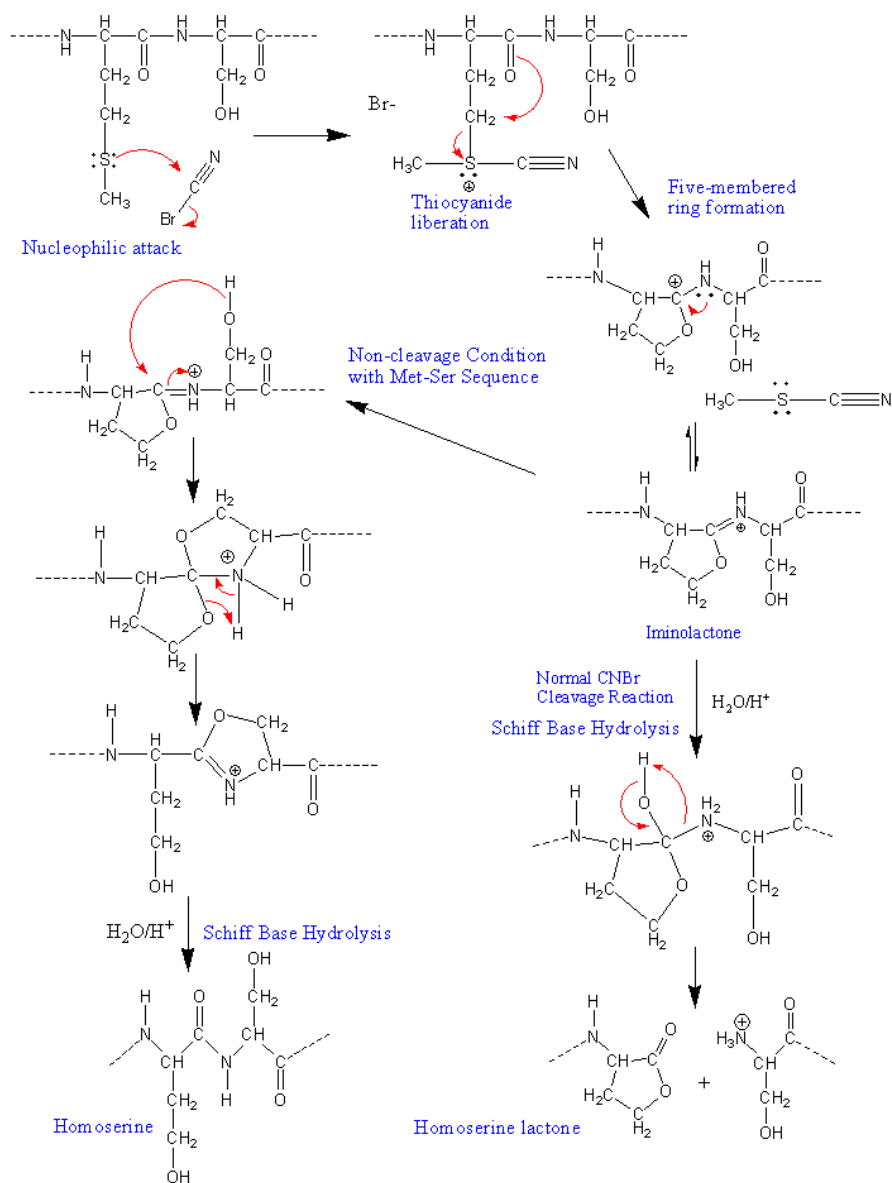
Figure 6-2. Mechanism of cyanogen bromide reaction proposed by Inglis and Edman (1970) *Analytical Biochemistry* **37** 73-80 (14).
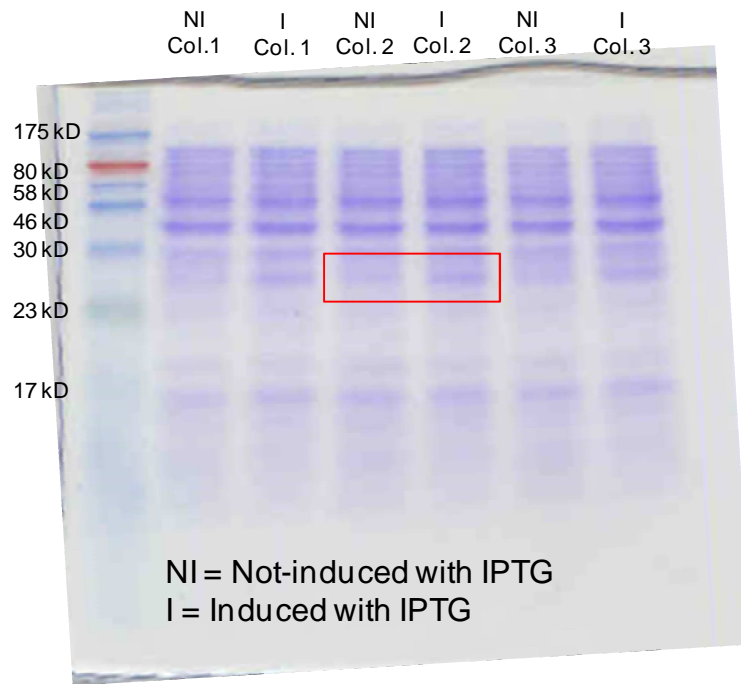
Figure 6-3. SDS-PAGE gel of TrpLE-Ubiquitin-WALP test expression. The appearance of a band can be seen when IPTG was added to the culture to induce expression. The newly visible band corresponds to the MW of TrpLE-Ubiquitin-WALP.

TrpLE-Ubiquitin-WALP(W) Post CNBr Cleavage
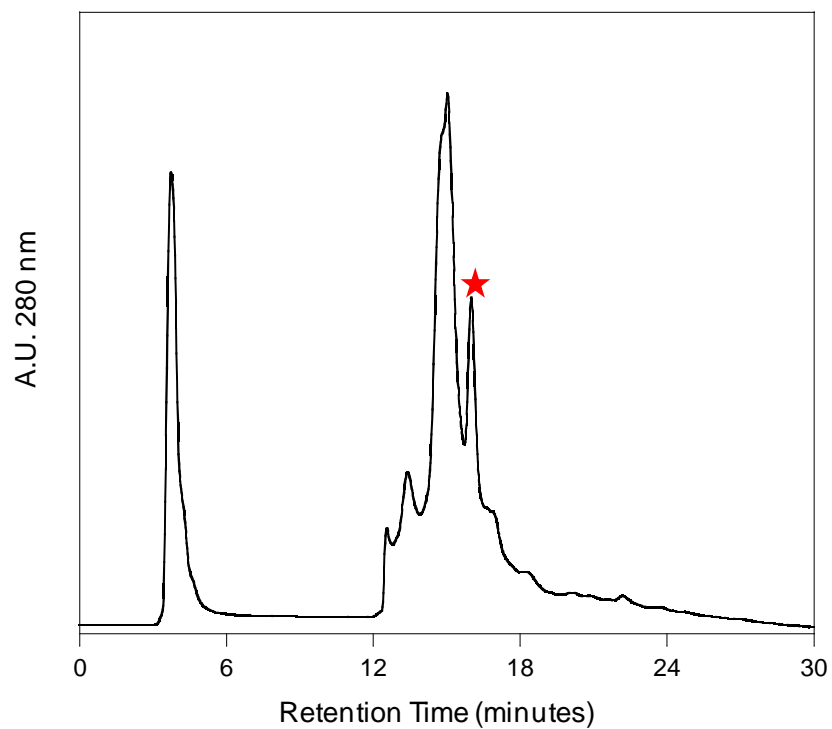
Figure 6-4. HPLC separation of cleavage products from CNBr reaction of TrpLE-Ubiquitin-WALP.

143

M + 1H$^+$ = 2473 Da

Intensity

m / z
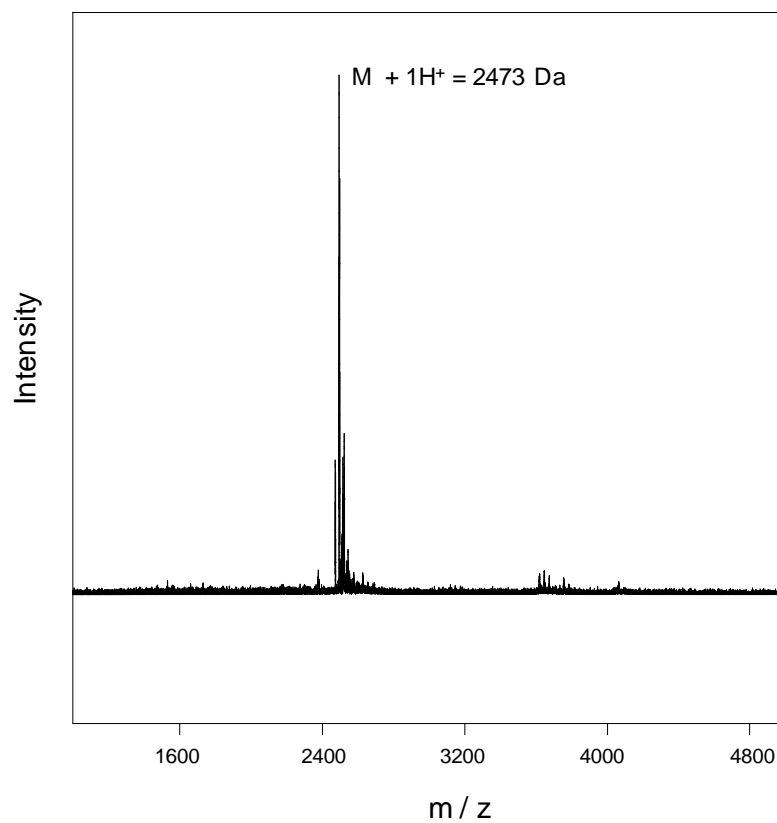
Figure 6-5. MALDI-TOF mass spectrometry of purified WALP peptide. The spectrum was obtained using a Bruker Microflex^{TM} in positive reflectron mode for 0-5 kD peptides.

144
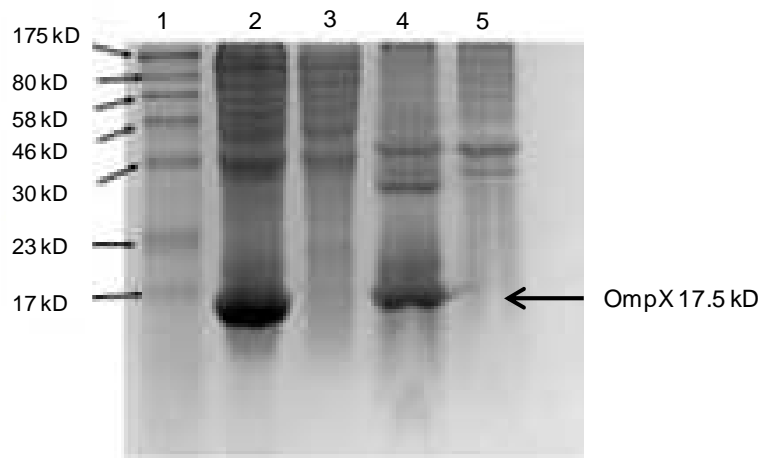
Lane 1 = MW protein ladder
Lane 2 = 20% sucrose, 20 mM Tris pre spin
Lane 3 = 20% sucrose, 20 mM Tris post spin
Lane 4 = 1% Triton, 20 mM Tris pre spin
Lane 5 = 1% Triton, 20 mM Tris post spin

Figure 6-6. SDS-PAGE gel of inclusion body prep. for OmpX.

Lane 1 = MW protein ladder
Lanes 2-10 = Fractions 1-9
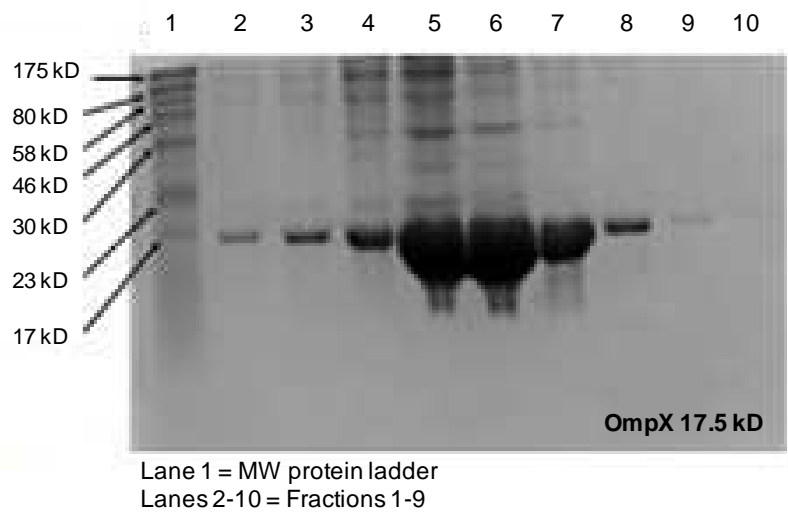
Figure 6-7. SDS-PAGE gel of Ni-NTA affinity column purification of OmpX

146
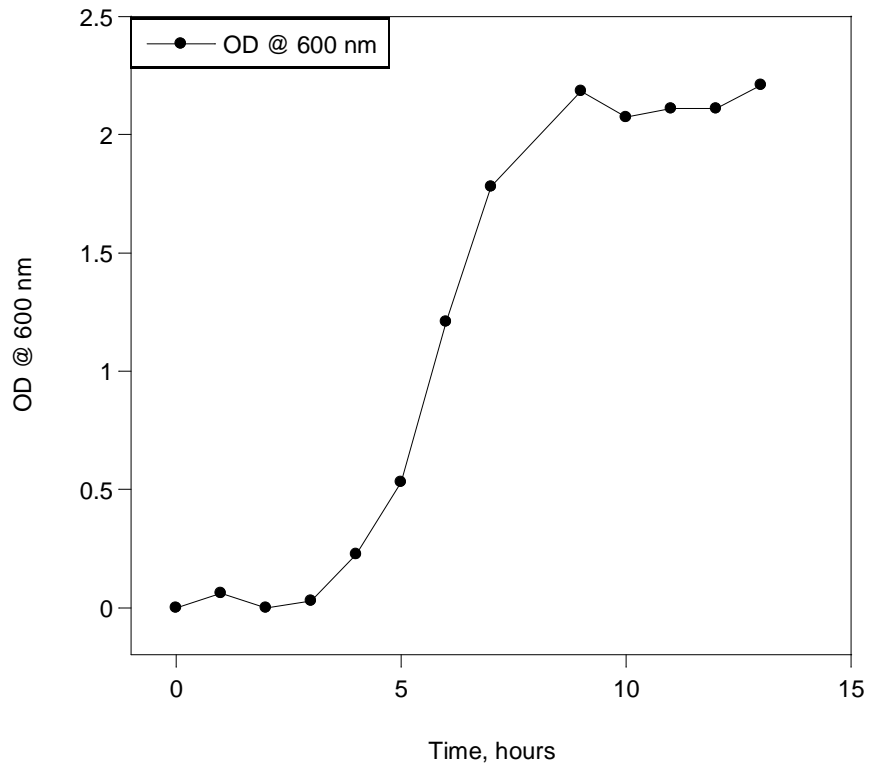
Figure 6-8. Growth profile of E. coli in auto-induction media. After the OD levels off, cells are harvested.
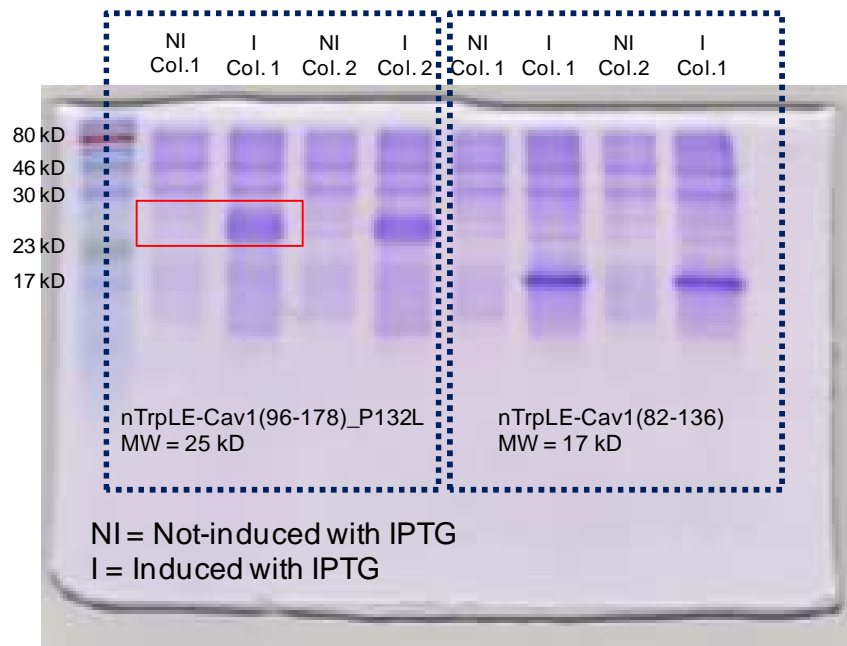
Figure 6-9. SDS-PAGE gel test expression of two Cav1(62-178) truncated mutants: Cav1(96-178) and Cav1(82-136). The red box highlights the appearance of a band corresponding to the expected molecular weight of the gene product upon induction with IPTG. Two colonies are show per construct.
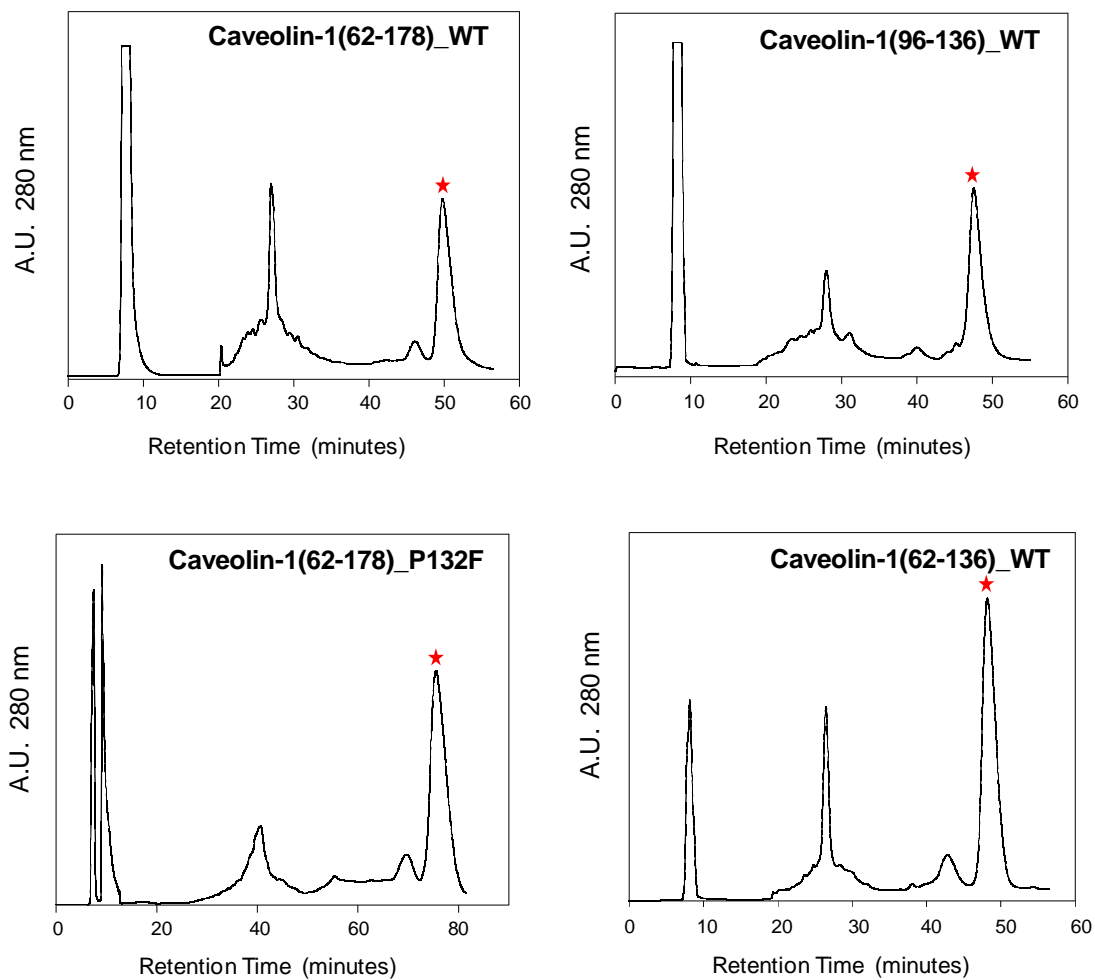
Figure 6-10. HPLC separation of cleavage products from CNBr reaction of nTrpLE-Cav1(62-178) and select Cav1(62-178) mutants. The red starred peaks represent Cav1(62-178) WT and mutants.

149

M + 1H$^+$ = 13451 Da
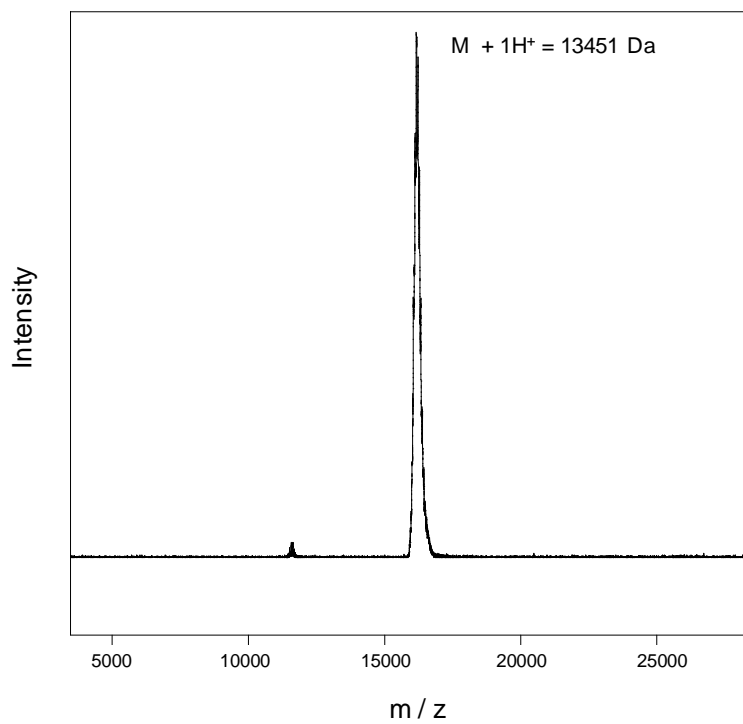
Figure 6-11. MALDI-TOF mass spectrometry of purified Cav1(62-178) peptide. The spectrum was obtained using a Bruker Microflex^{TM} in positive reflectron mode for 5-20 kD peptides.
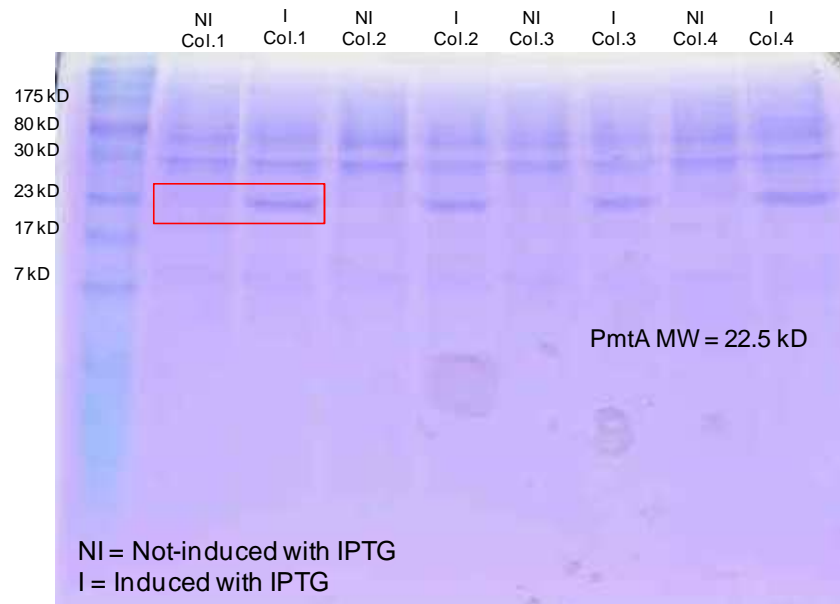
Figure 6-12. SDS-PAGE gel of PmtA test expression. The appearance of a band can be seen when IPTG was added to the culture to induce expression. The newly visible band corresponds to the MW of PmtA.

a.

| | 1 | 2 | 3 | 4 | 5 | 6 | 7 | 8 | 9 |

175 kD
80 kD
46 kD
30 kD
23 kD
17 kD

b.

| | 1 | 2 | 3 | 4 | 5 | 6 | 7 | 8 | 9 |

175 kD
80 kD
46 kD
30 kD
23 kD
17 kD

PmtA
MW = 22.5 kD

1 = ColorPlus™ Protein Ladder
2 = 20 mM Tris pH 8 / 20% Sucrose wash; pre spin
3 = 20 mM Tris pH 8 / 20% Sucrose wash; post wash
4 = 20 mM Tris pH 8 / 1% Triton X-100 wash; pre spin
5 = 20 mM Tris pH8 / 1% Triton X-100 wash; post spin
6 = 20 mM Tris pH 8 / 1% Triton X-100 wash; pre spin
7 = 20 mM Tris pH 8 / 1% Triton X-100 wash; post spin
8 = 20 mM Tris pH 8 / 8 M urea; pre spin
9 = 20 mM Tris pH 8 / 8 M urea; post spin

1 = BLANK
2 = BLANK
3 = BLANK
4 = Column Flow Through: 50 mM phosphate, 8 M Urea pH8
5 = Wash: 50 mM phosphate, 8 M Urea, 20 mM Imidazole pH8
6 = Elution: 50 mM phosphate, 8 M Urea, 250 mM Imidazole pH8
7 = BLANK
8 = BLANK
9 = BLANK

Figure 6-13. a) SDS-PAGE gel of PmtA inclusion body prep. A prominent 22.5 kD band can be tracked through the wash steps of the prep. Columns 8 and 9 show that PmtA is soluble when 8 M urea is present in the buffer. b) A Ni-NTA column was carried out after the inclusion body prep to further purify PmtA. Some of the protein was lost in the unbound fraction, lane 4, and in the wash step, lane 5. Lane 6 shows the eluted protein.
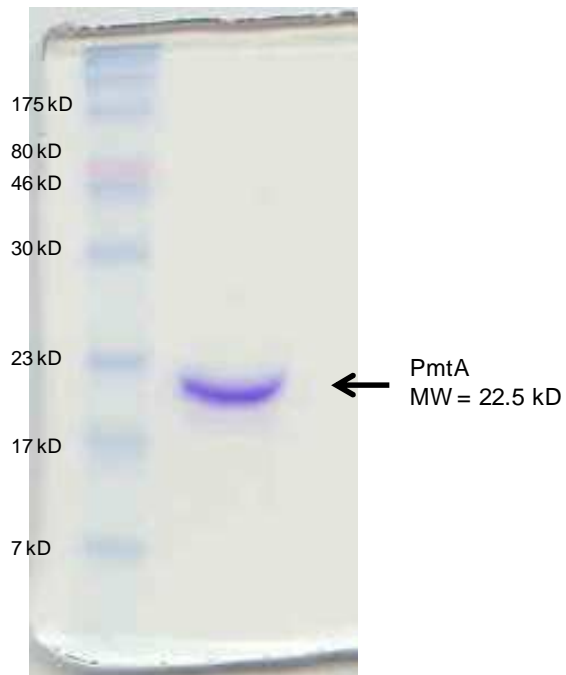
Figure 6-14. SDS-PAGE evaluation of PmtA purity. A single 22.5 kD band can be seen from the gel. Traces of contaminating proteins are too low to be detected by SDS-PAGE, which implies that the protein is highly pure and ready for downstream studies.

REFERENCES

1. Holt, A., and Killian, J. A. (2010) Orientation and Dynamics of Transmembrane Peptides: The Power of Simple Models. *Eur. Biophys. J. 39*, 609-621.

2. Siegel, D. P., Cherezov, V., Greathouse, D. V., Koeppe, R. E.,2nd, Killian, J. A., and Caffrey, M. (2006) Transmembrane Peptides Stabilize Inverted Cubic Phases in a Biphasic Length-Dependent Manner: Implications for Protein-Induced Membrane Fusion. *Biophys. J. 90*, 200-211.

3. Weiss, T. M., van der Wel, P. C., Killian, J. A., Koeppe, R. E.,2nd, and Huang, H. W. (2003) Hydrophobic Mismatch between Helices and Lipid Bilayers. *Biophys. J. 84*, 379-385.

4. Catoire, L. J., Zoonens, M., van Heijenoort, C., Giusti, F., Guittet, E., and Popot, J. L. (2010) Solution NMR Mapping of Water-Accessible Residues in the Transmembrane Beta-Barrel of OmpX. *Eur. Biophys. J. 39*, 623-630.

5. Burgess, N. K., Dao, T. P., Stanley, A. M., and Fleming, K. G. (2008) Beta-Barrel Proteins that Reside in the Escherichia Coli Outer Membrane in Vivo Demonstrate Varied Folding Behavior in Vitro. *J. Biol. Chem. 283*, 26748-26758.

6. Mahalakshmi, R., and Marassi, F. M. (2008) Orientation of the Escherichia Coli Outer Membrane Protein OmpX in Phospholipid Bilayer Membranes Determined by Solid-State NMR. *Biochemistry. 47*, 6531-6538.

7. Mahalakshmi, R., Franzin, C. M., Choi, J., and Marassi, F. M. (2007) NMR Structural Studies of the Bacterial Outer Membrane Protein OmpX in Oriented Lipid Bilayer Membranes. *Biochim. Biophys. Acta. 1768*, 3216-3224.

8. Fernandez, C., Hilty, C., Wider, G., Guntert, P., and Wuthrich, K. (2004) NMR Structure of the Integral Membrane Protein OmpX. *J. Mol. Biol. 336*, 1211-1221.

9. Fernandez, C., and Wuthrich, K. (2003) NMR Solution Structure Determination of Membrane Proteins Reconstituted in Detergent Micelles. *FEBS Lett. 555*, 144-150.

10. Arondel, V., Benning, C., and Somerville, C. R. (1993) Isolation and Functional Expression in Escherichia Coli of a Gene Encoding Phosphatidylethanolamine Methyltransferase (EC 2.1.1.17) from Rhodobacter Sphaeroides. *J. Biol. Chem. 268*, 16002-8.

11. Whiles, J. A., Glover, K. J., Vold, R. R., and Komives, E. A. (2002) Methods for Studying Transmembrane Peptides in Bicelles: Consequences of Hydrophobic Mismatch and Peptide Sequence. *J. Magn. Reson. 158*, 149-156.

12. Studier, F. W. (2005) Protein Production by Auto-Induction in High Density Shaking Cultures. *Protein Expr. Purif. 41*, 207-234.

13. Diefenderfer, C., Lee, J., Mlyanarski, S., Guo, Y., and Glover, K. J. (2009) Reliable Expression and Purification of Highly Insoluble Transmembrane Domains. *Anal Biochem. 384*, 274-8.

14. Inglis, A.S., Edman P. (1970) Mechanism of Cyanogen Bromide Reaction with Methionine in Peptides and Proteins I. Formation of Imidate and Methyl Thiocyanate. *Anal. Biochem. 37,* 73-80.

Appendix I. Common Lab Procedures and Protocols

Preparing and Running a DNA Agarose Gel

1. Prepare a 1.0% agarose gel by dissolving 1 gram of agarose (EMD Millipore, Billerica, MA) in 100 mL of 1X TAE buffer. Carefully boil the mixture to dissolve the agarose.

2. Cast the gel in a horizontal mini-gel system (C.B.S. Scientific, Del Mar, CA).

3. Fill the DNA gel box with 1X TAE buffer until the gel is completely submerged.

4. Load the DNA in the appropriate lanes. Do not exceed 12.5 µL of DNA per well.

5. 5 µL of 2-Log DNA ladder (NEB, Ipswich, MA) is included on the DNA gel for assessment of DNA size.

6. Once the DNA has been loaded on the gel, place the lid securely on the mini-gel box electrodes.

7. Run the gel at 140 Volts for 50 minutes using the BioRad PowerPac™ HC Power Supply (BioRad, Hercules, CA).

8. The gel is stained for 20 minutes using 0.5 µg / mL Ethidium bromide in 1X TAE buffer and destained for 20 minutes in dH_2O.

Purification of Digested DNA using Qiagen Gel Extraction kit (Valencia, CA)

1. To a 50 µL digest reaction add 12.5 µL of 5X Nucleic Acid sample loading buffer.

2. Load the sample across five lanes on an agarose DNA gel and run gel (see above).

3. Using a clean razor blade excise the correct DNA band from the gel taking care to eliminate excess agarose.

4. Transfer the excised band to a pre-weighed 15-mL centrifuge tube (VWR International).

5. Weigh the excised DNA. Add 3X the volume of QG buffer that is equivalent to the grams of weighed material. Ex. To 300 mg of agarose, add 900 µL of QG buffer (Qiagen Kit)

6. Place the centrifuge containing DNA and QG buffer in a 50 ºC water bath and vortex every few minutes until the agarose is completely dissolved (approx. 10 minutes).

7. Add another equivalent of isopropanol. Ex. 300 mg of agarose, add 300 µL of isopropanol

8. Vortex and add the mixture to a Qiagen spin column (max. capacity is 750 µL). Spin the column at 17,900 x g for 30 seconds and discard the material in the collection tube. Repeat until all of the mixture has been added and spun in the column.

9. Remove traces of agarose by adding 500 µL of QG buffer to the spin column. Spin at 17,900 x g for 30 seconds. Discard contents of collection tube.

10. Wash the DNA by adding 750 µL of Buffer PE (Qiagen kit) to the spin column and centrifuge at 17,900 x g for 30 seconds. Discard contents of collection tube.

11. Spin column again for 1 minute to remove all traces of ethanol from the Buffer PE.

12. Place the spin column in a sterile 1.5 mL Eppendorf tube (Axygen, Corning, NY). Add 1:10 buffer EB (Qiagen kit) directly to the column membrane and incubate for one minute.

13. Spin the column at 17,900 x g for 1 minute to elute the DNA from the spin column.

Transformation into Competent E. coli Cells

This procedure is adapted from Molecular Cloning Techniques; Volume 3, Cold Spring Harbor
(All steps to be carried out using sterile technique)

1. Remove a 50 µL aliquot of frozen chemically competent cells from the -80 ºC freezer and thaw on wet ice.

2. Chill a 10-mL sterile culture tube on wet ice for several minutes.

3. Transfer the contents of the 50 µL aliquot to the chilled culture tube.

4. Add 1-50 ng of DNA to the chemically competent cells and gently tap the tube to mix the DNA and cells.

5. Replace the culture on ice immediately and incubate for 30 minutes.

6. After 30 minutes heat shock the cells in the culture tube for 90 seconds in a 42 ºC water bath.

7. Replace the culture tube on ice for 2 minutes.

8. Add 450 µL of SOC broth to the culture tube and incubate at 37 ºC with shaking at 22-250 rpm for one hour.

9. Pre-warm a LB agar plate containing the appropriate selective marker at 37 ºC until cells are finished incubating.

10. Spread 450 µL of cells onto the pre-warmed LB agar plate containing the appropriate selective marker using a sterile spreader.

11. Allow 5-15 minutes for the broth to soak into the agar and incubate the plate upside down overnight (16-20 hours) at 37 ºC in the dark.

Note: For BL21-DE3 cells a 1:50000 dilution of the SOC broth into sterile LB broth is plated to avoid overgrowth of the plate.

Preparation of E. coli Glycerol Stocks for Growths

1. To a sterile cryotube (VWR International) 250 µL of sterile 60% (v/v) glycerol was added.

2. 750 µL of a bacterial culture is added to the crytoube and immediately vortexed for 1 second with the lid on.

3. The cryotube is then immersed in a beaker of liquid nitrogen for 3 minutes and stored at -80 ºC.

Procedure for DNA Test Digest

1. Pick a single colony from an LB agar plate. Grow in 5 mL of LB broth containing the desired antibiotic for 12-16 hours at 37 ℃ wit h shaking at 225-250 rpm.

2. Pellet all of the culture by spinning the material in a 2.0 mL Eppendorf tube and aspirating the supernatant.

3. Using the QIAprep Miniprep Kit (Qiagen, Valencia, CA) extract and purify the DNA from the pelleted cells.

4. To a sterile 1.5 mL Eppendorf tube add 10 µL of the purified, miniprepped DNA.

5. Add 1 µL of 10X restriction enzyme buffer (New England Biolabs, Ipswich, MA) to the DNA.

6. Add a small volume of restriction enzyme to the DNA:

      BamH1   0.25 µL   Add 1.0 µL 10X BSA
      EcoR1   0.25 µL
      NdeI   0.5 µL

7. Incubate the reaction at 37 ℃ for 30 minutes.

8. Analyze the test digest reaction on a 1.0% agarose gel for the presence of the gene product and the vector DNA (approx. 5000 bp).

Procedure for Protein Test Expression

1. Pick a single bacterial colony from an MDAG or LB plate and grow in 5 mL of MDAG or LB broth containing antibiotic overnight at 37 ºC.

2. Transfer 50 µL of the overnight culture to 1 mL of fresh MDAG or LB broth containing antibiotic and incubate with shaking at 220-250 rpm for three hours at 37 ºC in the dark.

3. After three hours remove 100 µL of the culture and immediately add 100 µL of 2 X SDS buffer. Boil the sample and vortex vigorously to kill cells.

4. To the remaining culture (900 µL) add 1 M IPTG to a final concentration of 1 mM (0.90 µL). Incubate the culture with shaking at 220-250 rpm for three hours at 37 ºC.

5. After three hours remove 100 µL of the cell culture and add 100 µL of 2X SDS buffer to the cells. Immediately boil and vortex vigorously to kill cells.

6. Run an SDS-PAGE gel of the sample loading the non-induced sample and induced samples side-by-side to compare.

Note: For protein test expression MDAG is often used since it does not contain any traces of lactose. Some batches of LB may contain traces of lactose which can prematurely induce protein expression.

Preparation of SDS-PAGE Gels

1. Using the Mini-Protean Gel Casting Stand (BioRad, Hercules, CA), set up two gel casting plate assemblies in the stand.

2. Prepare gel solutions based on the table below. For proteins ≤ 30 kDa a 15% T gel was used. For proteins 30 kDa-50 kDa a 12% T gel was used. For proteins ≥ 50 kDa a 10% T gel was used:

Gel Solutions	Stacking gel, 7.5% T	Running gel, 10% T	Running gel, 12% T	Running gel, 15% T
19:1 Bis acrylamide solution	675 µL		5.63 µL	6.75 µL
Acrylamide running buffer		4.5 µL	4.5 µL	4.5 µL
10% SDS solution	67 µL	180 µL	180 µL	180 µL
Water	4.1 mL			
TEMED	3 µL	6 µL	6 µL	6 µL
10% APS solution				

*The APS solution is added immediately before pouring the acrylamide solutions.

3. The acrylamide running gel is distributed evenly into each of the two gel casts leaving 2 mL of solution behind in the tube. A layer of water is added to the top of the poured acrylamide in each cast.

4. After the acrylamide has polymerized, the water is poured off and the acrylamide stacking gel is poured on top of the polymerized running gel distributing evenly across both casts. 2 mL of stacking acrylamide gel is left behind in the tube. A gel comb is added immediately to the top of the cast containing acrylamide stacking gel solution.

5. The gel is polymerized by assessing the small amount of acrylamide solution left behind in the tube.

6. The prepared gel is assembled in a BioRad Mini-PROTEAN gel box. 1X electrophoresis buffer is added to the gel box.

7. SDS-PAGE samples are prepared by adding 5X SDS reducing sample buffer to the protein sample. The sample is boiled in a water bath to denature the protein.

8. Samples are carefully loaded at the top of the SDS-PAGE gel (20-40 µL). A ColorPlus™ pre-stained protein marker (NEB, Ipswich, MA), range 7-175 kDa, is included in the first lane.

Appendix II. Buffers, Growth Media, Solutions

5X Nucleic Acid Loading Buffer

50 mM Tris-HCl, pH 8.0
25% Glycerol
5 mM EDTA
0.2% Bromophenol Blue
0.2% Xylene Cyanole FF

50X Tris-Acetate EDTA (TAE) Buffer

242 g of Tris base
57.1 mL of glacial acetic acid
100 mL of 0.5 M EDTA (pH 8.0)

1X Western Blot Transfer Buffer

57.6 g glycine
12.1 g Tris base
800 mL methanol
Final volume = 4 liters

10X TBS Buffer

24.2 g Tris base
292.4 g NaCl
Adjust pH to 7.5
Final volume = 1 liter

1X TBST Buffer

Dilute 10X TBS and add 500 µL Tween-20 per 1 liter

5X SDS Loading Buffer (Reducing)

20% (v/v) glycerol
100 mM Tris pH 6.8
200 mM β-mercaptoethanol
4% SDS (w/v)
0.2% bromophenol blue (from a 5% stock solution)

10X Electrophoresis Buffer

144 grams glycine
30 grams Tris base
5 g SDS
Final volume = 1 liter
*diluted to 1X when running an SDS-PAGE gel

Acrylamide Gel Buffer

1.5 M Tris adjusted to pH 8.8

Acrylamide Stacking Gel Buffer

0.5 M Tris adjusted to pH 6.8

Coomassie Blue Staining Solution / Destaining Solution

5 g Coomassie blue R-250
1000 mL of Methanol
200 mL of Acetic acid
800 mL of dH$_2$O
*omit the Coomassie blue for the destaining solution

ZYM-5052 Growth Media (Auto-Induction Media)
*Studier, F. W. (2005) Protein Production by Auto-Induction in High Density Shaking Cultures. *Protein Expr. Purif. 41*, 207-234.

For a 2-liter growth:

20 g NZ-Amine AS
10 g yeast extract
1916 mL ddH$_2$O
Autoclave on Fluid cycle for 20 minutes
Allow media to cool to room temperature
Add 4 mL of sterile 1 M MgSO$_4$ (sterile)
Add 400 µL 1000 X Trace Metals (sterile)
Add 40 mL of 50 X M (salts) (sterile)
Add 40 mL of 50 X 5052 (glucose and lactose) (sterile)

N-5052 Auto-Induction Growth Media (For ^{15}N-labeled growths)
*Studier, F. W. (2005) Protein Production by Auto-Induction in High Density Shaking Cultures. *Protein Expr. Purif. 41*, 207-234.

For a 2- liter growth:

14.196 g Na_2HPO_4
13.609 g KH_2PO_4
1.42 g Na_2SO_4
5.45 g [15]NH_4Cl
Autoclave on Fluid cycle for 20 minutes
Allow media to cool to room temperature
4 mL $MgSO_4$ (sterile)
400 µL 1000 X Trace Metals (sterile)
40 mL 50 X 5052 (glucose and lactose) (sterile)

MDG (MDAG) Starter Culture Growth Media
*Studier, F. W. (2005) Protein Production by Auto-Induction in High Density Shaking Cultures. *Protein Expr. Purif. 41*, 207-234.

For a 5 mL growth:
* All solutions are pre-sterilized)

4.6 mL ddH_2O (4.46 mL for MDAG)
10 µL 1 M $MgSO_4$
1 µL 1000 X Trace Metals
50 µL 50 X M
62.5 µL 40% Glucose

For MDAG, add amino acids
100 µL 17 amino acids
40 µL methionine

5 µL 1000 X antibiotic (typically kanamycin)

Monica D. Rieth

5635 Montauk Lane • Bethlehem, PA 18017
monica.rieth1@gmail.com
(610)-360-0535

EDUCATION

Doctor of Philosophy in Chemistry   January 2014
Lehigh University, Bethlehem, Pennsylvania
Advisor: Professor Kerney Jebrell Glover, Ph.D.
Concentration: Biochemistry

Master of Science in Chemistry
Lehigh University, Bethlehem, Pennsylvania   September 2007
Advisor: R. Samuel Niedbala, Ph.D.
Concentration: Clinical chemistry

Bachelor of Science in Biochemistry   May 2003
University of Delaware, Newark, Delaware
Advisor: Eugene Mueller, Ph.D.
Minor in Philosophy

AWARDS

Chemistry Departmental Fellowship   2010 - 2011

GRADUATE RESEARCH EXPERIENCE

Dissertation, Lehigh University, Bethlehem, PA   Fall 2007 –
Advisor: Kerney Jebrell Glover, Ph.D.   January 2014
Thesis: Characterizing membrane protein interactions in detergent and
lipid systems: Exploring caveolin oligomerization

Skills and Expertise:

- Molecular cloning, membrane protein expression, purification
- Reconstitution of membrane proteins into lipid mimics
- Analysis of membrane protein interactions in the analytical ultracentrifuge
- Circular Dichroism spectroscopy
- Reverse-Phase HPLC chromatography
- Size exclusion chromatography (SEC)
- Ni-NTA chromatography
- MALDI-TOF mass spectrometry
- Dynamic light scattering
- ^{31}P-phosphorus, ^{19}F-fluorine NMR
- SDS-PAGE and Western Blot

Research Assistant, Lehigh University, Bethlehem, PA   Fall 2006 –
Advisor: R. Samuel Niedbala, Ph.D.   Spring 2007
Project: HIV antibody detection in human oral fluid/sera

      Technical Skills:

- Handling of biohazardous specimens
- Application of conjugated antigens to nitrocellulose
- ELISA

UNDERGRADUATE RESEARCH EXPERIENCE

Summer Undergraduate Research, Lehigh University, Bethlehem, PA   Summer 2002
Advisors: Theodore Mellin, Ph.D., Richard Merritt, Ph.D.,
Robert Rapp, Ph.D.
Project: Alkylation of cyclodextrin hydroxyl groups to alter the polarity
of β-cyclodextrin

Summer Undergraduate Research, Lehigh University, Bethlehem, PA   Summer 2001
Advisors: Theodore Mellin, Ph.D., Richard Merritt, Ph.D.,
Robert Rapp, Ph.D., Dennis Patterson, Ph.D.
Project: Covalent linkage of β-cyclodextrin to a guest molecule

PROFESSIONAL EXPERIENCE

Research Intern, Orasure Technologies, Inc., Bethlehem, PA   Summer 2006
Supervisors: R. Samuel Niedbala, Ph.D., Keith Kardos, Ph.D.,
Bonnie Anstatt Martinez, Ph.D.

R&D Scientist I, Orasure Technologies, Inc., Bethlehem, PA   2003 – 2006
Supervisor: Bonnie Anstatt Martinez, Ph.D.

      Technical Skills:

- Protein A purification of antibodies from sera
- Bio-conjugation of small molecules to HRP, KLH, BSA
- ELISA
- Western blot
- Handling of oral fluid, urine specimens (Biohazardous samples)

TEACHING EXPERIENCE

Undergraduate Tutor, Lehigh University. Bethlehem, PA   Fall 2011
Course: General Chemistry

Teaching Assistant, Lehigh University, Bethlehem, PA   2006 – 2010

Courses: General Chemistry Lab: Spring 2006, Fall 2007, Spring 2008,
Spring 2009, Fall 2009, Spring 2010
Analytical Chemistry Lab: Fall 2008
Organic Chemistry I: Summer 2008
Organic Chemistry II: Summer 2009

Teaching Assistant, University of Delaware, Newark, DE   Spring 2002
Courses: Introduction to Biology, Introduction to Biochemistry

Teaching Skills:

- Prepared and executed pre-laboratory lecture
- Exam Proctor, Tutor
- Facilitated teaching discussions in a cooperative learning group

PUBLICATIONS

MD Rieth, J Lee, KJ Glover. Probing the caveolin-1 P132L mutant: Critical insights into its oligomeric behavior and structure. *Biochemistry.* **2012.** 3911-8.

POSTER PRESENTATIONS

Biophysics Meeting
Lehigh University, Bethlehem, PA   September 2010
An Inconvenient Truth: A Biophysical Analysis of Caveolin-1 Oligomerization

Delaware Membrane Protein Symposium
University of Delaware, Newark, DE   May 2012
An Inconvenient Truth: A Biophysical Analysis of Caveolin-1 Oligomerization

Federation of American Societies for Experimental Biology (FASEB)
The Westin Resort and Conference Center, Snowmass, CO   June 2012
An Inconvenient Truth: A Biophysical Analysis of Caveolin-1 Oligomerization

Delaware Membrane Protein Symposium
University of Delaware, Newark DE   May 2011
Dissecting the Oligomeric Behavior of Caveolin-1 Using Analytical Ultracentrifugation

Biophysical Society Conference
Baltimore Convention Center, Baltimore, MD   March 2011
Dissecting the Oligomeric Behavior of Caveolin-1 Using Analytical Ultracentrifugation

Delaware Membrane Protein Symposium
University of Delaware, Newark, DE   November 2009
Bicelles in the Analytical Ultracentrifuge: A Powerful Tool for Studying Membrane
Protein Interactions

PROFESSIONAL SOCIETIES AND AFFILIATIONS

Biophysical Society	2011 - Present
Alpha Chi Sigma Professional Fraternity	2007 - Present
American Chemical Society	2004 - Present

REFERENCES

Kerney Jebrell Glover, Ph.D.
Chemistry Department
Lehigh University
6 E. Packer Ave.
Seeley Mudd Bldg.
Bethlehem PA 18015
Email: kjg206@lehigh.edu

R. Samuel Niedbala, Ph.D.
Chemistry Department
Lehigh University
6 E. Packer Ave.
Seeley Mudd Bldg.
Bethlehem, PA 18015
Email: san204@lehigh.edu

Robert Flowers II, Ph.D.
Chemistry Department
Lehigh University
6 E. Packer Ave.
Seeley Mudd Bldg.
Bethlehem, PA 18015
Email: rof2@lehigh.edu